Aus dem Institut für Virologie
des Fachbereichs Veterinärmedizin
der Freien Universität Berlin

COWPOX VIRUS VIRULENCE DETERMINANTS

Inaugural-Dissertation
zur Erlangung des Grades eines
Doktors der Veterinärmedizin
an der
Freien Universität Berlin

vorgelegt von
Aistė Tamošiūnaitė
Tierärztin aus Kaunas, Litauen

Berlin 2017

Journal-Nr.: 3934

Gedruckt mit Genehmigung des Fachbereichs Veterinärmedizin

der Freien Universität Berlin

Dekan:	Univ.-Prof. Dr. Jürgen Zentek
Erster Gutachter:	Univ.-Prof. Dr. Nikolaus Osterrieder
Zweiter Gutachter:	Univ.-Prof. Dr. Robert Klopfleisch
Dritter Gutachter:	PD Dr. Sandra Blome

Deskriptoren (nach CAB-Thesaurus):
cowpox virus; DNA; plasmids; restriction fragment lenght polymorphism; immunohistochemistry; polymerase chain reaction; electrophoresis; antibiotics; antibodies

Tag der Promotion: 20.07.2017

Bibliografische Information der *Deutschen Nationalbibliothek*
Die Deutsche Nationalbibliothek verzeichnet diese Publikation in der Deutschen Nationalbibliografie; detaillierte bibliografische Daten sind im Internet über <http://dnb.ddb.de> abrufbar.

ISBN: 978-3-86387-832-0
Zugl.: Berlin, Freie Univ., Diss., 2017
Dissertation, Freie Universität Berlin
D 188

Choriner Str. 85 - 10119 Berlin
verlag@menschundbuch.de – www.menschundbuch.de

Parts of this thesis are based on following manuscript:

Tamošiūnaitė, A., D. Hoffmann, A. Franke, J. Schluckebier, K. Tauscher, B. K. Tischer, M. Beer, R. Klopfleisch, N. Osterrieder. 2016. Histopathological and Immunohistochemical Studies of Cowpox Virus Replication in a Three-Dimensional Skin Model. Journal of Comparative Pathology. **155(1):**55-61.

Table of Contents

List of Figures

List of Tables

List of Abbreviations

3D	Three-dimensional
µ	Micro
aa	Amino acid
APC	Antigen presenting cell
ATI	Acidophilic –type inclusion body
BAC	Bacterial artificial chromosome
BCE	Before Common Era
BR	Brighton Red
BSA	Bovine serum albumin
CMLV	Camelpox virus
CAM	Chicken chorioallantoic membranes
CE	Common Era
CECs	Chicken embryo cells
CEV	Cell associated enveloped virus
CEF	Chicken embryo fibroblast
co-int	Co-integrate clones
CPXV	Cowpox virus
Crm	Cytokine response modifier
CS	Chondroitin sulfate
DMSO	Dimethyl sulfoxide
DNA	Deoxyribonucleic acid
dNTP	Deoxyribonucleotide
dpi	Days post infection
dsDNA	Double stranded DNA
E.coli	*Escherichia coli*
ECTV	Ectromelia virus
EDTA	Ethylenediaminetetraacetic acid
EEV	Extracellular enveloped virus
FCS	Fetal calf serum
fw	forward
FWPV	Fowlpox virus
g	Gramm
GAAP	Golgi anti-apoptotic protein
GFP	Green fluorescent protein
HE	Heamatoxylin and eosin
HS	Heparan sulfate
HSPV	Horsepox virus
h	Hour
IV	Immature virus
IEV	Intracellular enveloped virus
IL	Interleukin
IL-18BP	Interleukin-18 binding protein
IMV	Intracellular mature virus
INF	Interferon
ITRs	Inverted terminal repeats
KANA	Kanamycin
kb	Kilo base pairs
l	Liter

LB	Lysogeny broth
LTα	Lymphotoxin α
m	Milli
M	Molar
mA	Milliampere
MCMV	Mouse cytomegalovirus
MEM	Minimal essential medium
min	Minute
mini-F	Minimal fertility factor
MOCV	Molluscum contagiosum virus
MOI	Multiplicity of infection
MPXV	Monkeypox virus
mRNA	Messenger RNA
MHC	Major histocompatibility complex
MVA	Modified Vaccinia Ankara
MYXV	Myxoma virus
m-slfn	Murine Schlafen gene
NF-κB	Nuclear factor-Kb
NGS	Next-Generation Sequencing
O/N	Overnight
OD_{600}	Optical density, 600 nm wavelength
OPV	Orthopoxvirus
ORF	Open Reading Frame
p	Plasmid or BAC
PBS	Phosphate buffered saline
PCR	Polymerase chain reaction
pfu	Plaque forming unit
pi	Post-infection
P/S	Penicillin/streptomycin
qPCR	Quantitative real time PCR
PKR	Protein kinase R
RFLP	Restriction fragment length polymorphism
RNA	Ribonucleic acid
rpm	Rounds per minute
RPO	RNA polymerase
RT	Room temperature
rv	reverse
SDS	Sodium dodecyl sulfate
sec	Second
SFV	Shope fibroma virus
SPF	Specific-pathogen-free
Slfn	Schlafen gene
TAE	Tris base acetic acid, EDTA
$TCID_{50}$	Tissue culture infective dose 50%
TGN	Trans-Golgi network
TK	Thymidine kinase
TNF	Tumor necrosis factor
UV	Ultraviolet
V	Volt
v	Reconstituted virus
v-slfn	Viral Schlafen gene

VACV	Vaccinia virus
VARV	Variola virus
WHO	World Health Organization
wt	Wild type

1. Introduction

1.1. Poxviruses

1.1.1. Classification of poxviruses

The Poxviridae is a family of large DNA (Deoxyribonucleic acid) viruses that multiplies in the cytoplasm of infected cells (1). Members of this family infect diverse genus of the animal kingdom that expanses from insects to mammals. Moreover, the Poxviridae family of viruses is divided into two sub-families based on differences in host range: Entomopoxvirinae, whose members infect insects, and Chordopoxvirinae, whose infect vertebrates (2). Viruses of the subfamily Chordopoxvirinae are subdivided into genera, primarily by serologic cross-reaction and cross-protection, host range, morphology and sequence similarity (3). The Chordopoxvirinae consists of ten genera: Suipoxviruses, Orthopoxviruses, Parapoxviruses, Yatapoxviruses, Molluscipoxviruses, Leporipoxviruses, Capripoxviruses, Cervidpoxviruses, Avipoxviruses and Crocodylipoxviruses. As Yatapoxviruses, Leporipoxviruses, Capripoxviruses, Cervidpoxviruses and Suipoxviruses form a sisterclade to Orthopoxviruses in phylogenetic analyses, viruses belonging to these clades are classified as “clade II” poxviruses (4, 5). The Orthopoxvirus (OPV), the most studied genus of the Chordopoxviruses, contains several important pathogens of man and animals, including the virus that caused smallpox, variola virus (VARV), as well as cowpox virus (CPXV) and vaccinia virus (VACV), zoonotic viruses, that made the worldwide eradication of smallpox possible (6, 7).

1.1.2. Historic hallmarks

The most known member of the Poxviridae family is variola virus. From the time of its suspected emergence after 10000 BCE (before the Common Era) to the time of its eradication, smallpox was a worldwide feared disease that took hundreds of millions of lives (8). It has even been hypothesized that smallpox caused the death of Ramses V in Egypt in around 1157 BCE, as poxvirus-like lesions were discovered on the mummy (9). The first recorded smallpox epidemic was in 1350 BCE during the Egyptian–Hittite war. Afterwards in-between the 5th and 7th century smallpox spread to Europe and later during the 17th-18th century, it reached the North American colonies. These widespread epidemics caused millions of deaths in Europe and Mexico. Additionally, smallpox was used to demolish select human populations. The first documented use of smallpox as a biological weapon was during the French and Indian War in 1763, when British forces dispersed blankets used by smallpox patients to Native Americans (10). Nonetheless, this terrible disease has had a profound impact on the modern practice of vaccination as well. Notably, the smallpox vaccination campaign, that stopped only after this disease was eradicated in 1980, is known to be one of the biggest public health accomplishments of modern medicine. The smallpox eradication through vaccination was possible at most due to one feature: there is no animal reservoir of smallpox, VARV spreads person to-person (11). Additionally, already early in the history those who bore pox scars were noted to be resistant to disease recurrence. Moreover, the persons who acquired smallpox through a scratch were witnessed to have attenuated course of disease. Buddhist nun sometime between 1022 and 1063 CE started an inoculation with smallpox pus or scabs either by a nasal or cutaneous route, a procedure known as variolation. This practice eventually spread to China, India and Turkey, and by the late 1700s, was practiced by European physicians (10). A much safer practice was established in 1798 by English physician Edward Jenner, when he started to use CPXV, a less dangerous poxvirus to prevent smallpox infections (10). After noticing, that milkmaids who developed cowpox lesions are resistant to smallpox, Jenner took a fluid from a cowpox pustule

on a dairymaid's hand and used it for inoculation of an 8-year-old boy. Consequentially, this boy did not develop symptoms of smallpox, when he was exposed to the disease, 6 weeks later. Thenceforth, Jenner extended this experiment to other children and the same outcome have been seen (12). This procedure was named vaccination, derived from "*Vacca*," the Latin word for cow. From these experiments, the practice of vaccination expanded around the globe. The use of cattle for amplification of the viral stocks was a widespread practice. Initially, vaccination was performed with cowpox virus, however, at some time during the 19th century, worldwide vaccinia virus was used for vaccination, but not cowpox virus (10). To this day, the reasons for this change are unknown, or as Fenner wrote „ obscure "(10). However, despite its indeterminate origin, vaccinia virus was the basis for effective vaccines. It provided a high degree of protection against smallpox, with minor risk to either the vaccinated individual or other members of community (10). It is important to notice, that Orthopoxviruses are known to be immunologically cross-reactive and cross-protective, therefore infection with any member of this genus provides protection against infection with any other member of the genus (10, 13). Even though, the systematic vaccination against smallpox have already begun in the early 19th century, the real breakthrough in the eradication of smallpox occurred in 1967 when the World Health Organization (WHO) introduced worldwide vaccination campaigns. The last known natural case of smallpox was registered in 1977 (14). Consequentially, in May 1980, the WHO announced, that smallpox had been eradicated and ceased the vaccination (10, 15 - 16). However, now, 37 years after the vaccination was ended, big part of the world human population doesn't possess immunity not only against smallpox, but also against any other Orthopoxvirus infections (17, 18). As a consequence of this new situation, there is a possibility for the Orthopoxviruses to circulate in the human population (17).

1.1.3. Structure of the poxvirus genome

The genomes of poxviruses consist of a linear, double-stranded DNA. Remarkably, the size of the genome varies from 130,000–134,000 base pairs (bp) for members of the Parapoxvirus and Yatapoxvirus genus (19, 20) to almost 360,000 base pairs for canarypox virus, a member of the Avipoxvirus genus (21). The genomic content and organization is greatly similar among poxviruses, and particularly within the Chordopoxviruses. Approximately 50 conserved genes have been found in all sequenced poxviruses. Moreover, additional 40 genes are commonly found in most of Chordopoxviruses (22-24). The products of the highly-conserved genes are the genes that are vital for poxviruses like RNA (Ribonucleic acid) processing, transcription, DNA replication, cell entry, virion assembly and release. Conserved genes are generally found in the central section of the poxvirus genomes. In the case of Orthopoxviruses, this central core region of the genome contains roughly 75% of the complete sequence and is the most conserved region of the genome, it is highly conserved within the family as well (25). Poxvirus genes that

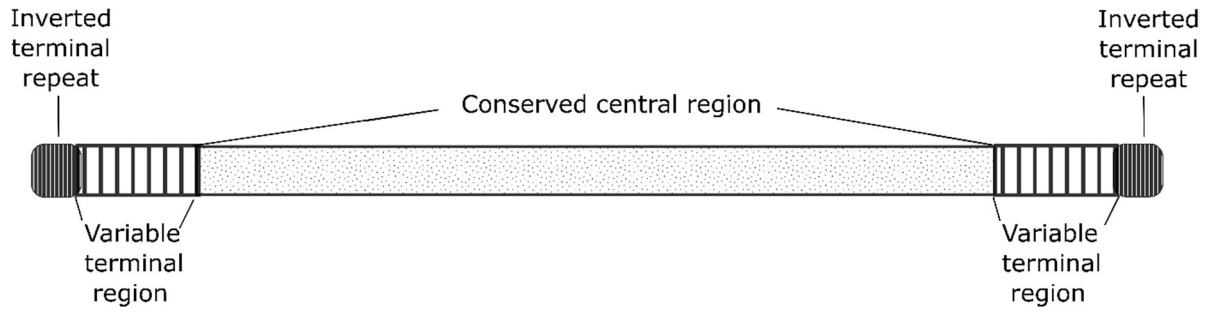

Figure 1: Schematic representation of the Orthopoxvirus genome. The double stranded DNA is enclosed by terminal hairpin loops and the ITRs are localized at both ends.

play a role in the interaction within the host, as well as genes that affect the host range, are involved in immunomodulation, and pathogenicity, are usually located at the terminal areas of the genome and often display lower sequence identity (26-31). Furthermore, inverted terminal repeats (ITRs) are found at the ends of the poxvirus genomes, these repeats can range from 0.1 to 13 kb in size. Since, ITRs hold matching sequences at both ends, however sequence at one end of the genome is being repeated in the inverse orientation at the opposite end (32, 33) (Figure 1). Poxvirus DNA strands are joined at their termini with a hairpin loop, this way forming a continuous polynucleotide chain (34, 35), that covalently closes the two genomic DNA strands. Analysis of terminal hairpin nucleotide sequences revealed that they consist almost completely of adenine and thymine residues and could be characterized as the F form, that is an inverted complementary to the sequence of the S form (34, 36). Near the termini there is incomplete pairing as well as two isomeric forms, F and S, are found. These two isomeric forms contain sequences responsible for concatemer resolution. Sequence of VACV open reading frames (ORF's) are generally named with a capital letter, which corresponds to *Hin*dIII restriction endonuclease genome fragment, an Arabic number, that indicates the position within the *Hin*dIII fragment in addition, letters L or R are added to the name, representing transcription to the left or right, respectively (37). Proteins have the equivalent designation, only the letter L or R is absent.

1.1.4. Poxvirus virion forms

During poxvirus infection four different types of infectious virus particles are formed: (i) intracellular mature virion (IMV) is the most abundant form, that is released during the cell lysis; (ii) intracellular enveloped virus (IEV) is an intermediate form of virus surrounded by an additional lipid envelope, (iii) cell associated enveloped virus (CEV) is responsible for cell-to-cell spread and (iv) extracellular enveloped virus (EEV or EV) is important for dissemination of the virus within the host (38-40). Naturally, IMV is the most basic infectious particle. The nucleoprotein core of IMV is surrounded by only one lipoprotein membrane (41-43) (Figure 2). These infectious particles are very stable. Furthermore, IMVs are assumed to be accountable for virus transmission between various hosts, whereas EEVs have an additional fragile outer membrane and depart the intact cell to spread inside the host (44, 45). The additional membrane of EEV, derived from endosomes or the trans-Golgi network (TGN), is altered by the inclusion of several cellular and viral proteins that are absent in IMV throughout morphogenesis (39, 40).

1.1.5. The poxvirus replication cycle

The poxvirus replication cycle starts with the virion attachment to the cell. However, the entry pathways differ, depending on the type of virion (Figure 2). For instance, IMV is surrounded by a single lipid envelope, so the virus core gains entry into the cytosol just after fusion of the virus membrane with the plasma membrane, in a low pH pathway (42, 46-48). Endocytosis can occur by dynamin-mediated fluid phase uptake or macropinocytosis (49-54). Several viral proteins were found to mediate IMV attachment. For example, VACV A27 binds heparan sulfate (HS) on the cell surface, when D8 binds chondroitin sulfate (CS) and soluble H3 binds HS (55-59). These multifunctional attachment proteins are not separately essential, nevertheless deletion of gene coding sequence for A27 and H3 were shown to severely reduce virulence of VACV (58, 60, 61). Additionally, the A26 protein were shown to mediate the assimilation of IMVs into acidophilic - type inclusion bodies (ATI) of some orthopoxviruses, like ectromelia virus (ECTV) and cowpox virus (62). ATIs are proteinaceous matrices which are assumed to shield infectious particles after they are released into the environment. Furthermore, the A25 protein, that is the A-type inclusion protein, were found to be a fusion suppressor (63-65) and to determine poxvirus strain-specific entry pathways (63, 67).

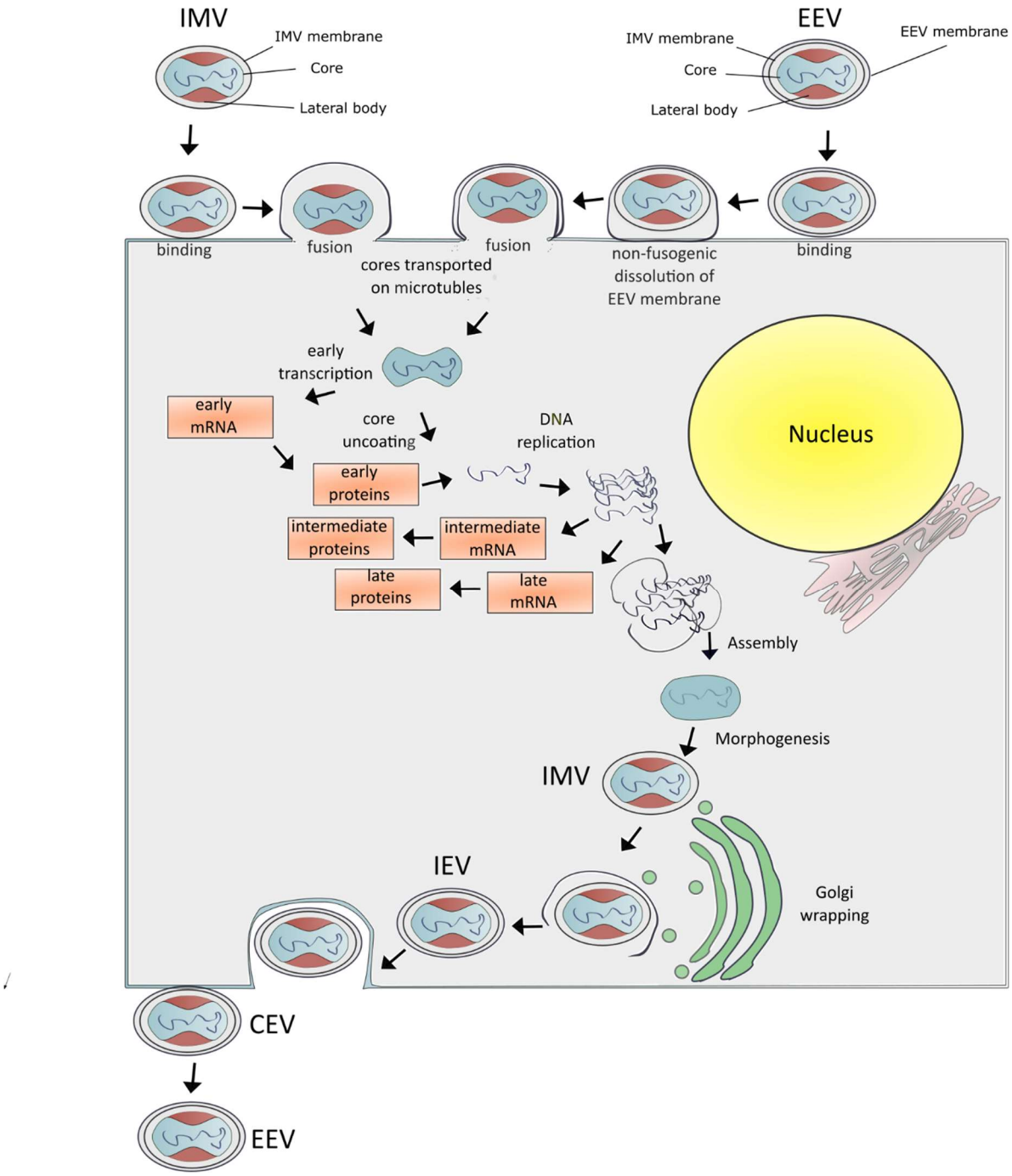

Figure 2: Schematic representation of the intracellular mature virion (IMV) and extracellular enveloped virion (EEV) structure and poxvirus replication cycle. Afterwards the infiltration of EEV or IMV into the host cell, the core is released into the cytoplasm. Immediately the early gene expression begins within the core, DNA replication follows, as the intermediate and late gene transcription. Thenceforth, the virus assembly follows and the formation of crescents. Next, the closed particle matures and is moved to the Golgi apparatus with the help of microtubules. After the Golgi wrapping the IEV is moved to the cell surface, again by microtubules. Finally, the virion fuses with the plasma membrane and is discharged out of the cell as EEV.

Consequentially MVs with functional copies of A25 and A26 proteins uses the endocytic pathway to enter the cell, while virions without functional copies of these proteins enter through the fusion with the plasma membrane (69).
Meanwhile EEV leaves the cell by exocytosis and possesses an additional membrane that is eventually ruptured before or during the next stages of infection, so the enclosed MV can fuse with the plasma membrane or endocytic machinery (54, 66, 67) (Figure 2). The early mRNA and protein synthesis as well as DNA replication begins after the virus core is introduced into the cytoplasm (70). Typically, DNA viruses replicate in the nucleus, using the cellular proteins. In contrast, poxviruses encode their own DNA replication and transcription machinery, hence they are capable to replicate in the cytoplasm, forming basophilic (B-type) inclusions (1). B-type inclusion bodies termed "virus factories", are spots of intense metabolic activity and production of viral components (71), surrounded by endoplasmic reticulum membranes (72). Vaccinia virus DNA replication begins with a nick of one of the DNA strands close to the terminal hairpin (73), approximately 1-2 hours after infection. Subsequently, strand cleavage provides a free 3'-OH end, which functions as a primer terminus for the viral DNA polymerase. Then, the strand extension proceeds towards the hairpin telomere, consequentially, forming dimeric tail-to-tail concatemer molecules, which are resolved by nicking with specific nucleases into unit length monomers. The newly replicated DNA delivers a template for intermediate and late mRNA synthesis (70). Succeeding a late gene expression, virus assembly follows. This process also takes place in the B-type inclusions. Subsequent, crescents associate with the virus DNA and protein complex and develop into a sealed oval or spherical particle called immature virus (41-43). By proteolytic cleavage of some capsid proteins and condensation IMV is assembled. Afterward, IMV particles are moved with from the virus factory on microtubules and wrapped by intracellular membranes forming the intracellular enveloped virions (IEVs). Hither, the newly constructed particles are transported by microtubules to the cell membrane (44, 45). Finally, the IEV outer membrane fuses with the plasma membrane exposing the virion on the cell surface by exocytosis (74) (Figure 2).

1.1.6. Immunomodulatory proteins of OPV

Because of the existence of countless host innate antiviral defense mechanism, in the course of evolution, poxviruses have evolved complex molecular strategies to inactivate or re-configure the host antiviral responses (75-77). OPV proteins that were shown to interfere with the host immune system can be separated into three categories: virotransducer, virostealth and viromimic proteins (27, 78, 79).
The first group, virotransducer proteins, act intracellularly. These proteins function to intervene with the intracellular response to infection, like the initiation of an antiviral state, the oxidative burst and apoptosis, an irreversible cascade of biochemical events orchestrated by caspase proteases that concludes in cell death (80). For instance, one of these mechanisms, activation of apoptosis by the intrinsic pathway, is controlled by a complex network of protein–protein interactions between anti-apoptotic and pro-apoptotic members of the Bcl-2 family of proteins. VACV directly subverts the intrinsic pathway by expressing proteins termed F1 and N1. Consequentially, protein F1 adopts a Bcl-2-like fold (81) and binds Bak at the mitochondrion (81 - 84). In addition, F1 also reduces the inflammatory response by binding NLRP-1, an upstream activator of caspase-1 (85). Moreover, protein N1 also has a Bcl-2 fold (86, 87). Furthermore, to interfere with activation of apoptosis, CPXV produces protein CrmA, which inhibits group I and group III caspases (88 - 90). Finally, few VACV strains, such as Evans, as well as camelpox virus (91) express a protein called viral Golgi anti-apoptotic protein (vGAAP) which is closely related (73% amino acid I dentity) to a human orthologue, hGAAP (92). Both proteins, hGAAP and vGAAP, were shown to protect cells from apoptosis deriving from both intrinsic and extrinsic pathways (92).

Another group of OPV proteins that interfere with the host immune response, are the virostealth proteins. These proteins act intracellularly, implementing a universal tactics to disguise the visible signs of infection, so the cell-mediated immune response machinery would not be able to identify and remove the infected cells. Moreover, the virostealth proteins downregulate immune recognition molecules, such as CD4 and major histocompatibility complex (MHC) class I, to reduce the chance of recognition by the immune system. For instance, it has been shown that CPXV evades antiviral CD8 T cell responses by suppressing the MHC class I (93) molecules. Two distinctly acting MHC class I regulating genes (D10L and B8R for CPXV-GRI) have been discovered. Protein D10 inhibits MHC class I expression by impairing endoplasmic reticulum (ER) peptide loading and dissociation of MHC class I from TAP, meanwhile protein B8 interferes with the intracellular trafficking of MHC class I molecules by sequestering them in the ER (94).
Extracellularly acting viral proteins are grouped as viromimics. These proteins mostly mimic cytokines produced by the host or the receptors for the host produced cytokines. Cytokines are extracellular signaling molecules. These molecules are the crucial regulators of the immune response, important for the fight against the various pathogen invasion. Early acting cytokines defend against the first steps of viral infection (95). In general, cytokine-mediated responses are responsible for the total elimination of viral infection (96). Moreover, large part of the damage imposed on pathogen infected cells is indeed the outcome of mechanisms that were started by pro-inflammatory cytokines like the interleukin-1 (IL-1) and IL-18, interferons (IFNs), chemokines and tumor necrosis factor (TNF) (97). Consequently, most viruses have established tactics for modulation of the cytokine signaling in infected cells (75, 98 - 99). Cytokine network viral deception proteins, the viromimics, can be further classified into virokines and viroreceptors. Viroreceptors are cell surface or secreted glycoproteins that competitively binds to host cytokines and chemokines in consequence disrupting their function. For example, viral tumor necrosis factor receptors (TNFr's) were identified in numerous members of the poxvirus family by sequence similarity to the extracellular part of host cell TNFRs. Interestingly, the cowpox virus encodes even four vTNFRs: cytokine response modifier (Crm) B, CrmC, CrmD and CrmE. Two of these, CrmB and CrmD, are secreted proteins that bind both TNF and lymphotoxin α (LTα), while CrmC and CrmE are specific to TNFα (100 - 104). During the path of evolution, pathogens, particularly viruses, have caught the genetic sequence needed to make their own forms of host molecules. Especially among large DNA viruses, stolen host genes are often found. Not surprisingly, large DNA viruses dedicate substantial part of their genome to the sequence of immune modulators. Viral proteins classified as virokines are largely secreted viral proteins. These proteins mimic host molecules, such as complement regulators, cytokines or even their inhibitors. One of the virokines encoded by poxvirus is interleukin-18 binding protein (IL-18BP). ECTV, MOCV, VACV and CPXV have been demonstrated to encode functional viral IL-18BP, which successfully blocks IL-18 (75, 76, 78, 105 - 108). Nevertheless, there has no immunomodulatory protein been found, that would be common to all poxviruses. Each virus species expresses its own unique combination of immunomodulatory proteins. This permits it effectively to evade its natural hosts immune system. Moreover, this by all poxviruses employed, remarkably host-specific, survival tactic, may also partly play part in the unpredictable outcome of infection, when poxvirus "jumps" into new host species.

1.2. Cowpox virus

Cowpox virus is one of the first described members of the Orthopoxvirus genus. It entered the medical history in Edward Jenner's publications "Inquiry" and "Further observations on the

Variolae Vaccinae" in 1798/99; where the physician revealed the efficacy of cowpox virus scarification to induce a protective immunity against smallpox infection (12, 109).
Phenotypically it is separated from other OPV species by the production of large eosinophilic cytoplasmic A-type inclusion bodies in infected cells and flattened pocks with a hemorrhagic center on the chicken chorioallantoic membrane (CAM) of embryonated eggs at 72 hours post infection. Moreover, among the OPVs, CPXV possesses the largest genome (224-228 kbp) and infects the widest range of host species (110, 111) (Table 1).
Today, CPXV is endemic in Europe and northern and central Asia (112). However, cowpox-like infection has also been described in Israel (113). The name cowpox virus is rather misleading, since the suspected reservoirs of this virus are wild rodents such as field voles (*Microtus agrestis*), bank voles (*Myodes glareolus*), common voles (*Microtus arvalis*) or wood mice (*Apodemus sylvaticus*) (114-119). The name cowpox originated in the 18th century, at what time CPXV was associated with clinical disease of cows and milkmaids. Today, however, the virus causes disease mostly in pet rats, cats and their owners (120-124). There has been a recent increase in the number of reports of CPXV infection of cats, rats, humans and other mammals, and the disease is considered to be an emerging infection (112, 122-128).
Interestingly, human cowpox predominantly affects young people, this might indicate, that the lack of smallpox vaccination may play a part in the increased susceptibility to variety OPV infections including cowpox (137-139). However, to date, no direct human-to-human transmission has been described (138, 140).

Species	Transmission to humans	Reference
Puma (*Felis concolor)*	-	[129]
Cheetah (*Acinonyx jubatus)*	yes	[129]
Lion (*Panthera leo)*	-	[129]
Ocelot (*Felis pardalis)*	-	[129]
Jaguar *(Felis onca)*	-	[129]
Lynx (*Lynx lynx)*	-	[125]
Far eastern cat *(Felis bengalis)*	-	[129]
Bearcat (*Aiulurus fulgens*)	-	[130]
Cat (*F. sylvestris f. catus*)	yes	[121, 122, 128]
Fox (*Vulpes vulpes*)	-	[131]
Common rat (*Rattus norvegicus*)	yes	[120, 123, 124]
Bank vole (*Myodes glareolus*)	-	[116-118]
Field vole (*Microtus agrestis*)	-	[116-118]
Wood mice (*Apodemus sylvaticus*)	-	[116-118]
House mice (*Mus musculus*)	-	[116-118]
Dog (*Canis lupus familiaris*)	-	[132]
Horse (*Equus caballus*)	-	[133]
Cow (*Bos taurus*)	-	[134]
Asian elephant (*Elephas maximus*)	-	[135, 136]
Llama (*Lama glama*)	-	[126]
White rhinoceros (*Ceratotherium simum*)	-	[135]
Okapia *(Okapia johnstoni)*	yes	[135]
Beaver (*Castor fibor canadensis*)	-	[130]
Anteater *(Myrmecophaga tridactyla*)	-	[129]

Table 1. CPXV host range. Registered CPXV infections in distinct species of mammals.

1.2.1. Clinical presentation

Even though human cowpox virus infections are in general characterized by mild and self-limiting lesions, cowpox may also lead to fatal outcome, especially in immune-compromised individuals including patients with atopic skin diseases (110, 141). The normal course of infection in humans was reconstructed by Baxby et al in an overview of 54 cases (140). It was shown, that in contrast to smallpox, CPXV infection in humans is spread through direct inoculation of CPXV into skin and/or oral mucous membranes by the use of small lesions. In consequence of the inoculation, the distinctive skin lesions develop. Next, inflamed macules occur that change to papulo-nodular or vesicular, then sterile pustules; later central hemorrhagic necrosis covered by a black eschar and frequently surrounded by erythema and indurated edema is formed (140). Cases of conjunctivitis and keratitis have also been registered. Nonetheless, fatal disease occurs seldom and is not completely characterized, even though isolated cases of encephalitis and heart failure have been reported (141). Furthermore, autoinoculation potentially contributes to the development of additional cutaneous and/or mucosal lesions. Lately increasing number of human CPXV infections, obtained through the contact with infected pet rats are recorded (123, 127, 150). In these cases, the animals exhibit skin lesions or respiratory signs and usually dies just after purchase. Natural CPXV infection in white rats has been investigated previously and 3 different clinical forms were defined: a pulmonary form, a milder dermal form, and a mixed form with the clinical signs typical to both previous forms (142). In the case of the pulmonary form dyspnea, loss of appetite, progressively increasing abdominal distention and flaccidity was registered. Inevitably, this form of the disease ended lethally within 3-4 days after the first clinical signs were registered. During the macroscopic examination, focal pneumonia with hemorrhagic pleural exudate was found. Furthermore, the intestines and stomachs were distended, but the skin and mucosal rash were not detected (142). When in the case of dermal form, papular rash, mainly on paws, tail and nose, together with rhinitis and conjunctivitis with hemorrhagic discharge were registered (Figure 3). Occasional anorexia and necrosis of the tail and paws was also documented. But the lethality was low. Necropsy findings were mucosal exanthema, dermal eruptions and focal pneumonia (142). Cats that are in contact with rodents are also disposed to possible CPXV infection (143). In the case of cat with CPXV, the ulcerated skin lesion develops at the site of viral entry (typically an infected bite wound on the head or forelimbs), followed by viremia. The secondary skin lesions develop 5 to 14 days post infection. Finally, the viremia is mostly transient and systemic clinical signs are absent or mild, and complete recovery is common (143, 144). Unfortunately, the clinical misdiagnosis of CPXV infections as eosinophilic granuloma, neoplasm or pyoderma are common. However, with the help of histopathological examination, CPXV infection can be detected and wrong clinical diagnoses rejected.

Figure 3: **Development of CPXV lesion in infected rats**. Picture 2. 6 days after intranasal CPXV infection, pox lesion at the dorsal view of the hind limb. Picture 3. 23 days after intradermal CPXV infection, lesion on a tail. Picture 4. 11 days after intradermal CPXV infection, swelling of the lips and tongue with superficial necrosis. Picture 5. 23 days after intradermal CPXV infection, necrosis of the distal phalanx. Reprinted by permission from SAGE Publications: (Veterinary Pathology) (158), copyright 2012

1.2.2. Variety of cowpox

The complete genomes of multiple CPXVs are presently available, including some well-known strains, like CPXV Brighton Red (BR), CPXV GRI-90 and CPXV Germany 91-3 which contain approximately 224, 224 and 228 kb, respectively (145). The knowledge of the *in vitro* and *in vivo* features of CPXVs is gathered largely from research achieved with the CPXV reference strain Brighton Red. This well-known strain was initially isolated in 1937 from a milkmaid and sustained by serial passage in rabbit skin (146). Although this strain has an unidentified passage history in countless laboratories worldwide after its isolation before 80 years, it is still considered to be a representative CPXV. Meanwhile, CPXV strains were found to differ to an extent that would even warrant reclassification as different species (23). Recently, a CPXV cluster whose genomes are closer to camelpox virus (CMLV), taterapox virus (TATV) and VARV has been acknowledged (147). Not only are the CPXVs genetically heterogeneous (23, 148), they also show marked differences in phenotypic properties (149). New CPXV infections occur naturally in Germany in increasing numbers. Starting in 2008 and continuing, numerous cases of human CPXV infections were described in the South and West of Germany and the Northern France, which could have been chased down to a contact with infected pet rats (123, 127, 150). It is striking, that an infection of pet rats with these newly occurring CPXV strains often had a lethal outcome (150).

1.3. Bacterial artificial chromosomes (BACs)

Bacterial artificial chromosomes (BACs) are DNA constructs based on circular minimal fertility factor (miniF) plasmids. BACs have revolutionized the directed mutation of large viral DNA genomes, by permitting viral genomes to be maintained at low copy number and manipulated in *Escherichia coli (E. coli*). Afterwards infectious virus can be reconstituted *via* transfection of eukaryotic cells (151, 152). Furthermore, mutagenesis in *E. coli* reduces the risk of compensatory mutations and allows mutagenesis of viruses that are difficult to grow and/or manipulate as well as the engineering of viruses with lethal mutations. This development has enabled the generation of transgenic animals, using modified clones of genomic BAC libraries (151). Moreover, it boosted the improvement in genome sequencing projects (153, 154). Mouse cytomegalovirus (MCMV) is the first large DNA virus, that was cloned as a BAC and successfully reconstituted. It has a genome size of approximately 230 kbp (154). Nonetheless, generating a poxvirus genome as a BAC has been technically challenging, largely because the genome has covalently closed ends and a helper virus must be used to reconstitute the virus, as pox virus DNA is not infectious on its own. However, these difficulties have been overcome and four VACV BACs and one CPXV BAC were generated (153, 155-157). The full-length genome of CPXV strain Brighton Red was cloned as a BAC in *E. coli*. For this purpose, the mini-F replicon of pBeloBAC11 was inserted *via* homologues recombination into the non-essential thymidine kinase gene of CPXV. Thenceforth, with the assistance of the transcriptional machinery of fowlpox virus (FWPV), infectious CPXV was effectively reconstituted in cell culture. BAC-derived virus, vBRF, shares the same growth properties as the parental virus (157). Besides, mini-F cassette inserted in BR BAC also contains a GFP (green fluorescent protein) encoding ORF that is under control of a late FWPV promoter to enable locating of infected cells.

1.4. Project Introduction

In 2009, in Southern Germany a CPXV strain was isolated from a CPXV infected pet rat, which had bitten and infected two girls. The isolate was named RatPox09 and exhibited viral growth characteristics *in vitro* that were very like those of reference strain Brighton Red (BR, AF482758). However, in *in vivo* experiments Wistar rats and fancy rats, infected with RatPox09, developed severe and often fatal disease. Similarly, after intradermal inoculation, RatPox09 caused systemic disease in rats, with several lesions, from proliferative to necrotizing and ulcerative. Histopathologic inspection found mixed cellular dermatitis and folliculitis with epithelial ballooning degeneration and necrosis (158). Meanwhile the infection of mice or Wistar rats with the CPXV strain BR results only in mild to asymptomatic course of disease (119, 158-160). The complete genomic sequence of RatPox09 was determined by Next-Generation Sequencing (NGS) and compared with BR and other published CPXV sequences. The calculated sequence identity between RatPox09 and BR was 92% (119). After comparison of all available CPXV sequences, there were no apparent virulence related viral genome pattern nor an individual ORF, which could be directly associated with the pathotype of the isolate, found (Figure 4) (119). Interestingly, four open reading frames (ORFs) are present in the RatPox09 genome, but absent in the BR genome. These ORFs are CPXV0002, CPXV0003, CPXV0030, and CPXV0284 (119). All genes have homologs in other othopoxviruses and encode the putative N-methyl-D-aspartate receptor-like (NMDAr) protein (CPXV0002), the cytokine response modifier E (CrmE) (CPXV0003), the putative 7-transmembrane-G-protein-coupled-receptor-like protein (7tGp) (CPXV0030) and the Kelch-like protein D7 (CPXV0284), respectively. In addition, there are two ORFs, ATI (CPXV158) and p4c (CPXV159), which are markedly different in the RatPox09 and BR genomes (Figure 5).

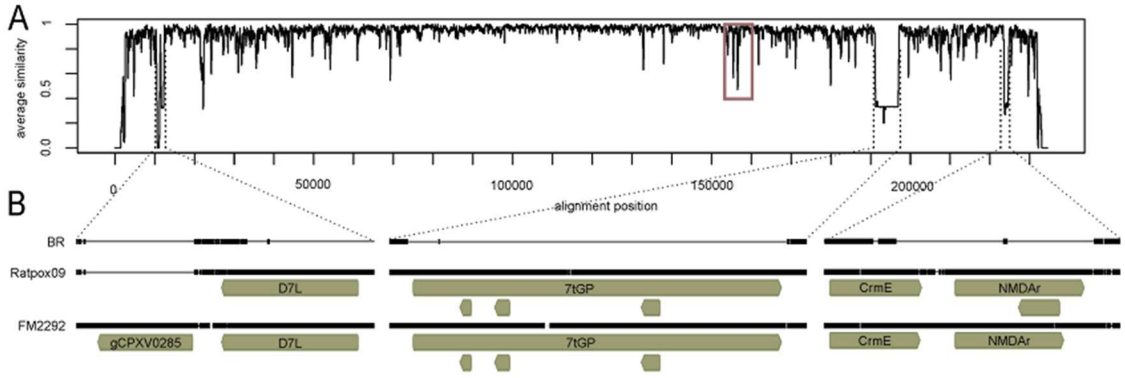

Figure 4: Nucleotide sequence comparison of RatPox09, FM2292, and Brighton Red (BR). (A) Normalized similarity plot of Brighton Red, FM2292, and RatPox09. A value of 1 indicates an identity of 100%, while a value of 0 indicates no conservation at all. Regions of special interest are enlarged. (B) Alignments of genes coding for CPXV0285, D7L-like protein, 7-transmembrane G protein-coupled receptor-like protein (7tGP), CrmE (CPXV0002) protein, and the NMDA receptor-like protein (NMDAr). Reprinted by permission from the American Society for Microbiology: (Journal of Virology) (119), copyright 2015.

1.5. Specific aims of the project

In this study, we aimed to identify new Orthopoxvirus virulence markers in the rodent host. The initial findings described in the previous section was the basis for this thesis, during which we focused on the new highly pathogenic CPXV isolate RatPox09. We generated BR mutants with Ratpox09 genes of interest inserted. Moreover, since, there are also minor sequence modifications of unknown impact found spread all over the genome. We also generated CPXV BR-RatPox09 chimeric viruses with large genomic segments exchanged between the two strains, so additional virulence factors can be identified.

Since it has been found that these two CPXV strains of different pathogenic potential *in vivo* show highly similar growth characteristics *in vitro*, animal experimentation seems to be the only suitable method to test the biological behavior of the recombinant viruses of both strains. Nevertheless, *in vivo* models are discouraged for many reasons, first most importantly for reasons of animal welfare but also the labor-intensive and time-consuming nature of such experiments. To reduce the need for animal experiments for testing of newly generated recombinant viruses, a second aim of the present study was to evaluate a three-dimensional (3D) skin model as a possible replacement for animal experiments. For this part of the project, we monitored lesion formation, viral gene expression and cell cycle patterns upon infection of the 3D skin cultures with CPXV BR and RatPox09.

Finally, BR mutants with NMDAr and CrmE ORFs inserted were selected for animal studies. The homologs of these two genes in VACV, VACV GAAP and VACV CrmE, were shown to influence the VACV virulence (92, 103). Moreover, the segment F chimera was as well selected for animal studies. The genomic segment F contains ATI and p4c genes, the sequence of these two genes differs between BR and Ratpox09.

2. Materials and Methods

2.1. Materials

All chemicals indicated below were used according to the instructions of the manufacturer.

2.1.1. Chemicals, consumables and equipment

2.1.1.1. Chemicals

Chemicals	Manufacturer
Acetone ((ch3) 2co)	Applichem, Darmstadt
CH_3COOH (acetic acid)	Applichem, Darmstadt
Agar (bacteriological)	Carl-Roth, Karlsruhe
Agarose- standard Roti®garose	Carl-Roth, Karlsruhe
L-(+)-Arabinose	Alfa aesar, Karlsruhe
BSA (Albumin Fraktion V), pH 7,0	Applichem, Darmstadt
Chloroform	Applichem, Darmstadt
Crystal violet	Merck, Darmstadt
DMSO (Dimethyl sulfoxide)	Merck, Darmstadt
dNTP mix	Bioline, Luckenwalde
EDTA (ethylendiamine tetraacetic acid)	Applichem, Darmstadt
Ethidium bromide 1%	Carl-roth, Karlsruhe
EtOH (ethyl alcohol) den. Absolute	Applichem, Darmstadt
FuGENE® HD	Promega, Mannheim
Glycerol	Applichem, Darmstadt
HCl 37% (hydrochloric acid)	Roth, Karlsruhe
Isopropyl alcohol (2-propanol)	Applichem, Darmstadt
KCH_3CO_2 (potassium acetate)	Applichem, Darmstadt
KH_2PO_4 (potassium dihydrogen phosphate)	Applichem, Darmstadt
KCl (potassium chloride)	Merck, Darmstadt
VECTASHIELD® Mounting Medium, with dapi	Vector laboratories inc, Burlingame
NaCl (sodium chloride)	Applichem, Darmstadt

Na_2HPO_4 (disodium phosphate)	Merck, Darmstadt
NaOH (sodium hydroxide)	Merck, Darmstadt
Phenol	Applichem, Darmstadt
SDS (sodium dodecyl sulfate)	Sigma-aldrich, St. Louis
Tris (2-Amino-2-Hydroxymethyl-1,3-Propanediol)	Applichem, Darmstadt
TRITON® X-100 detergent (Polyethylene Glycol-p-isooctylphenyl Ether)	Merck, Darmstadt
Water molecular biology grade	Applichem, Darmstadt

2.1.1.2. Consumables

Name	Feature	Manufacturer
Cell culture dishes	6-well, 24-well, 96-well	Sartsedt, Nümbrecht
Cell culture flasks	25 ml, 75 ml, 175 ml	Sartsedt, Nümbrecht
Petri dishes for cell culture	60 mm, 100 mm, 150 mm	Sartsedt, Nümbrecht
Conical test tubes	17x120 (15 ml)	Sartsedt, Nümbrecht
Conical test tubes	30x115 (50 ml), with and without feet	Sartsedt, Nümbrecht
Cryotubes	1.8 ml	Nunc, Kamstrupvej
Eppendorf tubes	1,5 and 2 ml	Sarstedt, Nümbrecht
Expendable cuvettes		Biodeal, Markkleeberg
PCR tubes		VWR International, West Chester
Pipettes	5, 10, 25 ml	Sarstedt, Nümbrecht
Pipette tips	P1000, 200, 100 and 10	VWR International, West Chester
Transfection polypropylene Tubes		TPP, Trasadingen
Microscope cover glasses		VWR, Sacramento
Parafilm M®		Bemis, Neenah
Nitrile gloves		Hansa-Medical 24, Hamburg
KIMTECH SCIENCE* Precision Wipes Tissue Wipers		Kimberly-Clark, Roswell

2.1.1.3. Equipment

Name	Feature	Manufacturer
Bacterial incubator	shaker Innova 44	New Brunswick Scientific, New Jersey
Bunsen burner, Cell incubators	Typ 1020	Usbeck, Radevormwald
Centrifuge 5424	Rotor FA-45-24-11	Eppendorf, Hamburg
Centrifuge 5804R	Rotors A-4-44 and F45-30-11	Eppendorf, Hamburg
Electroporator, GenePulser Xcell		Bio-Rad, München
Electrophoresis power supply Power Source	250 V	VWR International, West Chester
Inverted fluorescence microscope	Axiovert S 100	Zeiss, Oberkochen
Fluorescence microscope	Axiowert M1	Zeiss, Oberkochen
Freezer	-20°C	
Freezer	-80°C	GFL, Burgwedel
Galaxy mini centrifuge		VWR International, West Chester
Gel electrophoresis chamber	Big	Peqlab, Erlangen, Bio-Rad, München
Gel electrophoresis chamber	Small	VWR, Darmstadt
Ice machine	AF100	Scotsman, Vernon Hills
INTEGRA Pipetboy		IBS Integrated Biosciences, Fernwald
Inverse light Microscope	MOTIC AE20	Ehlert & Partner, Niederkassel-Rheidt
Microwave		Bosch, Stuttgar
Nanodrop spectrophoto-meter	ND-1000	Peqlab, Erlangen
Nitrogen tank	ARPEGE70	Air liquide, Düsseldorf
pH-meter		Hanna Instruments, Kehl am Rhein
Pipettes		VWR, Darmstadt
Thermocycler	Flexcycler ThermoFlex	Analytik Jena, Jena
Thermocycler	T-Gradient	Biometra, Göttingen
Thermomixer		Eppendorf, Hamburg
Transiluminator printer	P93D	Mitsubishi, Rüsselsheim
UV Transiluminator	Bio-Vision-3026	PeqLab, Erlangen
Vortex		Hartenstein, Würzburg
Water bath		Julabo, Seelbach
Water bath shaker	C76	New Brunswick Scientific, New Jersey

2.1.2. Enzymes and markers

Name	Manufacturer
*Asc*I	New England Biolabs, Ipswich
*Bam*HI	New England Biolabs, Ipswich
*Bam*HI-HF	New England Biolabs, Ipswich
*Dnp*I	New England Biolabs, Ipswich
FastAP™ Thermosensitive Alkaline Phosphatase	Thermo Fisher Scientific Inc.
*Fsc*I	New England Biolabs, Ipswich
Gene ruler 1kb plus DNA ladder	Fermentas, St. Leon-Rot
Gene ruler DNA ladder mix	Fermentas, St. Leon-Rot
*Hin*dIII	New England Biolabs, Ipswich
*Hin*dIII-HF	New England Biolabs, Ipswich
*Kpn*I	New England Biolabs, Ipswich
LongAmp® *Taq* DNA Polymerase	New England Biolabs, Ipswich
*Not*I	New England Biolabs, Ipswich
*Nru*I	New England Biolabs, Ipswich
*Pac*I	New England Biolabs, Ipswich
Phusion Hot Start High Fidelity DNA Polymerase	New England Biolabs, Ipswich
PrimeSTAR GXL DNA Polymerase	Takara, Clontech Laboratories, Inc, USA
Proteinase K	Finnzymes, Thermo Scientific, Rochester
*Pvu*II	New England Biolabs, Ipswich
*Pst*I	New England Biolabs, Ipswich
Quick-ligase	New England Biolabs, Ipswich
RNase A	Carl-Roth, Karlsruhe
*Sac*I	New England Biolabs, Ipswich
*Sbf*I	New England Biolabs, Ipswich
Solis 1 kb DNA Ladder Ready to Load	Solis BioDyne, Tartu, Estonia
*Sph*I	New England Biolabs, Ipswich
*Stu*I	New England Biolabs, Ipswich
Taq DNA-Polymerase	PeqLab, Erlangen
*Xcm*I	New England Biolabs, Ipswich
*Xma*I	New England Biolabs, Ipswich
*Xho*I	New England Biolabs, Ipswich

2.1.3. Kits

Name	Manufacturer
GF-1 AmbiClean Kit (Gel & PCR)	Vivantis, USA
Hi Yield® Small DNA Fragments Extraction Kit	Süd-Laborbedarf GmbH, Gauting

2.1.4. Buffers, media and solutions

2.1.4.1. Buffers

Buffer P1 (plasmid and BAC DNA purification)	50 mM Tris, pH 8.0 10 mM EDTA, pH 8.0
Lysis Buffer P2 (plasmid and BAC DNA purification)	0.2 N NaOH 1 % SDS
Neutralization Buffer P3 (plasmid and BAC DNA purification)	3 M KCH_3CO_2, pH 5.5
1x Phosphate saline buffer (1xPBS)	137 mM NaCL 2.7 mM KCl 10 mM Na_2HPO_4 2 mM KH_2PO_4
Lysogeny broth (LB) medium	10 g BactoTM Tryptone 5 g BactoTM Yeast Extract 10 g NaCl 15 g BactoTM Agar
1x Tris saline buffer (1xTBS), pH 7,5	50 mM Tris-Cl, pH 7.5 150 mM NaCl
1x Tris-acetate-EDTA buffer (TAE)	50 mM Tris-base 2.5 mM $Na_2EDTAx2H_2O$ 25 mM Acetic acid 99 %
0.8% Agarose Gel	80 mM Agarose 1x TAE buffer 4 µl Ethidium bromide 10 mg/ml
Blocking buffer for immunofluorescence staining	1 x TBS 5 % FCS 0.3 % Triton X-100
Virus DNA preparation Buffer I	1.5 ml 2 M NaCl 400 µl 1M Tris, pH 8.0 400 µl 0.5 M EDTA 17.7 ml ddH_2O
Virus DNA preparation Buffer II	400 µl 1 M Tris, pH 8.0 400 µl 0.5 M EDTA 1.5 ml SDS 10 % (w/v) 650 µl protein Kinase K 20 mg/ml 17.05 ml ddH_2O

2.1.4.2. Cell culture media and supplements

Cell culture media and supplements	Manufacturer
Fetal bovine serum (FCS)	GIBCO, Darmstadt
Methylcellulose (Methocel)	Sigma-Aldrich
Minimal Essential Medium (MEM)	Biochrom AG, Berlin
OptiMEM	GIBCO, Darmstadt
Trypsin	Biochrom AG, Berlin

2.1.5. Antibiotics

Antibiotics	Working concentration	Manufacturer
Ampicillin	100 µg/m diluted in ddH2O	Roth, Karlsruhe
Chloramphenicol	30 µg/ml diluted in 96% EtOH	Roth, Karlsruhe
Kanamycin	50 µg/ml diluted in ddH2O	Roth, Karlsruhe
Penicillin	100 U/ml diluted in MEM	Applichem, Darmstadt
Streptomycin	100 U/ml diluted in MEM	Applichem, Darmstadt

2.1.6. Antibodies

2.1.6.1. Primary antibodies

Name	Dilution	Manufacturer
Mouse monoclonal anti-human cyclin E	1:100	Biosciences, USA
Polyclonal rabbit anti human cyclin B1	1:100	Abcam, UK
Monoclonal rabbit anti-human cycline D1	1:100	Abcam, UK
Polyclonal rabbit anti-human histone H3 phospho S10	1:400	Abcam, UK
Monoclonal mouse anti-vaccinia A27 antibody	1:1000	provided by Dr. Andreas Nitsche, RKI, Germany

2.1.6.2. Secondary antibodies

Name	Dilution	Manufacturer
Alexa Fluor 647 goat anti-mouse IgG	1:1000	Invitrogen Life Technologies, Grand Island
Alexa Fluor488 goat anti-rabbit IgG	1:1000	Invitrogen Life Technologies, Grand Island

2.1.7. Bacteria, cells and viruses

2.1.7.1. Bacteria

Name	Features	Manufacturer/References
DH10B	FendA1 recA1 galE15 galK16 nupG rpsL ΔlacX74 Φ80lacZΔM15 araD139 Δ(ara,leu)7697 mcrA Δ(mrr-hsdRMSmcrBC) λ	Invitrogen
GS1783	DH10B λcI857 Δ(cro-bioA)<>araC-PBAD, I-SceI	(140)
Top 10	F- mcrA Δ(mrr-hsdRMS-mcrBC) φ80lacZΔM15 ΔlacX74 nupG recA1 araD139 Δ(ara-leu)7697 galE15 galK16 rpsL(StrR) endA1 λ -	Invitrogen

2.1.7.2. Cells

Name	Features	Source/References
CECs/CEFs	Chicken embryo fibroblasts/cells, VALO SPF Strain	Primary cells
Vero 96	African green monkey cells	Friedrich-Löfflers-Institut, Greifswald-Insel Riems, Germany

2.1.7.3. Organotypic epithelial raft cultures

Name	Features	Source
Phenion®FT	full-thickness skin model	Henkel AG & Co. KGaA, Düsseldorf, Germany

2.1.7.4. Viruses

Name	Features	Source/Reference
VACV WR		GQ923132, provided by Andreas Nitsche, RKI, Germany
CPXV BR		AF428758, provided by Dr. Philippa Beard, University of Edinburgh, UK
CPXV RatPox09		LN864565, (158)
CPXV BR_RatPox09_sB	reconstituted from pBRF_dsB and RatPox09_sB	This thesis

CPXV BR_RatPox09_sC	reconstituted from pBRF_dsC and RatPox09_sC	This thesis
CPXV BR_RatPox09_sB_C	reconstituted from pBRF_dsB_C and RatPox09_sB and RatPox09_sC	This thesis
CPXV BR_RatPox09_sD	reconstituted from pBRF_dsD and RatPox09_sD	This thesis
CPXV BR_RatPox09_sE	reconstituted from pBRF_dsE and RatPox09_sE	This thesis
CPXV BR_RatPox09_sF	reconstituted from pBRF_dsF and RatPox09_sF	This thesis
CPXV BR_RatPox09_sD_E_F	reconstituted from pBRF_dsD_E_F and RatPox09_sD, RatPox09_sE and RatPox09_sF	This thesis
CPXV BR_RatPox09_Ati_p4C	reconstituted from pBRF_RatPox09_Ati_p4C	This thesis
CPXV BR_RatPox09_D7L	reconstituted from pBRF_RatPox09:D7L	This thesis
CPXV BR_RatPox09_CrmE	reconstituted from pBRF_RatPox09_CrmE	This thesis
CPXV BR_RatPox09_NMDAr	reconstituted from pBRF_RatPox09_NMDAr	This thesis
CPXV BR_RatPox09_7tGp	reconstituted from pBRF_RatPox09_7tGp	This thesis
CPXV BR_RatPox09_D7L_CrmE_NMDAR_7tGp	reconstituted from pBRF_RatPox09_D7L_CrmE_NMDAR_7tGp	This thesis

2.1.8. Bacterial artificial chromosomes (BACs), plasmids and primers

2.1.8.1. BACs

Name	Features	Source/Reference
pBRF	Created from CPXV strain BR	(157)
pRatPox09Fapr22	Partial BAC of virulent strain RatPox09 with genome segments B and C	Xu Zhiyong, unpublished
pRatPox09Fdec3	Partial BAC of virulent strain RatPox09 with genome segments D, E and F	Xu Zhiyong, unpublished
pRatPox09FsB_dI	First removal of unnecessary sequence for RatPox09 segment B	This thesis
pRatPox09FsB_dII	Second removal of unnecessary sequence for RatPox09 segment B	This thesis
pRatPox09FsC_dI	First removal of unnecessary sequence for RatPox09 segment C	This thesis
pRatPox09FsC_dII	Second removal of unnecessary sequence for RatPox09 segment C	This thesis
pRatPox09FsD_dI	First removal of unnecessary sequence for RatPox09 segment D	This thesis

pRatPox09FsD_dII	Second removal of unnecessary sequence for RatPox09 segment D	This thesis
pRatPox09FsE_dI	First removal of unnecessary sequence for RatPox09 segment E	This thesis
pRatPox09FsE_dII	Second removal of unnecessary sequence for RatPox09 segment E	This thesis
pRatPox09FsF_dI	First removal of unnecessary sequence for RatPox09 segment F	This thesis
pRatPox09FsF_dII	Second removal of unnecessary sequence for RatPox09 segment F	This thesis
pBRF_dsB	Deletion of genome segment B	This thesis
pBRF_dsC	Deletion of genome segment C	This thesis
pBRF_dsB_C	Deletion of genome segment B and C	This thesis
pBRF_dsD	Deletion of genome segment D	This thesis
pBRF_dsE	Deletion of genome segment E	This thesis
pBRF_dsF	Deletion of genome segment F	This thesis
pBRF_dsD_E_F	Deletion of genome segment D, E and F	This thesis
pBRF_dATI_p4C	Deletion of ATI and p4C	
pBRF_RatPox09_Ati_p4C	Insertion of RatPox09 ATI and p4C	This thesis
pBRF_RatPox09_D7L	Insertion of RatPox09 D7L	This thesis
pBRF_RatPox09_CrmE	Insertion of RatPox09 CrmE	This thesis
pBRF_RatPox09_NMDAr	Insertion of RatPox09 NMDAr	This thesis
pBRF_RatPox09_7tGp	Insertion of RatPox09 7tGp	This thesis
pBRF_RatPox09_D7L_CrmE	Insertion of RatPox09 D7L and CrmE	This thesis
pBRF_RatPox09_D7L_CrmE_NMDAr	Insertion of RatPox09 D7L, CrmE and NMDAr	This thesis
pBRF_RatPox09_D7L_CrmE_NMDAr_7tGp	Insertion of RatPox09 D7L, CrmE, NMDAr and 7tGp	This thesis

2.1.8.2. Plasmids

Name	Features	References/Source
pepkanS2	Mammalian expression vector; T7prom, f1 ori, SV40 ori, SV40 pr, KanR, I-Sce-I restricion site, AmpR, ColE1 ori, NeoR	(162, 163)
pepkanS2_RatPox09_D7L	Insertion of RatPox09 D7L into *Kpn*I and *Bam*HI unique restriction sites	This thesis
pepkanS2_RatPox09_CrmE	Insertion of RatPox09 CrmE into *Kpn*I and *Bam*HI unique restriction sites	This thesis
pepkanS2_RatPox09_NMDAr	Insertion of RatPox09 NMDAr into *Kpn*I and *Bam*HI unique restriction sites	This thesis
pepkanS2_RatPox09_TK	Insertion of RatPox09 TK into *Kpn*I unique restriction site	This thesis

pCRII_CPXV TK	pCRII plasmid with insertion of CPXV BR TK .	(135)
puC19	*E.coli* cloning vector; AmpR, ColE1 ori	New England Biolabs
puc19_RatPox09_ATI_p4C	Insertion of RatPox09 ATI p4C into unique *Sbf*I and *Hind*III restriction sites	This thesis
puc19_RatPox09_ATI_p4C_kana	aphAI and Sce-I insertion into unique *Sbf*I restriction site	This thesis
puC19_RatPox09_7tGp	Insertion of RatPox09 7tGp into unique *Pst*I and *Sac*I unique restriction sites	This thesis
puC19_RatPox09_7tGp_kana	*aphAI* and I-*Sce*-I insertion into unique *Pst*I restriction site	This thesis

2.1.8.3. Primers

Primers for this study were designed by using Vector NTI 9.1 software from Invitrogen

2.1.8.3.1. Primers used for two-step Red mediated recombination

Number	Name	Sequence (5′–3′)
NT1	RatPox09_sB_d1fw	TATTTAGGTGACACTATAGAATACTCAAGCTTGGCCGGCCGGCGCGCCCATCCAATTTTAGAAATTGGGCCAGTGTTACAACCAATTAACC
NT2	RatPox09_sB_d1rv	GAAGAGATATGTAACACAGACCAATTTCTAAAATTGGATGGGCGCGCCGGCCGGCCAAGCTTGAGTATTAGGGATAACAGGGTAATCGATTT
NT3	RatPox09_sB_d2fw	TAATTAGATATAGAGAATATGATCCGTAACATATACAACTGGCGCGCCCCGGCCCTCGAGGCCGGCAATAGGGATAACAGGGTAATCGATTT
NT4	RatPox09_sB_d2rv	ATGAATTCCCAGATCCGGCCTTGCCGGCCTCGAGGGCCGGGGCGCGCCAGTTGTATATGTTACGGATCGCCAGTGTTACAACCAATTAACC
NT5	RatPox09_sC_d1fw	TATTTAGGTGACACTATAGAATACTCAAGCTTGGCCGGCCGGCGCGCCTCTATGCTATAAATGAATTCGCCAGTGTTACAACCAATTAACC
NT6	RatPox09_sC_d1rv	TATGAGCAGATGCAAAATGAGAATTCATTTATAGCATAGAGGCGCGCCGGCCGGCCAAGCTTGAGTATTAGGGATAACAGGGTAATCGATTT
NT7	RatPox09_sC_dI1fw	TACGGAACGGGACTATGGACGCATGATAAGAATAATTTTGGGCGCGCCCCGGCCCTCGAGGCCGGCAATAGGGATAACAGGGTAATCGATTT
NT8	RatPox09_sC_dI1rv	ATGAATTCCCAGATCCGGCCTTGCCGGCCTCGAGGGCCGGGGCGCGCCCAAAATTATTCTTATCATGCGCCAGTGTTACAACCAATTAACC
NT9	RatPox09_sD_d1fw	TCGAAATCATCGACATGGCTTCTTCCATAGTTAGAAGATCGGCGCGCCCCGGCCCTCGAGGCCGGCAATAGGGATAACAGGGTAATCGATTT

NT10	RatPox09_sD_d1rv	ATGAATTCCCAGATCCGGCCTTGCCGGCCTCGAGGGCCGGGGCGCGCCGATCTTCTAACTATGGAAGAGCCAGTGTTACAACCAATTAACC
NT11	RatPox09_sE_d1fw	GAAAGTGTTACATCGACTCATAATATTATATATTTTTATCGATATTTGATTTTTTTCCATGCCAGTGTTACAACCAATTAACC
NT12	RatPox09_sE_d1rv	TTTCGGAACTCTTGGATATCATGGAAAAAAATCAAATATCGATAAAAATATATAATATTATAGGGATAACAGGGTAATCGATTT
NT13	RatPox09_sE_d2fw	TATTTAGGTGACACTATAGAATACTCAAGCTTGGCCGGCCGGCGCGCCGAATACCAAGTGCTTAAATAGCCAGTGTTACAACCAATTAACC
NT14	RatPox09_sE_d2rv	GATTAATGAAGTAGTAGAAATATTTAAGCACTTGGTATTCGGCGCGCCGGCCGGCCAAGCTTGAGTATTAGGGATAACAGGGTAATCGATTT
NT15	RatPox09_sF_d1fw	GAATCACGTGTTCAACAATGGGTGATAGATACACTTAATGGGCGCGCCCCGGCCCTCGAGGCCGGCAATAGGGATAACAGGGTAATCGATTT
NT16	RatPox09_sF_d1rv	ATGAATTCCCAGATCCGGCCTTGCCGGCCTCGAGGGCCGGGGCGCGCCCATTAAGTGTATCTATCACCGCCAGTGTTACAACCAATTAACC
NT17	RatPox09_sF_d2fw	TATTTAGGTGACACTATAGAATACTCAAGCTTGGCCGGCCGGCGCGCCATCTGATGAGTATCTGAGCAGCCAGTGTTACAACCAATTAACC
NT18	RatPox09_sF_d2rv	AATGTTGGACCTGACTGTAGTGCTCAGATACTCATCAGATGGCGCGCCGGCCGGCCAAGCTTGAGTATTAGGGATAACAGGGTAATCGATTT
NT19	BRF_dsB_Cfw	CTATCAACTGATATCCGCTATTGCAAGAGTACGTTATACTGATGAAGGCCGGCCCTCGAGTAGGGATAACAGGGTAATCGATTT
NT20	BRF_dsB_Crv	CCAGATCCGGCCTTGCCGGCCTCGAGGGCCGGCCTTCATCAGTATAACGTACTCTTGCAAGCCAGTGTTACAACCAATTAACC
NT21	BRF_dsD_E_Ffw	GTAGAAAGTGTTACATCGACTCATAATATTATATATTTTTATCAAATACATTCGATGGTCTATGCCAGTGTTACAACCAATTAACC
NT22	BRF_dsD_E_Frv	TATAACACATAATAATCTGGTAGATAGACCATCGAATGTATTTGATAAAAATATATAATATTATAGGGATAACAGGGTAATCGATTT
NT23	BRF_dsBfw	CTATCAACTGATATCCGCTATTGCAAGAGTACGTTATACTCTTTCATATTTAGAATATATTAGGGATAACAGGGTAATCGATTT
NT24	BRF_dsBrv	TCTACTATATTTTTACATACATATATTCTAAATATGAAAGAGTATAACGTACTCTTGCAAGCCAGTGTTACAACCAATTAACC
NT25	BRF_dsCfw	ATACAGAATTTGTAACACTCTCGAAATCACACGATGTGTCGGCGATGAAGGCCGGCCCTCGAGTAGGGATAACAGGGTAATCGATTT
NT26	BRF_dsCrv	TTCCCAGATCCGGCCTTGCCGGCCTCGAGGGCCGGCCTTCATCGCCGACACATCGTGTGATTTGCCAGTGTTACAACCAATTAACC

NT27	BRF_dsDfw	GAAAGTGTTACATCGACTCATAATATTATATATTT TTATCGATATTTGATTTTTTTCCATGCCAGTGTTAC AACCAATTAACC
NT28	BRF_dsDrv	TTTCGGAACTCTTGGATATCATGGAAAAAAATCAA ATATCGATAAAAATATATAATATTATAGGGATAA CAGGGTAATCGATTT
NT29	BRF_dsEfw	CATAGTAGTTAGATTATCAGCGCATGCAGAAGAA CACCGCAAGACGATCGAACTCCATAAGCCAGTGT TACAACCAATTAACC
NT30	BRF_dsErv	AATCAAATCTTTGGAGAAGTTTATGGAGTTCGATC GTCTTGCGGTGTTCTTCTGCATGCGTAGGGATAAC AGGGTAATCGATTT
NT31	BRF_dsFfw	AACTATAGACCGTTACATTTCCAATATGTATCGTA TTCTAATTAAATACATTCGATGGTCTATGCCAGTG TTACAACCAATTAACC
NT32	BRF_dsFrv	TATAACACATAATAATCTGGTAGATAGACCATCG AATGTATTTAATTAGAATACGATACATATTAGGGA TAACAGGGTAATCGATTT
NT33	BRF_D7Lfw	TACATCATATACTATGATACCGTATCAGTTCCTAT CAATCTCTGTTTTGGGTG
NT34	BRF_D7Lrv	TATTTACATAGGATGTGATATTGACCACTCACTAC AGTCTATGAAAAGCGTCCAAACACAGACCCATGA ATGAGCCAGTGTTACAACCAATTAACC
NT35	BRF_CrmEfw	CGCTTATCATACTAGTTATATACTAAATGTTGATC ATATTCCACCAAATGATTGTGAAAGAG
NT36	BRF_CrmErv	CTTGGTTTCCAAATAGCTTAAGAAGGCATTTACGT ATGACCCATCCAGTAGATGCGAGTAAGTCTTATCT TGTCATTGGTGCCAGTGTTACAACCAATTAACC
NT37	BRF_NMDArfw	GATTAAATCGTCTAACAAACAATTAGTTTTTATGA CATTACTTACTCGCATCTACTGGATGGACATAAAT ATCCTCCTCGGCCAGTGTGATGGATATCTAGG
NT38	BRF_NMDArrv	TTCGTCATCGTTAAGTCAATAATGATTAATTTATA TATGTTTATTTCTTATTAGATACTTCCAAAAGCTGC AACAGATGCAAGAAC
NT39	BRF_7tGpfw	ATCGAATGACGTCATGACCGTGCTTAGCATGCTTG ACTAAATATTCTGGACAAATTCTAAATATTTTTTA TAAAAATTAAAAAATCACTTTCATTATCGATGACT CG
NT40	BRF_7tGprv	GGTAACCAGCGTATAATAGACGGTTTTATTTCATT TTTTTATACGGCATTAATAAAATTACTACGGTTAG TAGCAATAAAAACGCCAGTGTTACAACCAATTAA CC
NT41	BRF_dATIp4Cfw	AAACCATTAGATAAAGTTGATCTCAAACCGTCTTT TCTGGTTTAAACGCAGTAATGCTCGTAGGGATAAC AGGGTAATCGATTT
NT42	BRF_dATIp4Crv	GGTTCAAGATGTTAATGTTGCGAGCATTACTGCGT TTAAACCAGAAAAGACGGTTTGAGAGCCAGTGTT ACAACCAATTAACC
NT43	BRF_ATIp4Cfw	AAGACCTCCTTCGTTTTATAAACCATTAGATAAAG TTGATCTCAAACCGTCTTTTCTGGTGTAATATTGTT TAGTAGATATAGGGATAACAGGGTAATCGATTT

NT44	BRF_ATIp4Crv	AATTTATGGAACGGAATTGTACCAACGGTTCAAG ATGTTAATGTTGCGAGCATTACTGCG
NT45	BRF_D7L_CrmE_NMDAr_fw	ACCAATGACAAGATAAGACTTACTCGCATCTACTG GATGGACATAAATATCCTCCTCGCCAGTGTGATGG ATATCTAGGGAT
NT46	BRF_D7L_CrmE_NMDAr_rv	CTTGGTTTCCAAATAGCTTAAGAAGGCATTTACGT ATGACTTTCTTATTAGATACTTCCAAAAGCTGCAA CAGATGCAAGAAC

Table 2. Primers used for two-step Red mediated recombination. I-*Sce*I restriction sites are underlined.

2.1.8.3.2. Transfer plasmid generation primers

Number	Name	Sequence (5′–3′)
NT47	puC19_ATIp4Cfw	GCGCCTGCAGGCTCAAACCGTCTTTTCTGGT GT (*Sbf*I)
NT48	puC19_ATIp4Crv	CCCAAGCTTATGTTGCGAGCATTACTGCG (*Hin*dIII)
NT49	puC19_ATIp4C_kanafw	CGCCCTGCAGGTAGGGATAACAGGGTAATC GATTT (*Sbf*I)
NT50	puC19_ATIp4C_kanarv	CGCCCTGCAGGGCCAGTGTTACAACCAATT AACC (*Sbf*I)
NT51	puC19_7tGpfw	CGCGAGCTCACCGTGCTTAGCATGCTAGA (*Sac*I)
NT52	puC19_7tGprv	TGCCTGCAGCGGCATTAATAAAATTACTAC GG (*Pst*I)
NT53	puC19_7tGp_kanafw	GCGCTGCAGTAGGGATAACAGGGTAATCGA TTT (*Pst*I)
NT54	puC19_7tGp_kanarv	TGCCTGCAGGCCAGTGTTACAACCAATTAA CC (PstI)
NT55	pepkanS2_D7Lfw	TCTGGTACCCCTATCAATCTCTGTTTTGGGT G (*Kpn*I)
NT56	pepkanS2_D7Lrv	TATGGATCCCACTACAGTCTATGAAAAGCG TCC (*Bam*HI)
NT57	pepkanS2_CrmEfw	CGCGGTACCCCACCAAATGATTGTGAAAGA G (*Kpn*I)
NT58	pepkanS2_CrmErv	GGATCCCCATCCAGTAGATGCGAGTAAGTC GCG (*Bam*HI)
NT59	pepkanS2_NMDArfw	CGGGGTACCAGCTGCAACAGATGCAAGAAC (*Kpn*I)
NT60	pepkaS2_NMDArrv	GCGGATCCCTTACTCGCATCTACTGGATGG A (*Bam*HI)
NT61	pepkanS2_TKfw	CGGGGTACCCCTTCTCGTAGGCACACAATC T (*Kpn*I)
NT62	pepkanS2_TKrv	CGGGGTACCAGCTGTCCGCTATCTGAATCA G (*Kpn*I)

Table 3. Primers used for transfer plasmid generation. Enzyme cleavage sites used for cloning are indicated in brackets and underlined in the sequence of the primer.

2.1.8.3.3. Construct confirmation sequencing primers

Name	Name	Sequence (5′–3′)
NT63	RatPox09_seq1	AATCACACGATGTGTCGGC
NT64	RatPox09_seq2	GAGCAAGACGTTTCCCGTT
NT65	RatPox09_seq3	GCTATGACCATGATTACGCCA
NT66	RatPox09_seq4	CGTCATAACTATGGATCCCCAC
NT67	RatPox09_seq5	TGGTGATACGGAACCACTCA
NT68	RatPox09_seq6	CCGTAATCACCTACAGGTAGCT
NT69	RatPox09_seq7	CAGGCTAGATCAACTGCGTT
NT70	RatPox09_seq8	TATAGCTCTCGCCTGAAGAGTATG
NT71	RatPox09_seq9	AGAATAGTCGCGATGCTGCT
NT72	RatPox09_seq10	CTCCATTGCAGAGGACGTCAT
NT73	RatPox09_seq11	CGCTATTAGTGCCAAAGTGG
NT74	RatPox09_seq12	CTACTACAGGCGGAACATCAA
NT75	RatPox09_seq13	ACACGGCACTTCGAAATGG
NT76	RatPox09_seq14	ACCCGCTAGACAAGTATCCG
NT77	RatPox09_seq15	CAGCCTGGGATAATGATAAGTTGG
NT78	RatPox09_seqE3Lfw	CGCTCTACGAATATCTGTGACAGA
NT79	RatPox09_seqE3Lrv	CCAGAATCTCCAGAACCAGCAT
NT80	BRF_D7L_seq1	AATACGCGATTCCGATAGCAGT
NT81	BRF_D7L_seq2	TATATCTTGGGCCATGCAACAG
NT82	BRF_D7L_seq3	TATCTCTTCCGACCATCAAGCAT
NT83	BRF_CrmE_seqfw	GTGTCTGTGCATCCGGATACT
NT84	BRF_CrmE_seqrv	ACATGGATCATCAGAGGGAG
NT85	BRF_NMDAr_seq1	GGACATTGTCCGAGTGACACA
NT86	BRF_NMDAr_seq2	CGGACAATGTCCACAAAATGG
NT87	BRF_NMDAr_seq3	ATGTCATCCACGGTGTTCAGG
NT88	BRF_7tGp_seq1	TATAATAGATGAGTGCGTGGCG
NT89	BRF_7tGp_seq2	ATAACATCTTCTAACGCTGCCG
NT90	BRF_7tGp_seq3	TATTCTGTAAGGCATTCCAACGG
NT91	BRF_7tGp_seq4	TATGAGGGTGATGAGCGACAATAT
NT92	BRF_7tGp_seq5	TATCGTATCGGAGTACGGAGATCA
NT93	BRF_7tGp_seq6	ATACTGTTTCTGGTCGGAAGCTAT
NT94	BRF_7tGp_seq7	ACCGTGATGGCTATTACGCGAGAT
NT95	BRF_7tGp_seq8	ATAGGATATTCTCTGGTACACCGG
NT96	BRF_7tGp_seq9	TCTCTGACAGCCGCTATCTGTAAAC
NT99	BRF_7tGp_seq10	ACCCTGTTAAGAAGGCTACGGCAAT
NT100	BRF_ATIp4C_seq1	GTTACCACGTCTACACTCGGC
NT101	BRF_ATIp4C_seq2	TCCCATTCGACATTACGACG
NT102	BRF_ATIp4C_seq3	GGATAGCGAATACCTCATCGTC
NT103	BRF_ATIp4C_seq4	AGGGAACGAGAAATGCGTTC
NT104	BRF_ATIp4C_seq5	ATCTATCGCATGTGGATGGA
NT105	BRF_ATIp4C_seq6	CTCGAACGACAACTAGCAGC
NT106	BRF_seq1	CCGTAAACGCCGTCTTTATC
NT108	pBRF_67_seq	CTAGATTGGCATCCTATGGACTATA
NT109	miniF_seq1	GGTAACATAATACCCTTTTCCTGAA
NT110	BRF_seq2	CGATAATAGATACGGAACGGGAC
NT111	BRF_135_seq	TCAATGGATTCAGACGATGGTT
NT112	BRF_seq3	AGATGCGACAGATCCATGTCA

NT113	BRF_157_seq	CTCGCCTGTCATGTCTGGTAA
NT114	BRF_193_seqfw	TGAATATTGCGACGACATACG
NT115	BRF_193_seqrv	GGCTCCTTATACCAAGCACTC
NT116	BRF_seq4	AATGAGATACGGTAGACATCCTTCT

Table 4. Primers used for sequencing.

2.2. Methods

2.2.1. Cell culture.

2.2.1.1. Maintenance of cells

VERO cells were grown and maintained in growth medium MEM enhanced with 5% fetal calf serum (FCS), 100 U/ml penicillin and 0.1 mg/ml streptomycin and kept at 37°C under a 5% CO_2 atmosphere. Confluent cells were detached with the help of 10 min incubation with 0.25% trypsin EDTA at 37 °C with 5 % CO_2 atmosphere and then resuspended in the appropriate medium. Subsequently, cells were cultivated in 1:10 ratio.

Chicken embryo cells (CECs) were prepared fresh weekly from 10-days old specific-pathogen-free (SPF) VALO embryos by a standard protocol (161).

2.2.1.2. Cryoconservation

For long storing of eukaryotic cells, used in this study, the cell medium was discarded and the cells were washed with PBS. Next, 0.25% trypsin EDTA was added and the cells were kept at 37 °C with 5 % CO_2 atmosphere. When the cells detached, they were resuspended in 1.5 ml MEM and 3 ml of cryoconservation medium (MEM supplemented with 25% FCS and 20% DMSO) was added. Consequentially, cells were divided into the appropriate number of cryovials and frozen at -70°C in cryoconservation containers filled with isopropanol. Finally, frozen eukoryotic cells were stored at -196°C in liquid nitrogen.

For use of the frozen eukaryotic cell stock, cryovials were thawed in the 37°C water bath. In order to remove DMSO, cells were centrifuged for 10 minutes at 1,200 rpm at room temperature (RT). The pellet was resuspended in growth medium and the cells were transferred to cell culture flasks.

2.2.1.3. Transfection of VERO cells and CEF's

For transfection of Vero cells or CEF's, cells were seeded in 6-well plates (1×10^6 cells per well). 1 µg of plasmid DNA was diluted in 100 µl Optimem and briefly mixed. Next, 5 µl of FuGENE® HD transfection reagent was added to the DNA solution, following 10 – 15 s vortexing and 15 min incubation at room temperature. Eventually, the samples were added to the cells in a dropwise manner.

2.2.1.4. Organotypic epithelial raft cultures

The Phenion® full-thickness skin model (Phenion®FT) consists of a multilayered epidermis and a dermis sections. As it is stated by the provider (Henkel AG & Co. KGaA), the epidermis is generated from male neonatal foreskin keratinocyte stem cells and the dermis contains fibroblast. Both cell types used for tissue engineering are derived from a single human donor

and embedded in a bovine collagen matrix. For our study Phenion®FT was obtained at the age of 14 days at air–liquid interphase (Ø 1.32 cm; surface area 1.30 cm^2). According to the instructions of the supplier, fresh, pre-warmed medium was added and the tissue was kept at 37°C under 5% CO_2 overnight.

2.2.2. Virological methods

2.2.2.1. Virus reconstitution

To generate infectious virus particles, from BAC mutant stocks, virus reconstitution in vertebrae cells were used. VERO cells or CEFs were transfected with BAC DNA prep as described in section 2.2.1.3. (Transfection of VERO cells and CEF's). Moreover, chimeric viruses were generated as foll ows: 2 µl pBRF deletion mutant DNA prep was transfected simultaneously with 2 µl RatPox09 segments of interest DNA prep. Since BAC DNA, used in this study, encodes GFP under a late promoter, infected cells and formed plaques could be detected with the help of fluorescence microscopy. Since CPXV DNA is not infectious on its own, usage of helper virus for CPXV reconstitution is a widespread practice. Helper viruses like Shope fibroma virus in the case of CPXV reconstitution in CEF's or Fowlpox virus when CPXV is reconstituted in Vero cells, are indispensable for the efficient start of the gene transcription. Thenceforth, helper virus was added to cells 1 h post transfection and successful replication was observed with the help of fluorescence microscope 48 hours post transfection. Newly reconstituted virus was than passaged no less than four times to remove the helper virus.

2.2.2.2. Recovery of thymidine kinase (TK) gene and plaque purification

Since pBRF harbors mini-F sequence in TK gene, removal of mini-F sequence and recovery off full length TK gene were necessary. Therefore, foreign sequence in the newly generated mutants were removed by transfection of plasmid DNA harboring the full sequence of TK gene into cells as descripted previously in section 2.2.1.3. (Transfection of VERO cells and CEF's). 2 hours post transfection the cells were infected with a multiplicity of infection (MOI) of 0.01 of the mutant virus stock. The multiplicity of infection defines the ratio between virus particle and cell count. When MOI of 2 is chosen for an experiment, 2 infectious virus units per cell are used to infect cell monolayer. 48 pi infected cells were observed by fluorescence microscopy. CPXV infected cells that showed no GFP expression, were picked and passaged repeatedly. Successful TK gene recovery and elimination of mini-F sequence was confirmed by PCR and sequencing.

2.2.2.3. Virus stock preparation

Since the amount of cell free virus in the medium of infected cell culture is rather small, it is necessary to disrupt the cell membranes mechanically, so applicable virus stocks in high titers would be prepared. To achieve this goal, confluent cell monolayers were infected with the CPXV of interest. The virus infection rate was observed by fluorescence microscope and the percentage of the cells, that are expressing GFP, were evaluated. Once infection rates reached 70 % to 90 %, the cells were frozen and thawed three times. Thenceforth, thawed cells were transferred to centrifuge flasks containing glass beads and the solution was vortexed for 90 seconds so the disruption of the cell membranes would be achieved. Then, the glass beads and cell debris were centrifugated for 10 min at 3000 x g speed. After centrifugation step, the supernatant was aliquoted in 1.5 ml reaction tubes. These tubes with newly made virus stocks were kept at -70 °C.

2.2.2.4. Virus DNA preparation

To isolate viral DNA, infected cells and supernatant were collected by scraping, 48 h pi. The cells were transferred to ependorf tubes and centrifuged for 10 min, with the 20000 x g speed. Afterwards PBS was added to the cell pellet, and the suspension was centrifuged for another 10 min. Subsequently PBS was discarded and the pellet resuspended in 50 µl virus DNA isolation buffer I. Then, the proteinase K holding buffer II was added (250 µl) followed by 4 to 5 h incubation at 55 °C. Later 300 µl supersaturated NaCl (6M) was added and the tube was inverted several times. To precipitate the DNA 900 µl isopropanol was included. Subsequently the tube was inverted for 7 times and the suspension centrifuged 10 min at 20000 x g. Finally, the precipitated DNA was washed with 70 % ethanol, dried and dissolved in 50 µl of molecular water.

2.2.2.5. 3D Skin Model infection and immunohistochemistry

For the infection of The Phenion® full-thickness skin model 10^5 $TCID_{50}$ of CPXV was used. Infected cultures were incubated for 7 days at 37°C and lesion development was monitored macroscopically. Sliced Phenion® full-thickness model was fixed at 10% neutral buffered formalin, embedded in paraffin wax and used for histological analysis. Sections (2 µm) were mounted on adhesive glass slides and stained with haematoxylin and eosin (HE). Afterwards, expression of the CPXV and cell proteins was analysed using immunohistochemical labelling. For each treatment group, six slides were examined. Endogenous peroxidase was blocked with H_2O_2 3% in phosphate buffered saline (PBS, 0.1M, pH 7.4) for 20 min. For detection of cyclin B1, cyclin D1, cyclin E and histone H3 Phospho S10, antigen retrieval was performed by heating in citrate buffer (pH 6.0) for 12 min. Meanwhile, monoclonal mouse anti-vaccinia A27 antibody required no antigen retrieval. To block non-specific antibody binding, slides were incubated for 30 min with Roti-Immunoblock® (Roth, Karlsruhe, Germany) and normal goat serum. Thenceforth, sections were incubated overnight at 4°C with the primary antibody and afterwards secondary antibodies were applied. In each experiment, the slides that were incubated with irrelevant commercial mouse or rabbit immunoglobulins instead of primary antibodies were used as negative controls.

2.2.2.6. Virus growth kinetics

Overnight cultures of Vero cells were infected with BAC derived CPXV BR, wtCPXV RatPox09, wtCPXV BR and mutant viruses using MOIs of 0.01 or 3. After 1 h incubation at 37°C, the medium was removed and the cells were washed three times with PBS. Next, 1 ml of DMEM was added to each well. The samples for virus growth kinetics were attained at six time points after infection (0 h, 6 h, 12 h, 24 h, 48 h and 72 h). The infection of the cells was accomplished in duplicates for each dilution step. Endpoint dilution was used to determine virus titers. The virus titers were calculated as $TCID_{50}$ per milliliter.

2.2.3. Molecular biology techniques

2.2.3.1. Modified alkaline lysis at small scale - BAC DNA preparation

Bacterial cultures were grown in 5 ml of LB media with appropriate antibiotics overnight in an incubator shaker at 32 °C, 220 rpm. The cell pellet in 300 µl of plasmid or BAC DNA were resuspended in DNA purification buffer P1. Thenceforth, the culture was centrifuged at 4500 x g speed for 5 min and the supernatant was removed. Next, the cells were lysed by adding 300 µl of buffer P2 and precipitated by adding 300 µl of the neutralizing buffer P3 and then

incubated for 5 min on ice. Samples were centrifuged at 20000 x g speed for 5 min resulting in removal of cellular debris. Afterwards, the supernatant was relocated to a 2 ml ependorf tube and 900 µl isopropanol was added. Then, this tube was inverted few times and centrifuged for 15 min at 20000 x g speed. Then, the DNA pellet was washed with 70% ethanol and dried afterwards. Later 30 µl of TE buffer containing RNase A (40 µg/ml) was added to the tube containing the pallet. Finally, the prepared BAC DNA preps were stored at 4 °C until further use.

2.2.3.2. Polymerase Chain Reaction (PCR)

For amplification of different DNA fragments, standard and modified PCR reactions were used.

For simple fragment amplification, Taq DNA polymerase was used with standard conditions. Reaction setup:

Component	50 µl reactions	Final concentration
10X Standard *Taq* Reaction Buffer	5 µl	1X
10 mM dNTPs	1 µl	200 µM
10 µM Forward Primer	1 µl	0.2 µM
10 µM Reverse Primer	1 µl	0.2 µM
Template DANN	variable	<1,000 ng
Taq DNA Polymerase	0.25 µl	1.25 units/50 µl PCR
Nuclease-free water	to 50 µl	

Thermocycling condition:

Step	Temp	Time
Initial Denaturation	95°C	30 seconds
30 Cycles	95°C 45-68°C 68°C	30 seconds 30 seconds 1 minute/kb
Final Extension	68°C	5 minutes
Hold	4°C	

For amplification of PCR products with long extensions for Red recombination Longamp *Taq* polymerase was used. Reaction setup:

Component	50 µl reaction	Final Concentration
5X Standard Longamp *Taq* Reaction Buffer	10 µl	1X
10 mM dNTPs	1,5 µl	300 µM
10 µM Forward Primer	2 µl	0.4 µM
10 µM Reverse Primer	2 µl	0.4 µM
Template DNA	variable	<1,000 ng
Longamp *Taq* DNA Polymerase	2 µl	5 units/50 µl PCR
Nuclease-free water	to 50 µl	

Thermocycling condition:

Step	Temp	Time
10 Cycles	98°C 55-60°C 68°C	10 seconds 15 seconds 1 minute/kb
20 Cycles	98°C 65-68°C 68°C	10 seconds 15 seconds 1 minute/kb
Hold	4°C	

For amplification of long PCR products (3-7 kb) with long extensions for Red recombination PrimeSTAR GXL polymerase was used. Reaction setup:

Component	50 µl reaction	Final Concentration
5X PrimeSTAR GXL Buffer	10 µl	1X
10 mM dNTPs	4 µl	800 µM
10 µM Forward Primer	1 µl	0.2 µM
10 µM Reverse Primer	1 µl	0.2 µM
Template DNA	variable	<1,000 ng
PrimeSTAR GXL DNA Polymerase	1 µl	1.25 units/50 µl PCR
Nuclease-free water	to 50 µl	

Thermocycling condition:

Step	Temp	Time
Initial Denaturation	94°C	30 seconds
10 Cycles	94°C 50-55°C 65°C	30 seconds 30 seconds 1 minute/kb
20 Cycles	94°C 60-65°C 65°C	30 seconds 30 seconds 1 minute/kb
Final Extension	65°C	10 minutes
Hold	4°C	

2.2.3.3. Restriction fragment length polymorphism (RFLP)

To confirm generated BAC's or plasmid the RFLP was used. For this purpose, the DNA was cleaved by an appropriate enzyme in a 20 µl reaction mixture (20 µl). The reaction setup as follows:

Plasmid DNA	1 µl
or BAC	6 µl
Buffer (10 x)	2 µl
Enzyme	1 µl
add to 20 µl with ddH_2O	x µl

2.2.3.4. Gel electrophoresis

To visualize PCR products or fragments of DNA for RFLP, samples were mixed with 6 X DNA loading buffer and loaded into the slots of a freshly poured and solidified 0.8 % agarose gel. For plasmid RFLP or PCR confirmation agarose gels were prepared in 0.5 x TAE buffer containing ethidium bromide at a final concentration of 0.5 µg/ml. A voltage of 100 V was used for 35 min. Cleaved BAC and virus DNA was exposed to 70 V for 20 h or more in an ethidium bromide free 0.8 % gel, prepared in 1 x TAE. Then, the gel was stained in an ethidium bromide bath for 30 min and washed with water to remove excess ethidium bromide. In the case of both gel sorts the DNA was detected under 260 nm UV light.

2.2.3.5. Viral DNA extraction from agarose gels

To extract viral DNA fragments from agarose gels, the DNA fragment containing gel slice was cut out, diced and placed in 1.5 ml micro centrifuge tube, equal volume phenol (200-500 µl) saturated with TE buffer, pH 8.0, added. Then, the mixture was vortexed for 10 s and incubated for at least 5 min at –80 °C, in order to freeze the phenol. Afterwards, the samples were centrifuged for 5 min at 15000 × g at room temperature. The aqueous layer was removed to a new tube, the phenol layer left in the same tube. Next, 200 µl of water added to the phenol layer, vortexed 10 s and centrifuged for 5 min at 15000 × g, room temperature. Thenceforth, the top (aqueous) layer was removed and combined with the aqueous layer removed in the previous step. For DNA precipitation, 200 µl of chloroform: isoamylalcohol (24:1) added, the samples gently mixed by inverting and centrifuged (15000 × g, 1 min, RT). Next the top aqueous phase was transferred into a new tube and to the saved aqueous layer, 0.1 volumes of 3 M sodium acetate, pH 5.2 and 2.5 volumes of 100 % ethanol was added. Later the mixture was incubated 20 min at RT and DNA was palleted at 15000 × g, 20 min, 4-20 °C. Afterwards the supernatant was carefully remove and discarded and the pellet sustained. Subsequently the pellet was washed with 500 µl of 70 % ethanol, centrifuged for 5 min, 15000 × g. Followed by careful remove and discard of the supernatant. Finally, the samples were centrifuged shortly and the remaining aqueous remains were discarded. When all 70 % ethanol is removed, the DNA pellet can be immediately dissolved The DNA pellet was dissolved in a minimal volume of EB buffer (e.g. 20-50 µl of 10 mM Tris-HCl, pH 8.0) or water.

2.2.3.6. Purification of DNA by column purification and recovery of DNA from agarose gels

To purify DNA amplified by PCR or cleaved DNA fragments from agarose gels Hi Yield Gel/PCR DNA Fragments Extraction Kit (SLG) was used according to the manufacturer´s instructions.

2.2.3.7. Sequencing

To determine DNA nucleotide sequences, plasmids or PCR-amplified DNA fragments were column purified, eluted in H_2O and sent for DNA sequencing to LGC Genomics in the required amounts. Received sequence data was examined by the Vector NTI software (Invitrogen). Full genome sequencing of final mutants was completed in Friedrich-Loeffler-Institut by Maria Jenckel.

2.2.3.8. Cloning

2.2.3.8.1. Restriction digests and sticky end ligation for cloning in vectors

In order to, generate of plasmids with specific fragments inserted, the cleaved and purified insert DNA were ligated with the vector backbone. The main principle of “sticky ends” DNA ligation is that, DNA ligase catalyzes formation of phosphodiester bonds between the 3'-OH of one nucleotide and the 5'-PPP of a second nucleotide and such ligates DNA fragments having complementary, so-called “sticky ends”. The “sticky ends” ends were generated by incorporation of the restriction enzyme recognition sites required for cloning into the forward and reverse PCR primers. Next vector and PCR product were cleaved with the appropriate restriction enzymes to obtain sticky ends. In case only a single restriction site was used for the cloning procedure the vector was dephosphorylated with FastAP™ Thermosensitive Alkaline Phosphatase (2µl of phosphatase for 1 µg of DNA in 20 µl reaction volume with 10X reaction

buffer) to avoid self-ligation of the vector. The dephosphorilization mixture was incubated for 10 min at 37°C followed by heat inactivation at 75°C for 5 minutes. The amount of vector and insert DNA was measured spectrophotometrically using the Nanodrop spectrophotometer (Peqlab): the vector backbone was ligated in different vector/insert ratios ranging from 5:1 to 1:2 with a total volume of 10 µl for 5 min at 25 °C. The Quick-ligase ligase buffer system was used. The ligation reaction was mixed and incubated for 3 h. at RT before chemically competent or electrocompetent *E. coli* cells were transformed with 1 to 10 µl of the ligation reaction.

2.2.3.8.2. Preparation of chemically competent cells with calcium chloride ($CaCl_2$)

A single colony of *E. coli* (TOP10, DH10B) was grown O/N in 5 ml LB medium at 37°C at 220 rpm in a shaking incubator. Next day, 4 ml of o.n. culture was added to 400 ml fresh LB medium and incubated at 37 °C and 220 rpm until optical density 600 nm wavelength (OD_{600}) of 0,45-0,6 was reached. Thenceforth, the culture was transferred to 50 ml ice cold polypropylene tubes and incubated for 5-10 min on ice. Next, the bacteria were pelleted for 2 min at 1000 x g at 4°C and resuspended in 10 ml ice-cold 50 mM $CaCl_2$. Subsequently a second centrifugation step at 600 x g for 10 min at 4°C followed. Then the supernatant was removed and each pellet was resuspended in 10 ml ice-cold 50 mM $CaCl_2$ and incubated on ice for 30 min. Subsequent cells were centrifuged for one more time at 4 °C for 10 min at 500 x g, the supernatant was discarded and the pellet resuspended in 2 ml ice cold 100 mM $CaCl_2$ and 15 % glycerol solution. Finally, 100 µl aliquots of the culture were prepared and stored at -70 °C.

2.2.3.8.3. Transformation of chemically competent cells

To transform the ligation product to chemically competent bacteria, the product was added in a dropwise manner to bacteria and incubated for 30 min on ice. Thenceforth a 45-sec heat shock was completed in a 42°C water bath, followed by a short (~2 min) incubation on ice. Bacteria were then grown in 1 ml SOC medium for 1 h at 37°C. Finally, the transformed bacteria were plated on LB plates containing the appropriate antibiotics. These plates were then incubated at 37 °C overnight.

2.2.3.8.4. Preparation of electro competent cells

The *Escherichia coli* strain MegaX was incubated at 37˚C O/N in 5 ml of LB medium. Then, 100 µl of the O/N culture were added to 5 ml of fresh LB and the following was incubated at 37˚C and 220 rpm until it reached a logarithmic growth of OD_{600} of 0.5 to 0.7. Next, cultures were transferred to a water-ice bath and incubated for 20 min at 220 rpm on a shaker. Afterwards bacteria were pelleted by centrifugation for 2 min at 4500 rpm and 4˚C. Later, pellets were washed three times with ice-cold 10% glycerol in H_2O and shortly centrifuged at 4500 rpm after each washing step. Finally, the bacteria pallet was resuspended in 60 µl of 10% glycerol.

2.2.3.8.5. Transformation of electro competent cells

To transform the ligation product to electro competent bacteria, the product was added to bacteria and immediately transferred to electroporation cuvette. Thenceforth, electroporation was completed at 1.25 kV, 25 µF and 200 Ω. Next, bacteria were resuspended in 1000 µl of preheated SOC medium and incubated 1 h shaking at 37˚C before plating on selective LB agar plates.

2.2.3.9. Generation of recombinant viruses *via en passant* mutagenesis

The key principle of DNA editing used in this thesis is a technique termed *en passant* mutagenesis. This two-step system developed by Tischer and colleagues is based on Red mediated recombination and *in vivo* cleavage in *E. coli* (162, 163). The key features of the Red-recombination system are from λ phage proteins: Exo, Bet and Gam. These three proteins mediate homologous recombination of double-stranded DNA. During the Red recombination, the protein Gam takes a vital role in the recombination event since it defends free double-stranded DNA ends from degradation by the *E. coli* RecB/C/D system. Meanwhile, the 5'-3' exonuclease Exo generates free 3' single strand overhangs in the DNA template and Bet serves as a protector of those free strands. Moreover, during the amplification of the BAC DNA, Bet mediates the strand invasion which is essential to attain homologous recombination with the target sequence. Therefore, the *E. coli* strain used in this study, GS1783, a derivative of the DH10B strain, was engineered to express the Red system under a temperature inducible promoter, which is activated at 42˚C. Furthermore, GS1783 also express I-*Sce*I, a *Saccharomyces cerevisiae* homing endonuclease, under an arabinose inducible promoter. I-*Sce*I cleaves a very large and therefore rarely found a restriction site of 18bp, which makes a specific cleavage of the mutated region possible, in final recombination the selection marker cassette can be removed from the mutated sequence. Briefly, first a selection marker with an adjoining I-*Sce*I restriction site and to the target sequences homologous 40–50 bp sequence extensions are introduced into the the sequence of interest. Next, I-*Sce*I is expressed to allow a cleavage of the marker cassette which results in a seamless excision of the selection marker (Figure 6). This modern technique allows a broad range of different modifications of BAC cloned sequences. Using this technique, it is possible to edit single base pairs, to delete sequences of any size and to insert sequences of interest (157, 162 - 164).

Preparation of electrocompetent *E.coli* for *en passant* mutagenesis

The *E.coli* GS1783 culture holding the chosen parental BAC clone was incubated in LB medium with chloramphenicol overnight at 32 °C. The following day, 5 ml of chloramphenicol containing LB medium was inoculated with 100 µl of O/N culture and incubated at 32°C and 220 rpm until logarithmic growth reached OD_{600} 0,5 - 0,8. Next, a flask with bacterial culture was moved to a 42°C water bath for 15 min with 220 rpm shaking and afterwards kept in an ice bath for 20 min with 220 rpm shaking. Thenceforth, bacteria were palleted at 4°C for 5 min at 4500 x g. The supernatant was removed and the pellet was resuspended in 1 ml of 10% ice-cold glycerol or H_2O. Before a second centrifugation, washing step followed. After three washing steps, 50 µl 10 % ice-cold glycerol or H_2O was added to resolve the bacterial pellet. Finally, bacteria were positioned on ice or stored at -70 °C until the electroporation.

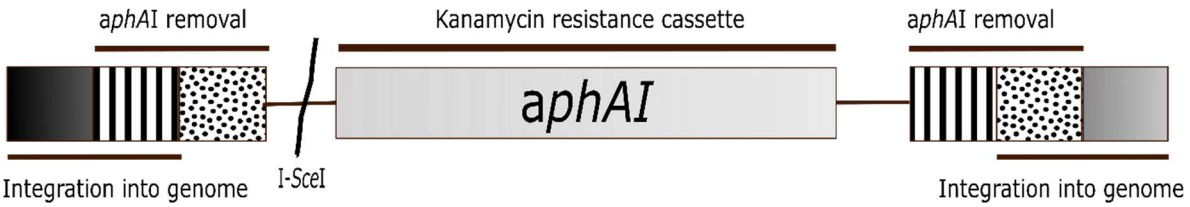

Figure 5. Schematic illustration of PCR product for *en passant* mutagenesis. Kanamycin resistance cassette serves as the positive selection marker, homologous flanks to the target sequence, and duplicated sequences (stripe and dot boxes) for removal of the positive selection marker.

1st Red recombination

For the first mutagenesis step, bacteria were electroporated in ice-cold 0,1 cm cuvettes with 2-5 µl (~100 ng) *Dpn*I-digested and gel purified PCR product. The PCR product electroporated in competent bacteria contained homologous flanks required for sequence integration into the BAC DNA, kanamycin cassette with an *I-Sce*I restriction site and duplicated homologous sequences that allow the complete removal of the kanamycin cassette during the second Red recombination step (Figure 5). After electroporation, the bacteria were carefully removed from the cuvette by adding 900 µl 32°C LB. Then bacteria were incubated for 2 h at 32ºC, 220 rpm. Afterwards, bacteria were plated on plates with chloramphenicol and kanamycin and incubated for 2 days at 32 °C.

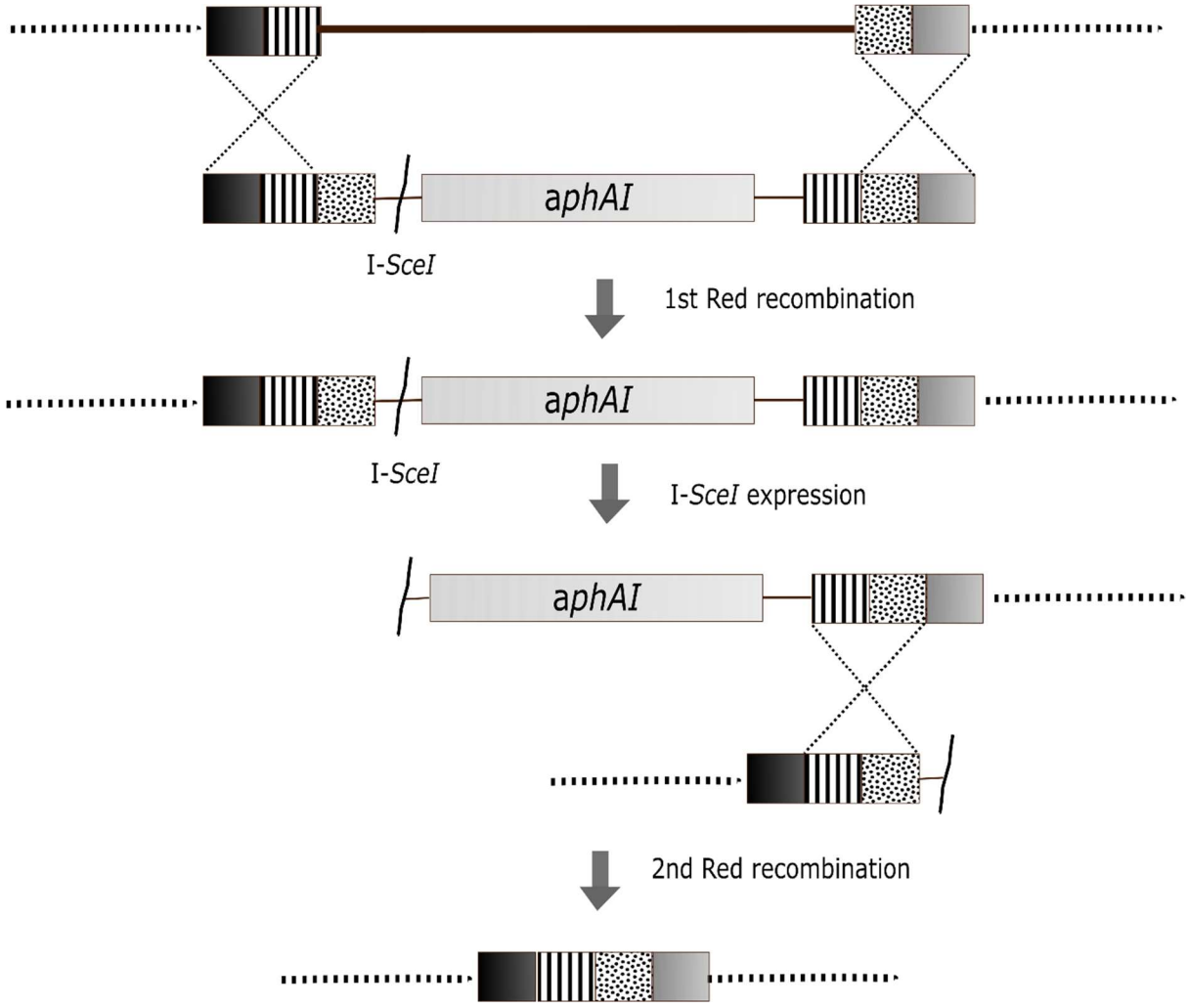

Figure 6. Deletion of selected sequences *via* two-step Red mediated recombination. The sequence is deleted integration of the kanamycin cassette with the help of homologues flanks during the first Red recombination step. After I-*Sce*I induction with L-arabinose and incubation at 42ºC, the second recombination step occurs, resulting in recombination between the homologous sequences (stripe and dot boxes); the kanamycin cassette is then removed. Figure adapted from Tischer et al. (162, 163)

2nd Red recombination or resolution of co-integrates

The correct clones were selected, after RFLP and colony PCR screen. Then bacterial colony, containing selected mutant, was inoculated in 1 ml LB medium with chloramphenicol and incubated under shaking conditions while waiting for the culture to became faintly cloudy, around 2 – 3 hours. Afterwards, the *I-Sce*l cleavage site was activated with the help of adding 1 ml 32°C LB medium cwith chloramphenicol and 2 % L-Arabinose. Afterward incubation at 220 rpm for another 60 min at 32°C, the Red recombination system was activated by incubation at 42°C at 220 rpm for 30 min. Next, bacteria were grown at 32°C, 220 rpm shaking conditions for another 2 hours. Finally, 5-10 µl of a 1:100 and 1:1000 dilutions of the bacteria culture were plated on LB-plates with chloramphenicol and 1 % L-Arabinose. These plates were then incubated for 2 days at 32 °C. Grown colonies were moved to replica plates with kanamycin and chloramphenicol to eliminate the colonies, that are false positive. Finally, positive clones were confirmed by RFLP and colony PCR.

2.2.4. Animal Studies

In vivo experiments were conducted in Friedrich-Loeffler-Institut, approved by the Ministry of Agriculture of Mecklenburg-Western Pomerania, Germany. Mixed-sex Wistar rats at 6 weeks old (outbred; Charles River, Sulzfeld, Germany) were kept in groups of 2 to 3 animals in standard laboratory rodent cages. The experimental design, used in this study, complied with the experiments published earlier (119, 158, 160). Rats were infected intranasally with mutant viruses: BR_RatPox09_NMDAr, BR_RatPox09_CrmE and BR_RatPox09_sF, control viruses wild type BR, RatPox09 and BAC derived, vBR, and correspondingly 2 control rats were used. The infectious dosage of $10^{5,5}$ $TCID_{50}$/animal was used. General health status, weight and body temperature of all animals were registered everyday over a period of 15 days, and then on 17th, 19th and 21st day post infection. Oropharyngeal swabs (Bakteriette; EM-TE Vertrieb, Hamburg.) were taken every other day. Wistar rats were either humanely killed for autopsy 21 dpi or when the clinical score was indicated to be higher than 7. All Wistar rats, used in this study, were dissected and organ specimens were collected. The scoring system was developed by Annika Franke and Donata Hoffmann (Friedrich-Loeffler-Institut, unpublished data). The following measurements and clinical symptoms were summarized for calculation of the clinical score: body temperature, weight, nasal discharge, activity, respiratory distress, wheezing, pox lesions, inflated stomach, rough fur. The clinical scoring system is presented in the Table 5. The oropharyngeal swab samples were resuspended in 2 ml of cell culture medium with antibiotics (gentamicin, 0.05 mg/ml, lincomycin, 1 mg/ml; enrofloxacin, 1 mg/ml;). Samples of organ tissue were homogenized, the the DNA from all collected organ samples and swabs was extracted using BioSprint 96 and a MagAttract Virus Mini M48 kit (Qiagen). The real-time PCR was completed by OPV DNA-specific protocol (165). Additionally, endpoint dilution assays using the Spearman-Kaerber algorithm, were completed for each collected sample. For detection of virus-specific antibodies in serum of infected animals, indirect immunofluorescence was used. For this purpose, serum samples were incubated for 30 min at 56°C. Afterward, CPXV virus-infected Hep2 cells were incubated for 1 hour at room temperature with a 1:200 or 1:500 dilution of serum. After three PBS washing steps, anti-rat and anti-mouse secondary antibodies (Life Technologies) were used. Finally, Evans Blue (Sigma-Aldrich, Deisenhofen, Germany) was inroduced to stain the cytoplasm of the infected cells. Statistical analyses were performed with Graphpad and XLSTAT for Windows. Values were compared using one-way ANOVA followed by Dunn's and Bonferroni t-test for pairwise

comparisons. In all analyses, two-tailed p values less than 0.05 were considered statistically significant.

Clinical parameters		Points
Body temperature	above 36°C	0
	35-36°C	1
	34-35°C	2
	below 34°C	3
Nasal discharge	Absent	0
	Doubtful	1
	clearly present	2
Respiratory distress	normal breathing	0
	Light	1
	Moderate	2
	Severe	3
	Absent	0
Pox lesions	Present	1
Activity	Normal	0
	moderate activity	1
	Inactive	2
Body weight loss	Absent	0
	> 10 %	1
	> 20 %	2
	> 30 %	3
Wheezing	Absent	0
	Present	1
Inflated stomach	Absent	0
	Present	1
Rough fur	Absent	0
	Present	1

Table 5. Clinical scoring system for rats infected with CPXV.

3. Results

3.1. Generation of the knock-in mutants

In the present study, we aimed to identify new orthopoxvirus virulence markers in a rodent host model. For this purpose, we analyzed the sequence of two CPXV strains with different course of the disease, recognized the ORF's that might possibly be responsible for the change in CPXV virulence and generated recombinant viruses with individual RatPox09 genes introduced into the BR-genome. However, first, we analyzed the sequence of the putative virulence markers. The analysis of each of possible virulence determents is given in the following section.

3.1.1. Sequence analysis of genes of interest

The major differences between the two CPXV isolates are four ORFs (CPXV0002, CPXV0003, CPXV0284 and CPXV0030,), that are absent in BR, but found in RatPox09. One of these ORFs, CPXV0002, is positioned between CPXV222 and CPXV0003. BLAST searches identify CPXV0002 highly similar sequence in multiple newly isolated cowpox viruses as well in some older isolates (Germany_1998_2, Germany_1980_EP4, Germany_2002_MKY), likewise in multiple Vaccinia virus strains (Lister, L-IVP, USSR) and some camelpox virus isolates (0408151v, CMS, M-96) (91, 119, 145, 147, 166 – 169). The protein encoded by CPXV0002 is 273 amino acid long. It has 99 % identity with CPXV N-methyl-D-aspartate (NMDA) receptor like protein (145). Therefore, further in this study it will be named NMDAr. Nevertheless, various predictions showed no indication, to the similarity of CPXV0002 to NMDA receptor like proteins (173). Furthermore, this protein sequence also has 98 % identity with Vaccinia Golgi anti apoptotic protein (VACV GAAP) (Figure 7) as well as similarity to CMPV proteins CMP6L and CMP006 (91, 92, 169). Moreover, BLAST searches with CPXV0002 identified closely related, lifeguard protein in cattle (78% identity), mouse (74% identity), and rat (74% identity) to be highly related to CPXV0002 (Figure 7). In addition, there are related proteins of equivalent size predicted to be encoded by goat (78% identity), European hedgehog (74% identity), water buffalo (77% identity) and wild boar (74% identity). Consequently, the PFAM program indicated the protein family UPF0005 domain with multiple transmembrane motifs, between the 32 and 231 aa (173).

Figure 7. Alignment of CPXV strain RatPox09 putative protein NMDAr sequence with related proteins from other species: VACV GAAP and Rattus Norvegicus protein lifeguard 4. Blue coloring indicates identical sequence.

Another investigated protein, CPXV0003, is positioned between CPXVCrmD and CPXV0002. Sequence in high similarity to CPXV0003 is found in multiple newly isolated cowpox viruses as well in some older strains (Germany_1998_2, Germany_1980_EP4, Germany_2002_MKY), additionally in multiple Vaccinia virus strains (Lister, L-IVP, WAU86/88-1), camelpox isolates (0408151v, CMS, M-96) and even monkeypox virus isolates (Yambuku_DRC_1985, Boende_DRC_2008, Gabon-1988) (91, 145, 147, 166, 168 – 169, 174). The protein encoded by CPXV0003 is 167 amino acid long. It has 99 % identity with VACV CrmE protein. Therefore, further in this study it is named CrmE (103). This protein also has high similarity with CMLV protein CMLV007 (169). Subsequently, The PFAM program indicated the TNFR/NGFR cysteine-rich region between the 22 and 58 aa (173).

Thenceforth, we analyzed sequence of CPXV0284, which is located between CPXV010 and CPXV011. Sequence in high similarity to CPXV0284 is found in numerous newly isolated cowpox viruses as well in some older isolates (Germany_1998_2, UK2000_K2984, Germany 91-3,) moreover, in some horsepox (MNR-76) and ectromelia virus isolates (Naval, ERPV, Moscow) (147, 166, 167, 170 - 172). The protein encoded by CPXV0284 is 273 amino acid long. It has 92 % identity with D7L protein of CPXV GRI -90, 95 % identity with horsepox virus (HSPV) protein HSPV008 and 94 % identity with ECTV protein EVM004 (167, 172). Due a high similarity to recognized CPXV protein, the protein encoded by CPXV0284, will be named D7L further in this study. Pfam prediction of CPXV0284 was performed. The BTB/POZ domain is indicated, found between the 31 and 131 aa (173).

CPXV0030 is positioned between CPXV202 and CPXV203. To CPXV0030 similar sequence is found in multiple newly isolated cowpox viruses as well in some older isolates (Germany 91-3, France_2001_Nancy, EP-2) (145, 147, 166, 167). Some residues of the sequence are also found in some camelpox virus and even variola virus isolates. The protein encoded by CPXV0030 is 1898 amino acid long. It has 99 % identity with CPXV 7-transmembrane G protein-coupled receptor-like protein (7tGp) (145). Therefore, further in this study it will be named 7tGp. However, multiple structure predictions indicate only one transmembrane domain and even 2 Poxvirus_B22R domains, between 10 and 777, 786 and 1053 aa. (173)

We considered it to be likely that ATI and/or p4c contribute to CPXV virulence in rats as both these gene sequences have quite a few modifications between BR and RatPox09. Moreover, RatPox09 p4c amino acid sequence (A26; CPXV161 protein for RatPox09 and CPXV159 and CPXV161 in BR) results in a 59-amino-acid (aa) truncation at the N terminus, which likely is responsible for incapability to place IMVs in ATI (119), as BR p4C gene is disrupted, due premature stop codon introduced by frame shift mutation. Furthermore, CPXV BR and RatPox09 ATI (CPXV159 in RatPox09 and CPXV158 for BR), corresponding to VACVA25) show modifications in length and sequence, particularly in the repeat regions, but the translational initiation and stop codons of these two ORFs are identical. The overall identity of CPXV BR and RatPox09 ATI genes is 87 %.

3.1.2. Transfer constructs

For transfer plasmid construction, the ORF's coding RatPox09 proteins D7L, CrmE, NMDAr, TK, 7tGp and ATI/p4C together with the estimated promoter sequence were amplified by PCR using primer pairs: NT53, NT54; NT55, NT56; NT57, NT58; NT59, NT60; NT49, NT50; NT45, NT46, respectively (Table 3). The amplificated products were extended with a *Kpn*I restriction site upstream and a *Bam*HI site downstream of the respective ORF, in the case of D7L, CrmE and NMDAr, for RatPox09 TK PCR product was extended with *Kpn*I restriction sites upstream and downstream and for 7tGp *Sac*I restriction site upstream and *Pst*I restriction

site downstream. In the case of ATI/p4C *Sbf*I restriction site upstream and a *Hin*dIII site downstream were used. The PCR products were column purified and cloned into the vector pepkanS2 in the case of D7L, CrmE and NMDAr and to puC19 in the case of 7tGp and ATI/p4C. The vectors have been digested with *Kpn*I and *Bam*HI for cloning of ORF's D7L, CrmE, NMDAr; *Kpn*I for cloning of RatPox09 TK, *Sac*I and *Pst*I for ORF 7tGp cloning and *Sbf*I, *Hin*dIII for ATI/p4C. Afterwards the vectors were dephosphorylated with FastAP before cloning. TOP 10 chemical competent cells or MegaX electro competent cells were used for transformation as described in sections 2.2.4.8.3. (Transformation of chemically competent cells and 2.2.4.8.5 (Transformation of electro competent cells), respectively. Correct clones were determined by PCR and RFLP. Finally, the PCR products were confirmed by sequencing. For 7tGp and ATI/p4C transfer plasmid construction, a second PCR using primers NT51, NT52 and NT47, NT48, respectively, combined with pEPkanS2 plasmid as template was performed (Table 3). This PCR amplified the I-*Sce*I-*aphAI* recombination cassette and extensions *Pst*I restriction site for 7tGptransfer plasmid and *Sbf*I for ATI/p4C transfer plasmid. Thenceforth, the PCR products were gel purified and cloned into the appropriate transfer plasmids which had been digested with suitable restriction enzyme, as well as dephosphorylated with FastAP. Thus, selection for resistance to ampicillin and kanamycin was possible. Correct transfer plasmid clones were also confirmed by RFLP, PCR and sequencing (schematic representation of the transfer constructs is given in Figure 8).

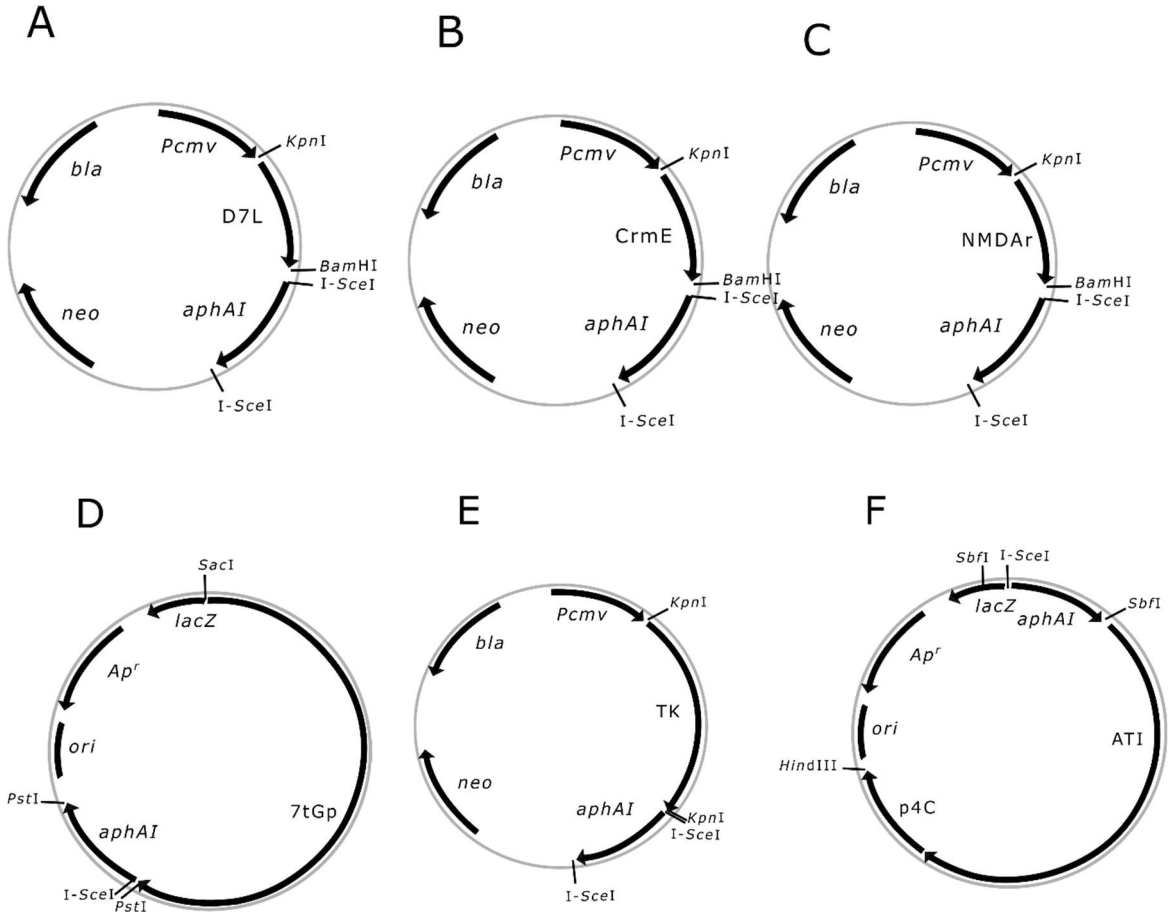

Figure 8. Schematic representation of transfer constructs generated in this study. Generated constructs pEPkan-S2_RatPox09_D7L (A). pEPkan-S2_RatPox09_CrmE (B), pEPkan-S2_RatPox09_NMDAr (C), puC19_RatPox09_7tGp kana (D), pEPkan-S2_RatPox09_TK (E), puC19_RatPox09_ATI_p4C_kana (D)

3.1.3. Recombination

The putative CPXV virulence markers were inserted in pBRF using *en passant* Red recombination as described in section 2.2.4.9. (Generation of recombinant viruses *via en passant* mutagenesis). Only in the case of ATI/pr4C gene, due to numerous similarities in the sequences of these genes between the two examined CPXV strains, the original sequence in BR required to be deleted. For this purpose, also *en passant* mutagenesis was performed as

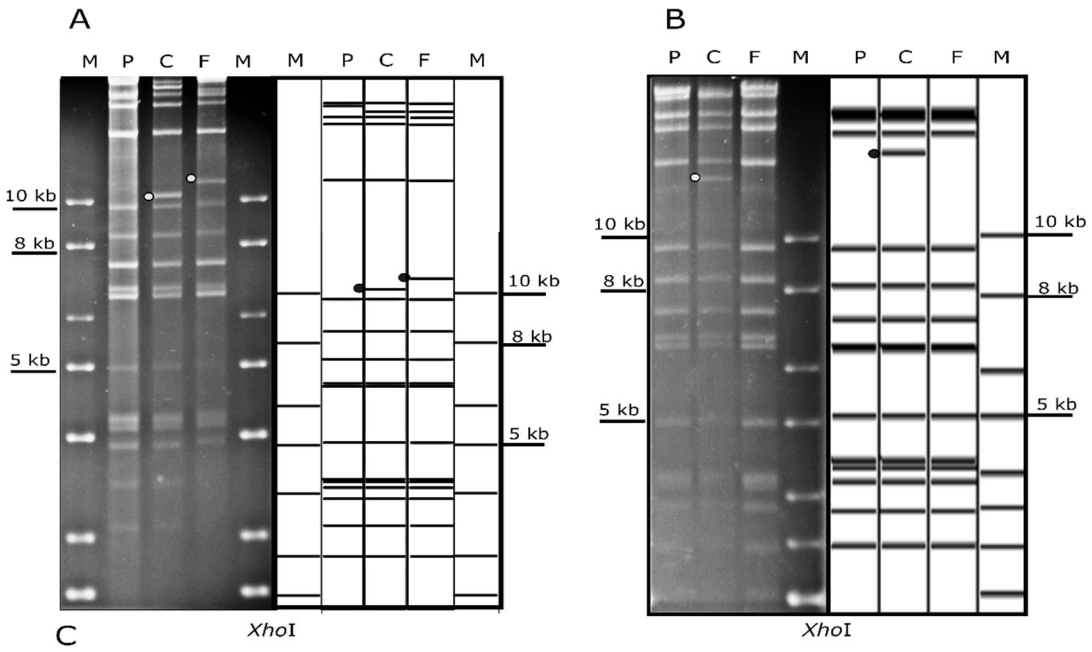

C

BAC	Restriction enzymes	Sequencing primers
pBRF_Ratpox09_D7L	*Xcm*I, *Xho*I	80-82
pBRF_Ratpox09_CrmE	*Xcm*I, *Pst*I	83, 84
pBRF_Ratpox09_NMDAr	*Xcm*I	85 - 87
pBRF_Ratpox09_7tGp	*Xho*I	88 - 99
pBRF_Ratpox09_D7L_CrmE	*Xcm*I, *Pst*I	80-84
pBRF_Ratpox09_D7L_CrmE_NMDAr	*Xho*I	80 - 87
pBRF_Ratpox09_D7L_CrmE_NMDAr_7tGp	*Xho*I	80 - 99
BRF_Ratpox09_ATI_p4C	*Xho*I	100 -105
pBRF_dATI_p4C	*Xho*I	100, 105

Figure 9. RFLP analysis of BR_RatPox09_NMDAr and BR_RatPox09_ATI_p4C, sequencing primers and restriction enzymes used for confirmation of pBRF mutants. **(A)** RFLP analysis of the parental BAC (P), the kanamycin cassette containing cointegrate (C) and the resolved final clone pBRF_RatPox09_NMDAr, respectively (F) with restriction enzymes *Xho*I. The maker used: Solis 1kb DNA (M). **(B)** RFLP analysis of the parental BAC (P), the kanamycin cassette containing cointegrate (C) and the resolved final clone pBRF_RatPox09_ATI_p4C, respectively (F) with restriction enzymes *Xho*I. The maker used: Gene ruler DNA ladder mix (M). Dots indicate the fragment length variation caused by deletion and the insertion of the kanamycin cassette which is removed in the final**. (C)** Sequencing primers and restriction enzymes used for confirmation of pBRF mutants.

described previously in section 2.2.4.9. A list of all primers used in this study for construction of the transfer plasmids as well as for Red-mediated recombination is given in the Materials and Methods section (Table 2 and 3). The resulting sensitivity to kanamycin of successfully resolved clones was confirmed by replica-plating on appropriate selection plates. We confirmed successful insertion by RFLP analysis. Sequences covering deleted ORFs were amplified by PCR. The PCR products were analyzed by agarose gel electrophoresis and sequenced. A list of restriction enzymes and sequencing primers used to confirm the deletion mutants is given in the Figure 9C. The detected restriction patterns and the sequencing results were in complete agreement with the *in silico* predictions (Figure 9A and B). We have successfully generated mutants with one RatPox09 gene inserted in pBRF genome: pBRF_RatPox09_D7L, pBRF_RatPox09_CrmE, pBRF_RatPox09_NMDAr and pBRF_RatPox09_7tGp, pBRF_RatPox09_ATI_p4C as well as mutants with multiple genes inserted: pBRF_RatPox09_D7L_CrmE, pBRF_RatPox09_D7L_CrmE_NMDAr, and pBRF_RatPox09_D7L_CrmE_NMDAr_7tGp.

3.1.4. Reconstitution and TK recovery of gain of function mutants

Vero cells were transfected with BAC DNA of pBRF mutants. Infectious virus was recovered with the help of fowlpox virus. Thenceforth, the gained virus clones were passaged three times on Vero cells to eliminate FWPV helper virus. Later, mini-F vector sequences present in pBRF were removed and the thymidine kinase (TK) gene repaired by transfection with a TK-containing plasmid and plaque purification. Figure 10 illustrates the BR knock-in mutants generated over the course of this study.

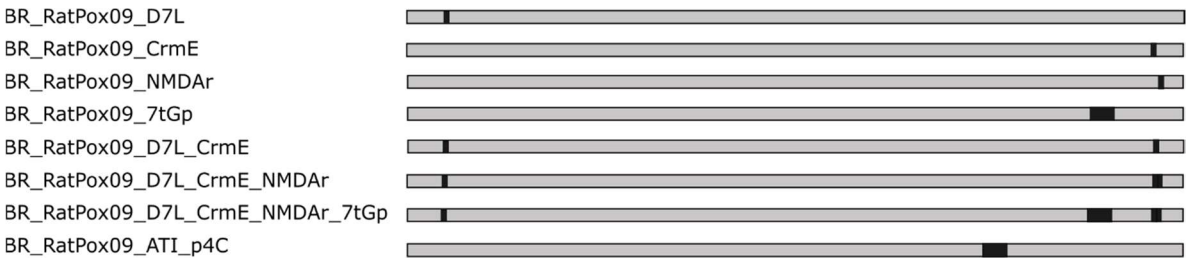

Figure 10. Schematic illustration of generated BAC knock-in mutants. Gray boxes BR sequence, black, boxes – RatPox09 sequence.

3.2. Generation of the chimeric viruses

In order to identify the additional virulence factors within the "background noise" of the proteome comparison we decided to swap segments of the virulent isolate RatPox09 with the authentic sequences of the low-virulent strain BR. For this purpose, we divided CPXV genome into seven 20 – 40 kb size segments, the sequence of each segment was chosen in a way that every single segment would harbor at least 800 bp of overlapping sequence that is identical between the two investigated CPXV strains (Figure 11, Table 6). Unfortunately, we were not able to generate chimeric viruses of segment A and G, since these segments were not harbored by the partial RatPox09 BAC's, generated by Xu Zhiyong (unpublished data) and used in our study. Nevertheless, the six genes that represent the major genetic differences between these two strains, were separately introduced into the BR genome as described in section 3.1.

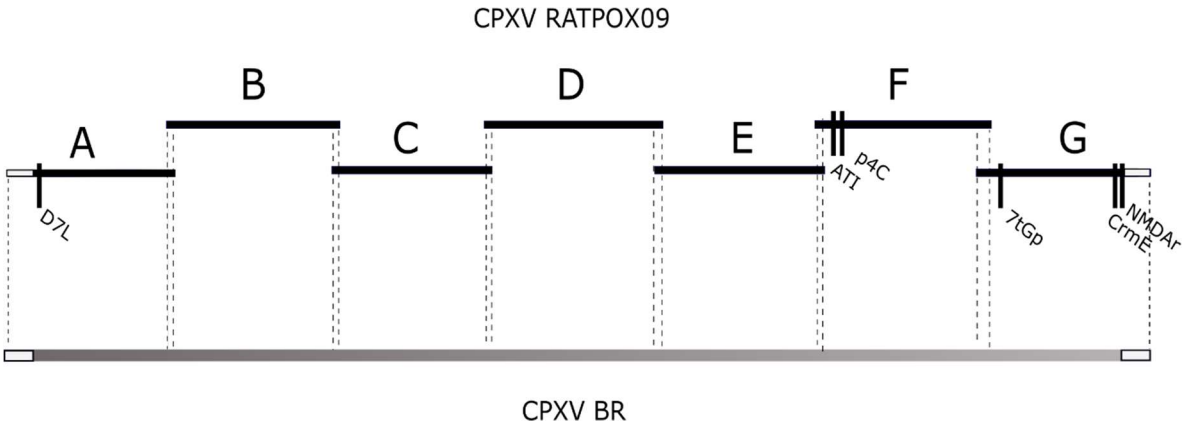

Figure 11. Schematic illustration of the exchange of genomic segments between CPXV RatPox09 and CPXV BR. Gray boxes represent CPXV BR sequence, black boxes – RatPox09 sequence segments, white boxes – sequence of the repeats.

(Generation of the knock-in mutants). In order to achieve this complicated task, we combined two techniques: seamless *en passant* Red mutagenesis and an older well-known method: virus recombination in the cell culture. *En passant* from pBRF and mostly two *en passant* mutagenesis reactions were necessary to obtain RatPox09 segment of interest from partial BACs. (Figure 12). Primers for the amplification of the transfer cassette were generated as follows: the 40bp sequence for alignment were joined with 20 bp duplication sequence for the release of the marker cassette in the resolution step, each (Figure 5). In the case of genomic segment recovery from the partial pRatPox09F also an 8bp *Asc*I unique restriction site (GGCGCGCC) for the final release of the segment were added to the primer design. The amplification of the marker cassette was completed by adding 24 bp of the kanamycin sequence to the forward primer and 23 bp corresponding to the kanamycin resistance gene cassette to the reverse primer. For amplification of marker sequences pepkanS2 plasmid was used, it also encodes a unique *I-Sce*I restriction site together with kanamycin resistance cassette. The *en passant* mutagenesis were performed as described in 2.2.4.9. (Generation of recombinant viruses *via en passant* mutagenesis). A list of all primers used in this study for Red-mediated recombination is given in Table 2. Furthermore, two *en passant* mutagenesis reactions were necessary to recover segments B, C, E and F from partial RatPox09 BAC's (pRatPox09F_sB, pRatPox09F_sC pRatPox09F_sE, pRatPox09F_sF) and only one *en passant* reaction were necessary to recover segment D (pRatPox09F_sD) (Figure 12) and to delete segments of interest from pBRF. The resulting sensitivity to kanamycin of successfully resolved clones was confirmed by replica-plating on appropriate selection plates. Moreover, we confirmed successful sequence deletion by RFLP and PCR analysis (Figure 13 and 14). The PCR products were analyzed by agarose gel electrophoresis and sequenced. A list of restriction enzymes and sequencing primers used to confirm the deletion mutants is given in the Table 7. In all cases, the observed restriction pattern and the sequencing results were in complete agreement with the *in silico* predictions (Figures 13 and 14). Moreover, the exact ORFs that were deleted in pBRF and were rescued from partial pRatPox09F is listed in the Table 6. We have successfully generated deletion mutants of single segment B, C, D, E and F in pBRF (pBRF_dsB; pBRF_dsC; pBRF_dsD; pBRF_dsE; pBRF_dsF). As well as mutants with segments B and C or D, E and F deleted (pBRF_dsB_C; pBRF_dsD_E_F). Since the attempts to insert 20 kb to 40 kb fragments to CPXV BR genome via Red recombination were not successful due to the high amount of mutations in the final PCR products, the final modifications were made in the cell culture. The miniF sequence were removed from the RatPox09 BAC harboring only one

genomic segment by *Asc*I cleavage and gel electrophoresis, in the case of segment D, *Asc*I and *Fsc*eI cleavage were used.

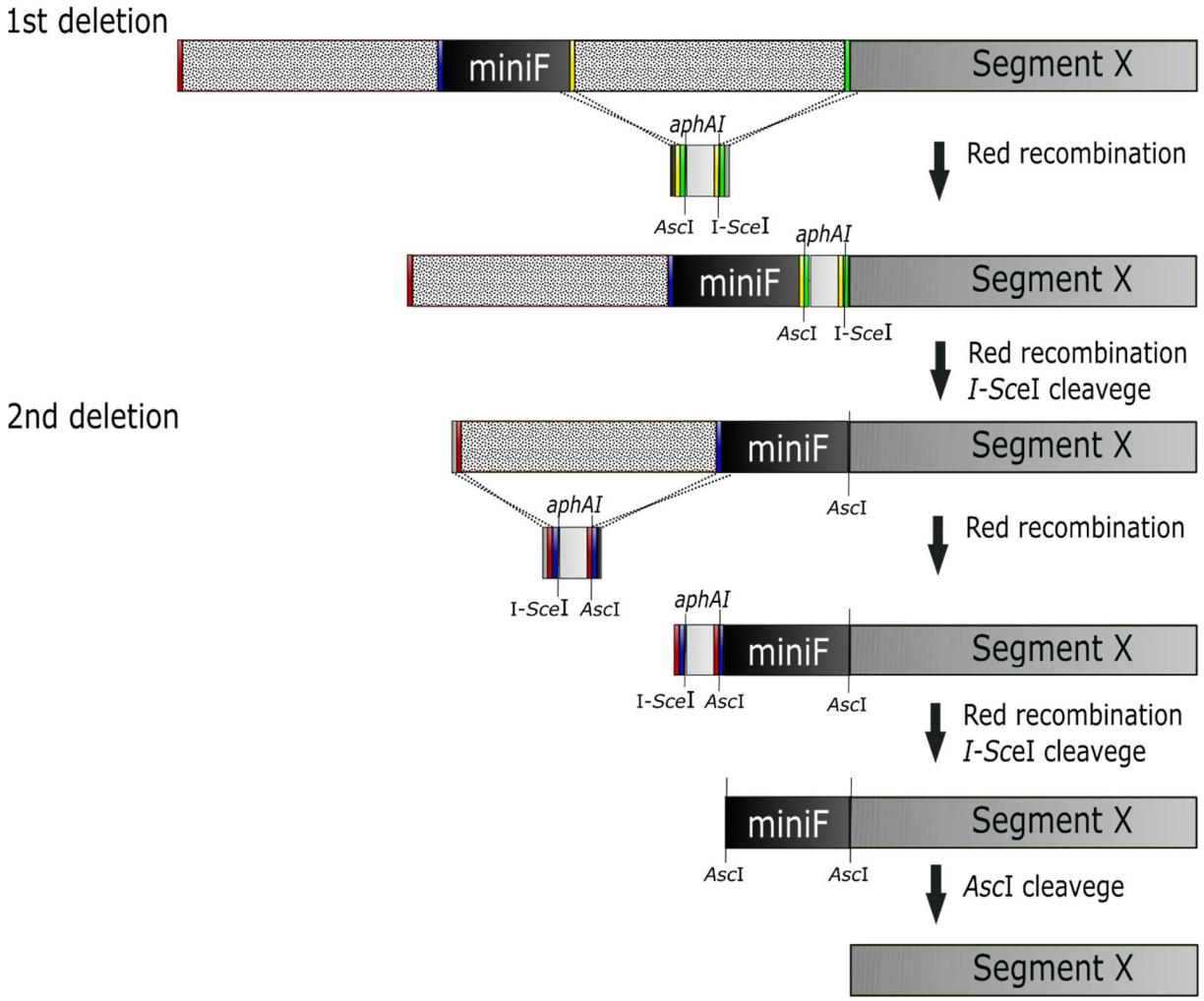

Figure 12. Schematic illustration of the strategy used to recover segments of interest from partial RatPox09 BACs. Two en passant deletions were necessary. Marker inserted cassette (aphAI) also contained alignment sequence, duplication sites, *I-Sce*I and *Asc*I expression sites.

BR_Ratpox09 sX	Ratpox09_sX	pBRF_dsX
Segment B	ORF 34 - ORF 66	ORF 35 - ORF 65
Segment C	ORF 66 - ORF 105	ORF 68 - ORF 104
Segment D	ORF 105 - ORF 134	ORF 106 - ORF 133
Segment E	ORF 133 - ORF 158	ORF 134 - ORF 157
Segment F	ORF 156 - ORF 198	ORF 157 - ORF 190
Segment B_C	ORF 34 - ORF 66; ORF 66 - ORF 105	ORF 35 - ORF 104
Segment D_E_F	ORF 105 - ORF 134;ORF 133 - ORF 158; ORF 156 - ORF 198	ORF 106 - ORF 190

Table. 6. Organization of generation of chimeric viruses. BR_RatPox09 sX: generated CPXV chimera; pRatPox09F_sX: segments rescued from pRatPox09F for the generation of chimeric virus; pBRF_dsX: ORF's deleted in pBRF for the generation of chimeric virus.

BAC	Restriction enzymes	Sequencing primers
pRatpox09FsB_dI	*Kpn*I, *Pst*I	65, 66
pRatpox09FsB_dII	*Hind*III, *Pst*I	63, 109
pRatpox09FsC_dI	*Kpn*I, *Nru*I	65, 108
pRatpox09FsC_dII	*Pst*I, *Kpn*I	109, 110
pRatpox09FsD_dI	*Nru*I, *Stu*I	106, 109
pRatpox09FsE_dI	*Nru*I, *Hind*III	100, 109
pRatpox09FsE_dII	*Nru*I	65, 111
pRatpox09FsF_dI	*Hind*III, *Stu*I	109, 116
pRatpox09FsF_dII	*Pst*I, *Nru*I	65, 112
pBRF_dsB_C	*Nru*I	76, 109
pBRF_dsD_E_F	*Nru*I, *Xho*I	65, 114, 115
pBRF_dsB	*Pac*I, *Xho*I	76, 108
pBRF_dsC	*Kpn*I, *Pst*I	63, 109
pBRF_dsD	*Xho*I	65, 111
pBRF_dsE	*SpH*I	105, 106
pBRF_dsF	*SpH*I, *Nru*I	113 - 115

Table. 7. Enzymes and sequencing primers used for confirmation of deletion mutants.

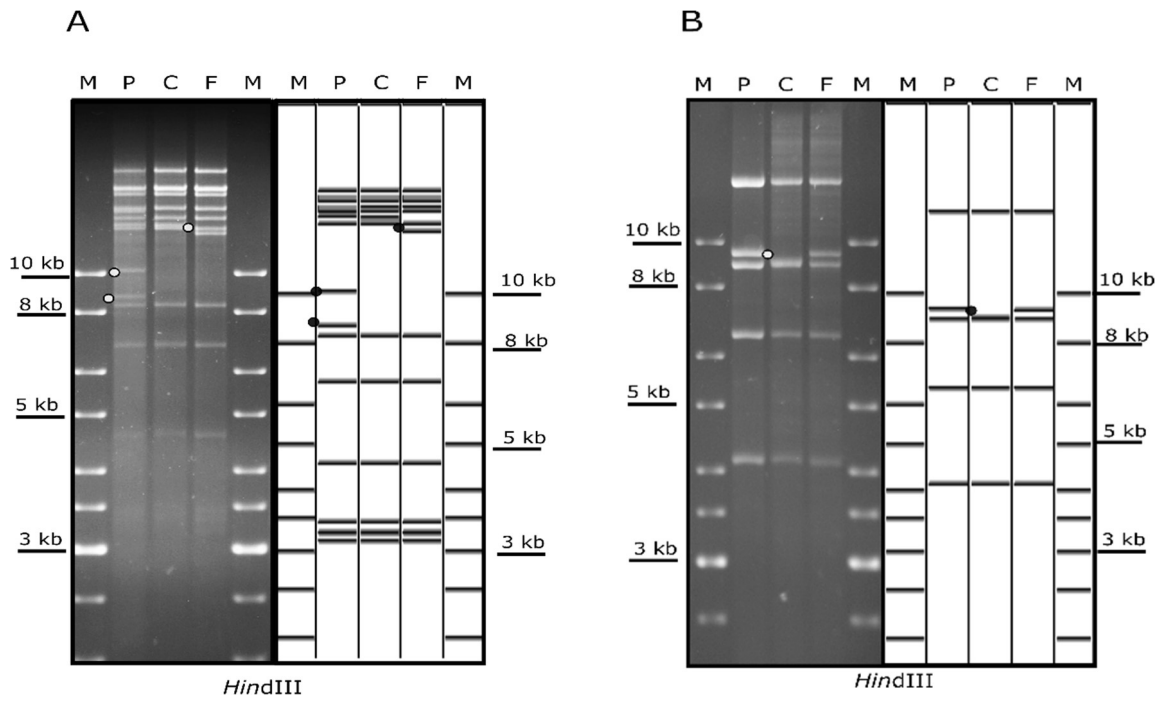

Figure 13. RFL analysis of pBRF segment C deletion mutant (A), and pRatPox09apr22 second deletion mutant for segment C recovery (B). RFLP analysis of the parental BAC (P), the kanamycin cassette containing cointegrate (C) and the resolved final clone pBRF_dsC and pRatPox09_sC, respectively. (F) with restriction enzymes HindIII. The maker used: Gene ruler DNA ladder mix (M). Dots indicate the fragment length variation caused by deletion and the insertion of the kanamycin cassette which is removed in the final.

Finally, Vero cells were then transfected with pBRF deletion mutants and RatPox09 segments of interest. The chimeric viruses were recovered using fowlpox virus as a helper. The completed virus mutants were passaged three times on Vero cells to eliminate FWPV helper virus. Thenceforth, mini-F vector sequences present in pBRF were removed and the thymidine kinase (TK) gene repaired by infection of with a TK- containing plasmid transfected Vero cells and plaque purification. Using this strategy, we managed to generate chimeric viruses of single genomic segments B, C, D, E, and F (BR_RatPox09 sB, BR_RatPox09 sC, BR_RatPox09 sD, BR_RatPox09 sE, BR_RatPox09 sF) and segments B and C or D, E and F combined (BR_RatPox09 sB_C, BR_RatPox09 sD_E_F) (Figure 15). All final mutants were confirmed by full genome sequencing.

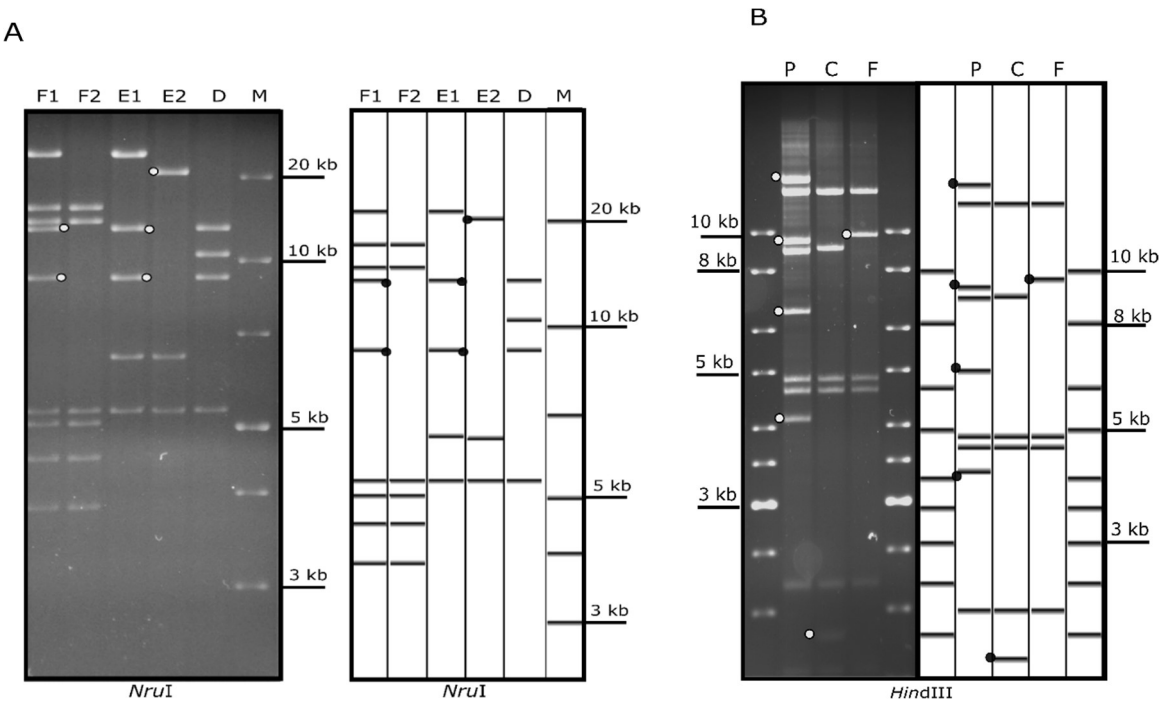

Figure 14. RFL analysis of pRatPox09 deletion mutants for segment recovery. A: RFLP analysis of the pRatPox09_sF_d1 (F1), pRatPox09_sF_d2 (F2), pRatPox09_sE_d1 (E1), pRatPox09_sE_d2 and pRatPox09_sD (D) with restriction enzyme *Nru*I. The maker used: Gene ruler 1kb Plus (M). **B:** pRatPox09apr22 second deletion mutant for segment B recovery (B). RFLP analysis of the parental BAC (P), the kanamycin cassette containing cointegrate (C) and the resolved final clone pBRF_dsB and pRatPox09_sC, respectively. (F) with restriction enzymes *Hin*dIII. The maker used: Gene ruler DNA ladder mix (M). Dots indicate the fragment length variation caused by deletion and the insertion of the kanamycin cassette which is removed in the final.

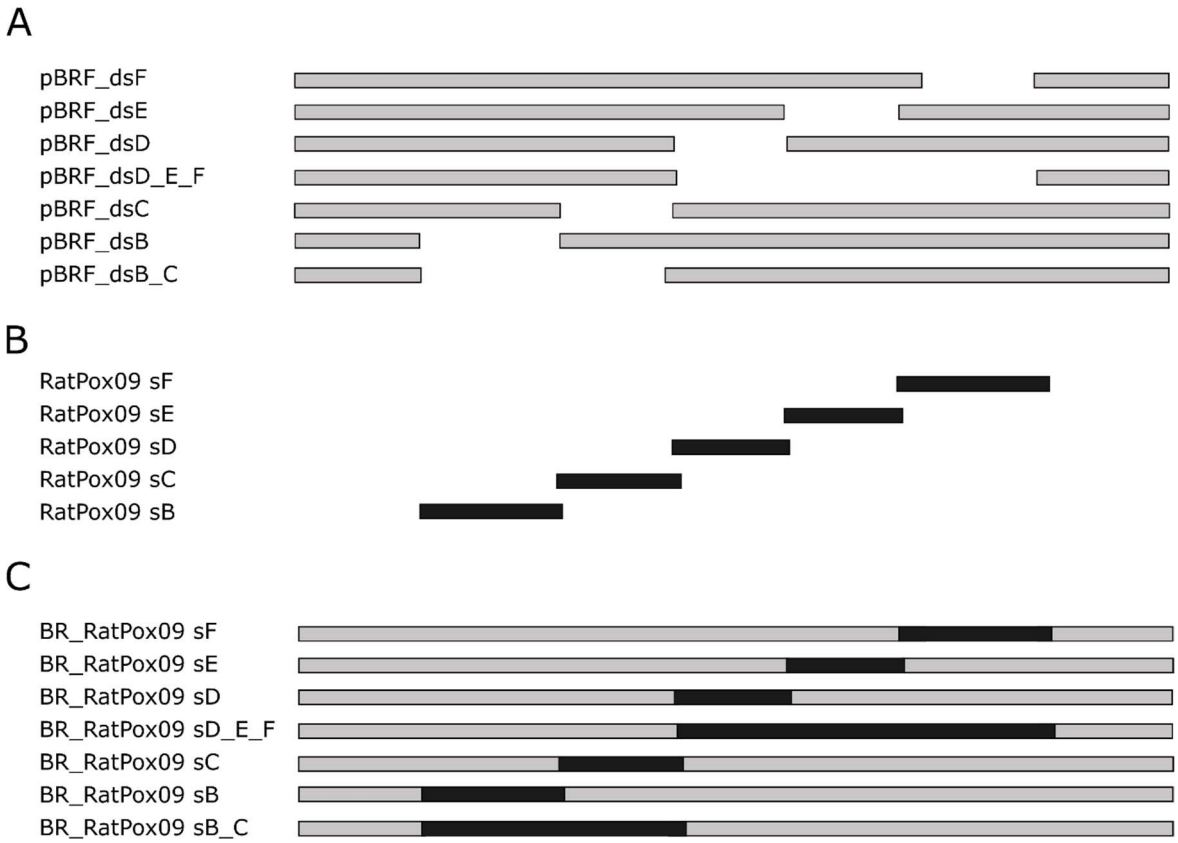

Figure 15. Schematic illustration of generated BAC mutants and chimeric viruses. (A) Schematic representation of pBRF deletion mutants (B), segments won from RatPox09 partial BAC's (C) and chimeric viruses. Gray boxes BR sequence, black, boxes – RatPox09 sequence.

3.3. Phenion® full-thickness 3D skin model as possible replacement for animal experiments

To reduce number of animal experiments needed for this study, we aimed to test Phenion® full-thickness 3D skin model as a possible replacement for animal model.

3.3.1. Histopathological studies of the Uninfected and CPXV-Infected the Phenion® full-thickness skin model Skin Model

In order to test the pathological effect of CPXV on The Phenion® full-thickness skin model, the skin model was infected with 10^5 $TCID_{50}$ of CPXV BR and RatPox09 virus as described in section 2.2.3.5. (Infection 3D Skin Model and immunohistochemistry). Correspondingly, a MOCK control group was included. Cultures were incubated for 7 days at 37°C and the lesion development was monitored macroscopically. There were no major differences noticed between the infected and uninfected skin models macroscopically, during the time of incubation. Microscopically, for each treatment group, six slides were analyzed. The HE and immunohistochemical staining and microscopy were conducted by Prof. Robert Klopfleisch. Histological images obtained from uninfected rafts stained with HE revealed a fully differentiated epithelium consisting of epidermis and dermis. Four epidermis cell layers were distinguished: the *stratum basale* with keratinocytes arranged in a palisade-like pattern, a thin

layer of *stratum spinosum*, the *stratum granulosum* keratinocytes, with a predominantly flattened appearance and the *stratum corneum*, where individual cells could no longer be distinguished (Figure 16). The 3D skin tissue infected with CPXV BR and RatPox09 allowed virus replication with evidence of a cytopathic effect. Infection led to epithelial necrosis as well as epithelial and stromal proliferation, cytoplasmic swelling and ballooning of keratinocytes (Figure 16). The necrotic epithelial structures contained intracytoplasmic Guarnieri bodies (B-type inclusions) within the affected keratinocytes and showed. hyperplasia of epithelial cells and eosinophilic inclusion bodies in epithelial cells. However, we were unable to detect any differences in the tissue damage between the two CPXV strains (Figure 16).

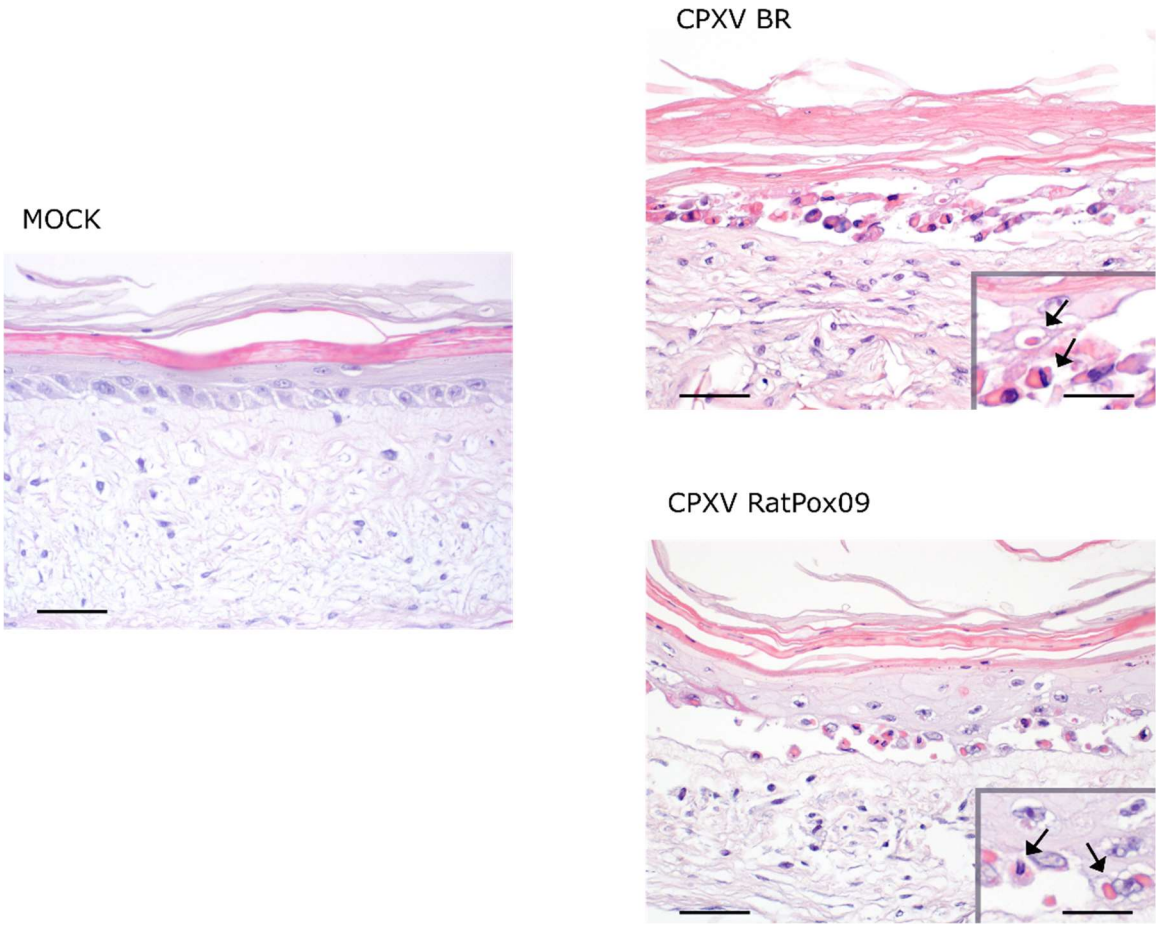

Figure 16. Sections of 3D skin models, mock-infected (MOCK) and infected with CPXV BR and CPXV RatPox09 and stained with HE. Infection with both virus strains led to epidermal necrosis and the presence of intracytoplasmic inclusion bodies. Bars, 50 µm. Insets show higher magnifications of epidermal cells with ballooning degeneration and intracytoplasmic inclusion bodies (arrows). Bars, 25 µm. Figure from a publication of Tamosiunaite et al (175). Reprinted by permission from Elsevier.

3.3.2. Analysis of Cell Cycle and Gene Expression in the Infected 3D Skin Culture Model

To confirm successful CPXV infection, the skin model was stained with CPXV anti-A27 protein antibody. The protein expressed by was detected in keratinocytes and some fibroblasts in all CPXV-infected skin tissues, while no A27 protein was detected in MOCK-infected skin

(Figure 17). In order to test the changes of cell cycle regulation in CPXV infected cells, skin models were stained with anti-histone H3 phospho S10 and cyclin B, D1 and E antibodies. The histone H3 phospho S10, cyclin B1, D1 and E expression was recognized both in mock- and

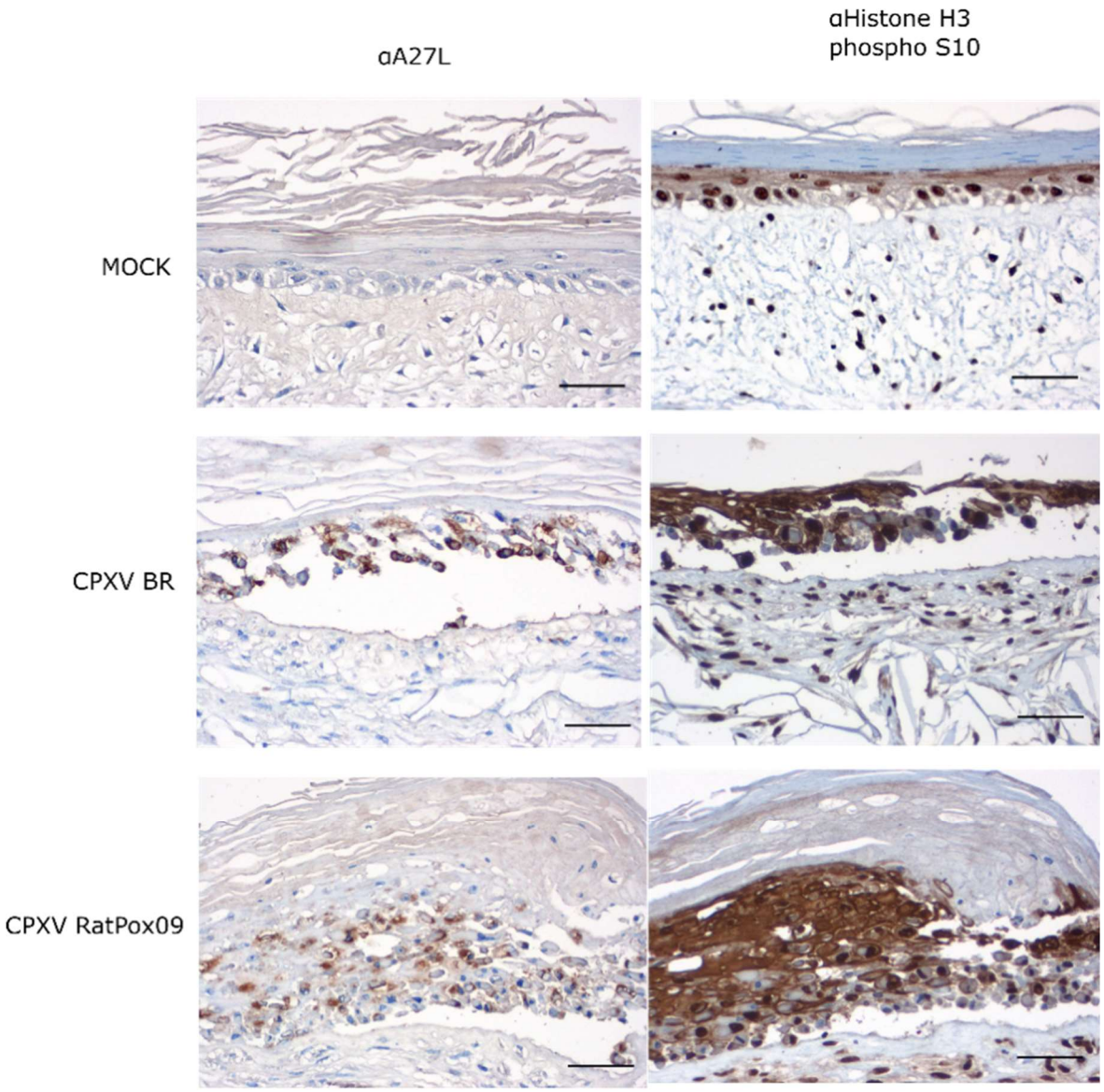

Figure 17. Sections of 3D skin models, mock-infected (MOCK) and infected with CPXV BR and CPXV RatPox09 were labelled with anti-A27L and anti-histone H3 phospho S10 antibodies. A27 and histone H3 phospho S10 expression was detected in epidermal cells infected with both virus strains. In addition, infected epidermal areas showed an increased expression of phosphorylated histone H3 phospho S10. Bars, 50 µm. Figure from a publication of Tamosiunaite et al (175). Reprinted by permission from Elsevier.

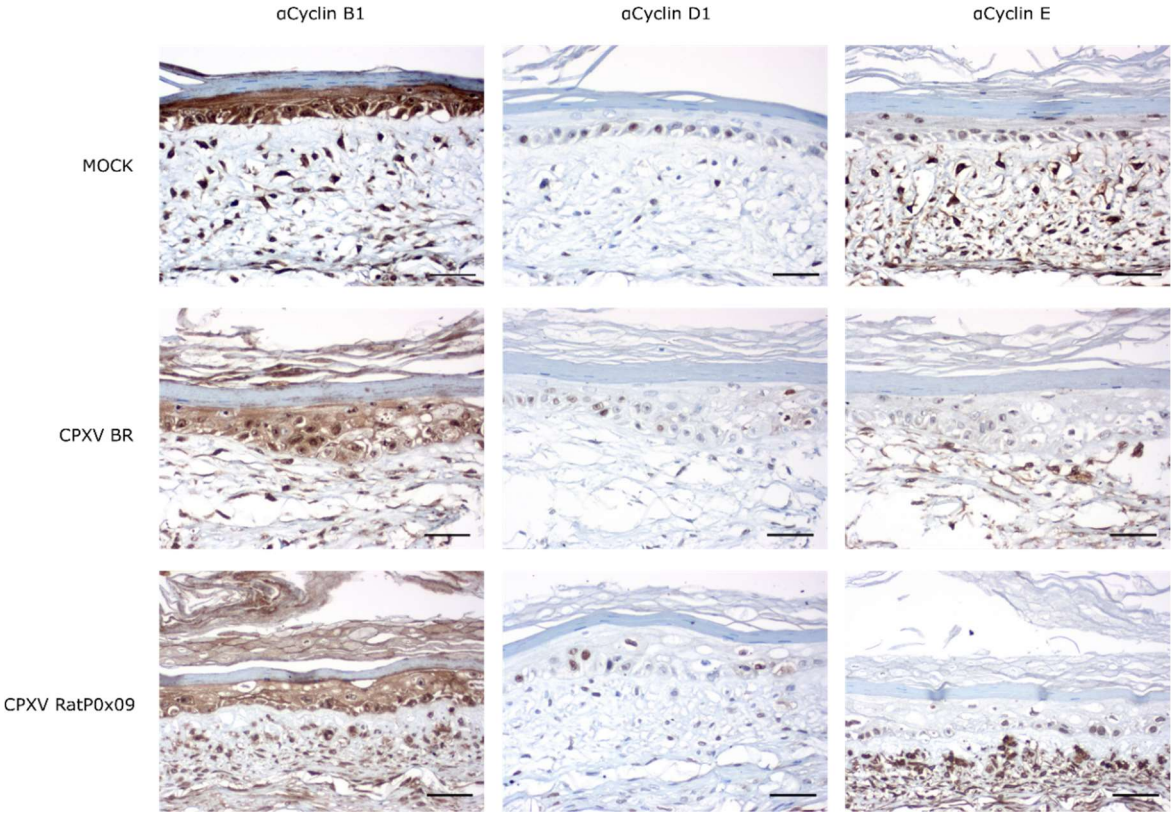

Figure 18. Sections of 3D skin models, mock-infected (MOCK) and infected with CPXV BR and CPXV RatPox09 were labelled with antibodies against cyclins B1, D1 and E. Infected epidermal areas showed a decreased labelling intensity for cyclin D1, while cyclins B1 and E expression was not altered. IHC. Bar, 50 µm. Figure from a publication of Tamosiunaite et al (175). Reprinted by permission from Elsevier.

CPXV-infected skin. Histone H3 phospho S10 was expressed more strongly in infected than non-infected cells (Figure 17). Cyclin D1 was expressed at slightly reduced levels in infected tissue when compared with non-infected cells (Figure 18). However, no differences in the cell cycle patterns between BR, RatPox09 or chimeric virus-infected raft cultures were detected (Figure 18).

3.4. Virus growth kinetics

The replication abilities of the parental wt Ratpox09 and the BAC derived BR and the knock-in mutants, as well as chimeric viruses, that were confirmed by NGS, were measured. Multiple-step growth analyses were conducted by Annika Franke in Vero76 cells at different time points. The various recombinant viruses replicated in titers comparable to those of parental viruses and no statistically significant differences could be revealed. (Figure 19) (Kruskal-Wallis test, $p>0.05$).

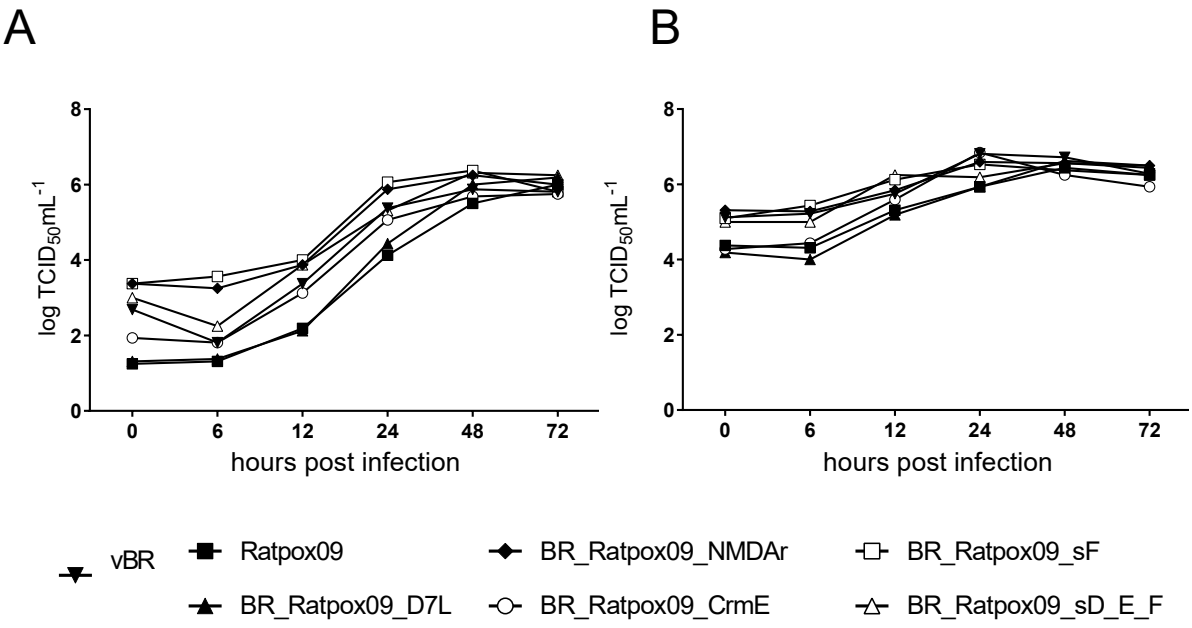

Figure 19. Comparison of replication characteristics of vBR, RatPox09, BR_Ratpox09_NMDAr, BR_Ratpox09_D7L, BR_Ratpox09_CrmE, BR_Ratpox09_sF and BR_Ratpox09_sD_E_F on Vero76 cells infected with MOI of 0.01 (A) or 3 (B). Virus growth was measured time points post infection and virus titers were determined by endpoint dilution assays. The means of two independent experiments are shown, including technical replicates.

3.5. *In vivo* experiments

In order to test the impact of insertion of single RatPox09 genes, NMDAr and CrmE, and genomic segment F into BR, on the course of the disease in rats, animal studies were completed. *In vivo* experiments were conducted in the Friedrich-Loeffler-Institut by Annika Franke and Donata Hoffmann. Rats were infected intranasally with $10^{5,5}$ TCID 50 /animal of wt CPXV BR, BAC derived BR; wt RatPox09, BR_RatPox09 CrmE, BR_RatPox09 NMDAr, BR_Ratpox sF, respectively. Following infection, rats were observed daily for clinical signs of disease. On days 4 to 6 pi, the first clinical signs were registered: nasal discharge, rough fur and loss of activity. Later in the course of the disease the body weight loss, respiratory distress and inflated stomach were absorbed. In addition, one with BR_RatPox09 CrmE infected Wistar rat developed pox-like rash on the nose 9 dpi (Figure 20). Moreover, Wistar rats infected with wildtype strain CPXV BR, BAC derived CPXV BR or Segment F chimeric virus showed no or only very mild clinical symptoms, these Wistar rats survived the infection and recovered. Unsurprisingly, rats infected with RatPox09, BR_RatPox09 NMDAr, BR_RatPox09 sF attained clinical score significantly higher than parental BAC derived BR infected animals

Figure 20. Pox-like lesions of a Wistar rat. Wistar rat- infected with BR_Ratpox09_CrmE developed pox-like lesion on the nose. Image was taken at 9 days' pi. Picture taken by Annika Franke (Friedrich-Loeffler-Institut).

($p \leq 0.05$, Anova) (Figure 21 A). As can be seen in Figure 21 B, 6 out of 8 RatPox09, 2 out of 10 BR_RatPox09 NMDAr and 1 out of 10 BR_RatPox09 CrmE infected rat had to be euthanized between 8 and 13 dpi as their health declined. Viral shedding was detected in all animal groups, between 3 and 13 dpi (Figure 21 C). The most virus was shed on 7th day post infection. Generally, animals infected with BR_RatPox09 CrmE and RatPox09 shed the most virus. (Figure 21 C). On day 7 pi, single RatPox09 infected rats shed up to $10^{4,9}$ TCID 50 ml^{-1} or $10^{3,3}$ TCID50 ml^{-1}, in the case of BR_RatPox09 CrmE infection. The highest virus shedding patterns were seen in the rats, that also had the strongest clinical symptoms. The clinical score of these animals reached 7 and higher, therefore they were euthanized on 9th pi. 15 days after inoculation, no virus shedding was detected in any of the infected Wistar rats (Figure 21C). Virus distribution in various organs was determined by real-time PCR and by end point dilution assay (Table 8). All rats that reached high clinical scores, scored positive for virus in trachea samples (9/9 animals) as well. Nonetheless, the highest viral loads were found in the rhinarium. Rats infected with RatPox09 had viral loads of up to $10^{7,8}$ TCID50 ml^{-1} in this organ, while virus titers in the trachea of Wistar rats reached $10^{5,18}$ TCID50 ml^{-1}. In the blood samples from RatPox09 infected Wistar rats that had succumbed to infection on day 7th dpi no CPXV-specific antibodies were found. Nonetheless, antibodies against CPXV were detected in all the other infected rats (data not shown).

		Rhinarium	Trachea	Lung 1	Lung 2	Liver	Spleen	Skin
	wt BR	0/8	0/8	0/8	0/8	0/8	0/8	0/8
	vBR	0/8	0/8	0/8	0/8	0/8	0/8	0/8
21 dpi	BR_RatPox09_NMDAr	0/8	0/8	0/8	0/8	0/8	0/8	0/8
	BR_RatPox09_CrmE	0/9	0/9	0/9	0/9	0/9	0/9	0/9
	RatPox09	0/2	0/2	0/2	0/2	0/2	0/2	0/2
	BR_RatPox09_sF	0/10	0/10	0/10	0/10	0/10	0/10	0/10
8 dpi	BR_RatPox09_NMDAr	0/2	0/2	0/2	0/2	0/2	2/2	2/2
8 -11 dpi	RatPox09	6/6	6/6	3/6	5/6	4/6	4/6	5/6
13 dpi	BR_RatPox09_CrmE	0/1	1/1	0/1	0/1	0/1	0/1	1/1

Table 8. Virus detection in various organs. qPCR and virus titration results for the infection experiments with CPXV wt BR, vBR (BAC derived BR), BR_RatPox09_NMDAr, BR_RatPox09_CrmE, BR_RatPox09_sF and RatPox09.

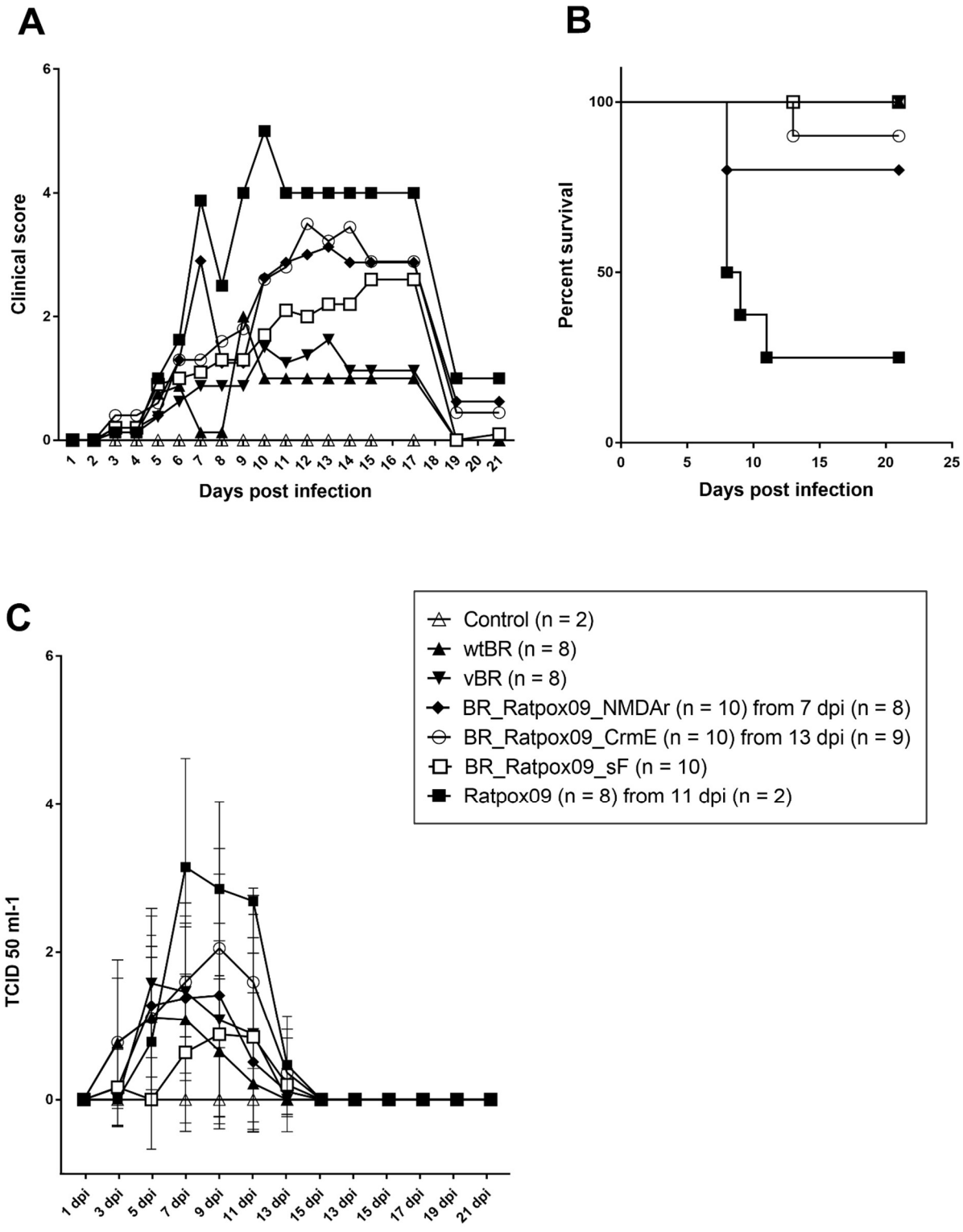

Figure 21. Characterization of the CPXV infection in rats. (A) Rat CPXV infection clinical score over time of rats infected with $10^{5.5}$ TCID 50 /animal. (B) Rat survival over time (C) Viral shedding patterns of infected Wistar rats.

4. Discussion

Molecular characterization of OPVs isolated from different geographic regions or hosts is a valuable tool, that helps to identify their geographic distribution, phenotypic variability and evolution. Even more importantly, it is crucial for monitoring the emergence of new atypical OPV strains with enhanced virulence. Today, DNA sequence data provide the key information for defining of the phylogenetic relationships between species, which sequentially provides the basis for comparative approaches for biological investigation.

Most of the earlier studies about OPVs were performed with VACV, which lacks functional copies of several OPV genes (25), although, CPXV, less investigated OPV, owns the most complete genome not only in terms of number of genes, but also in terms of the most of unique ORFs (167). Consequently, CPXV was even proposed to be the closest to the common ancestor of OPVs (167). Therefore, investigation of the genetic organization of cowpox virus is of special interest. Moreover, this species has the widest host range among the poxviruses, it can even cause disease in humans. Clearly, CPXV is a pathogen, that is able to multiply in different molecular environments and to overcome defensive mechanisms of various mammalian species (110). In recent years, the interest in this zoonotic disease has been renewed, due to increasing cases of human cowpox virus infections (137-139, 150). Moreover, these infections mostly affect young nonvaccinated persons.

The knowledge of virulence factors of newly appearing CPXV field strains is vital for the risk assessment of the viruses sustained in rodents and cats. With this in mind, we focused our work on newly isolated CPXV strain RatPox09. CPXVs RatPox09 and reference strain BR are genetically highly similar. However, the disease outcomes after infection with these two strains differ substantially (119).

4.1. Generation of recombinant BR, with putative RatPox09 virulence markers inserted

Comparison of all available CPXV sequences shows that there is no identifiable virulence related pattern of viral genome sequence nor a specific ORF, which would directly associate with the pathotype of the highly pathogenic isolate, Ratpox09. Nevertheless, a set of four genes: CPXV0284, CPXV0030, CPXV0002, and CPXV0003, which are encoded by RatPox09, but not by the low-virulent BR nor most of the sequenced CPXV, was recognized. Moreover, the sequence of the poxvirus genes ATI and p4C differ highly between these two strains (119). In this study, my aim was to generate BR gain-of-function mutants. But beforehand we analyzed the sequence of gene products of major difference and related literature, if available data supports a possibility of these genes being virulence markers.

The protein encoded by CPXV0002 has 99 % identity with CPXV protein, indicated and named N-methyl-D-aspartate (NMDA) receptor like protein by Carrol et al (145). Therefore, further in this study CPXV0002 were named NMDAr. However, various predictions showed no indication to the similarity of CPXV0002 to NMDA receptor like proteins (173). Furthermore, this protein has 98 % identity with Vaccinia Golgi anti apoptotic protein (VACV GAAP). Even more surprisingly, database searches found high sequence similarity to a human protein S1R (73% identity, h-GAAP) of unknown function. Moreover, BLAST searches with CPXV0002 identified closely related, lifeguard protein in various mammals, like cattle (78% identity),

mouse (74% identity), and rat (74% identity) to be highly related to CPXV0002 (Figure 7). The comparison of the sequences of all putative GAAPs revealed, that GAAPs are very conserved in sequence and even lenth. All putative GAAP's show conserved hydrophobicity profile and are predicted to have six or seven transmembrane domains (92). Consequently, The PFAM program recognized CPXV0002 similarity to the UPF0005 protein family. Members of this family are as well predicted to contain six to seven transmembrane domains (173). A characterized UPF0005 family member, Bax inhibitor-1, were shown to protect cells against ER stress. This protein was found to have 45% similarity to VACV GAAP. (176, 177). Both human and VACV GAAPs were shown to inhibit a various proapoptotic stimuli (92). The human GAAP (hGAAP) is abundantly found in all human tissues tested, it was also shown to be crucial for cell viability (92, 178). Taken together, we identified RatPox09 NMDAr as possible, immunomodulatory protein, which could contribute to increase of pathogenicity in the CPXV strain RatPox09.

CPXV-BR CrmE was shown to be not functional, due to stop-codons and sequence deletions, some of which are found as well in MPXV and ECTV CrmE pseudogenes (103). Interestingly, CPXV0003 (CrmE) is fully intact in CPXV RatPox09. CrmE has been shown to be a soluble TNFα receptor with both soluble and membrane vTNFR activity and it is encoded by many OPV (179). In addition, VACV CrmE binds to TNFα from rat, mice and human but it was showed to only protect against human, but not mouse or rat TNF cytolysis *in vitro* (103, 180, 181).

CPXV0284 has 92 % identity with D7L protein of CPXV GRI-90, therefore in this study it was named D7L. Data analysis revealed D7L to be kelch-like protein with unknown function. The kelch motif is a motif, that is 44–57 aa long and commonly occurs as 4–7 repeats, forming a tertiary b-propeller structure (182). The PFAM program indicates the BTB/POZ domain, between the 31 and 131 aa of D7L (173). BTB/kelch proteins are the largest subgroup of the kelch superfamily (183). These proteins are recognized by a BTB (broad-complex, tramtrack and bric-a-brac) domain in the N-terminal end and kelch repeats in the C-terminal part. BTB/kelch proteins are expressed by several poxviruses. The BTB domain was reported to play part in protein–protein interactions and to dimerize the BTB/kelch protein, while the kelch domain mediates a variety of binding interactions with other molecules (185). The POZ domain was shown to mediate homo- or heteromeric protein interactions and is present in several zinc-finger proteins and in a subgroup of kelch proteins (184, 185). It has been speculated, that proteins containing the BTB domains function as substrate-specific adapters for the cullin-3 ubiquitin ligase complex (186-189). Consistent with the prediction, the ectromelia virus kelch-like proteins EVM018, EVM027, EVM150, and EVM167 indeed associate with conjugated ubiquitin, when interacting with cullin-3 and the ubiquitin ligase Roc1 (184, 190). Recently, EVM150 was identified as an inhibitor of the NF-κB pathway, hence innate immune signaling (191). It also has been experimentally demonstrated that a deletion of individual ectromelia virus genes, EVM18, EVM27, or EVM167, radically decreases the ECTV virulence in white mice, even though the damage of EVM150 gene has no effect on the virulence (192). Deletion mutants of four kelch like proteins in CPXV resulted in a significant reduction of weight loss in infected mice (193). It is tempting to speculate, that the RatPox09 D7L homologue CPXV0284 is also involved in the formation of active CUL3-containing ubiquitin ligase complexes and interferes with innate immune signaling in a species-specific fashion.

The protein encoded by CPXV0030 has 99 % identity with CPXV 7-transmembrane G protein-coupled receptor-like protein (7tGp) (145), a receptor-like protein of unknown function. This ORF coding sequence could only found in two other CPXV virus strains, Ger91-3 and FRA2001. Although named after known chemokine receptors featuring 7 transmembrane

helices, various secondary structure predictions do not confirm such a topology. Rather, the 7tGP-like protein, while featuring several hydrophobic helices, likely is more alike to the B21R/B22R proteins. Recently the CPXV and MPXV B21/B22R proteins, encoded by the genes with the longest sequence of these viruses, were shown to be expressed early in infection and cleaved into C - terminal fragments and N- terminal fragments in the case of CPXV 219 (194). These proteins have a signal peptide and are transited through the secretory pathway where extensive glycosylation and proteolytic cleavage occurred. Previous reports have indicated, that these proteins make human T cells unresponsive to stimulation by both MHC-dependent antigen presentation and by MHC-independent stimulation (194, 195). Main mechanism that CD4+ T cells use to identify APCs (antigen – presenting cell) and CD8+ T cells use for identification and removal of virus-infected cells is indeed the T cell activation with peptide and MHC complexes. Not surprisingly numerous viruses are in use of various tactics to disrupt antigen presentation or to inhibit the ability of T cells to respond to antigen. (196). However, most of MHC-inhibitors are unable to stop T cell activation by MHC-I cross-presentation or by non-infected APC processing exogenous antigens by MHC-II presentation. Interestingly, B22 proteins seem to permit poxviruses to affect the TCR-dependent T cell activation no matter what stimulatory pathway is being used. This protein function could be even restored in a MPXV197 deletion mutant by its CPXV homologue, CPXV219. The detailed function of MPXV197 and its CPXV homologue have not yet been elucidated, but secondary structure predictions of the proteins of MPXV and CPXV are strikingly similar to that of the 7tGP-like protein. However, the authors discuss that the MPXV197 protein is a determinant of host specificity (194). We hypothesize that the relative of MPXV197 and CPXV219 has a similar immunomodulatory function and is a determinant of host range.

ATI and the p4c gene are shorter in RatPox09 in comparison to BR which is unique to CPXV strain RatPox09. ATIs are composed of multiple copies of the ATI viral protein (64). The embedding of mature virions (MV) within ATIs, that leads to their occlusion and possibly ensures extra-host survival, requires the p4C protein (197, 198). P4C is a protein anchored in the mature virions membrane by interactions with the A27-A17 complex (62, 199). Kastenmayer and coworkers (200) constructed and characterized ATI and p4c deletion mutants of the GER1991_3 CPXV strain. Mice inoculated intranasally with the ATI deletion mutant lost significantly more weight, indicating that ATI may be a virulence determinant. In previous studies, both CPXV strains were shown to be capable of composing ATI's but not directing IMVs to ATI, probably due to deletions in p4C gene (62, 119). Moreover, the C-terminal part of BR and RatPox09 p4C remains intact, and most possibly functional. Chang and colleagues have showed that a synthetic A26 peptide, containing the C-terminal coiled-coil region of the A26 protein, can partially inhibit cell fusion, when it is induced by WR A26L deletion mutant infections in a dosage-dependent manner (63). This implies that the A26 protein can inactivate viral fusion through modulation of the coiled-coil interaction with the A27 protein even in the absence of the A25 protein (63).

Markerless *en passant* Red recombination, a technique developed by Tischer et al (162, 163), was used to generate mutants with individual and multiple RatPox09 genes introduced in BR genome (Figure 10). One of the main advantages of *en passant* Red recombination is that the marker cassette is removed from the final construct and integrity of the mutated region is largely restored. Moreover, this technique allows the introduction of very small and larger modifications, keeping the overall sequence changes and bystander effects low (162, 163). With the help of this method, all of the previously discussed genes were successfully inserted in the BR genome. This allows the analysis of the impact of individual putative virulence factors, combination of putative virulence factors for the overall pathotype of the virus. All mutants were analyzed by full genome sequencing. Thenceforth, the mutants constructed correctly were

characterized *in vitro*. *In vitro* growth curves did not reveal any significant differences between RatPox09, BR or generated mutant viruses, that were later used in animal experiments (Figure 19).

4.2. Generation of chimeric viruses.

Besides these six analyzed genes we found small genetic modifications of unknown impact scatter all over the RatPox09 genome. To make an analysis of the impact of minor genetic change in parts of genome on the increase of RatPox09 virulence possible, we used a novel approach to generate BR-RatPox09 chimeric viruses in which blocks of 20 to 40 kbp genome segments or combinations of multiple genome segments from RatPox09 replaced the authentic BR sequences (Figure 15). This was accomplished by combining seamless *en passant* Red recombination and homologues recombination in cell culture. Red recombination was used for deletion of segments of interest from pBRF and recovery of segments of interest from partial RatPox09 BACs. Unfortunately, there was no full length RatPox09 BAC available and the partial RatPox09 BACs, used in this study, didn't cover the sequence of the segments A and G (Figure 11). Poxviruses do not produce a circular form of virus genome during replication, what makes the transfer of the recombinant poxvirus constructs into *E.coli* a significant challenge. To overcome this issue, infected cells were treated with isatin-β-thiosemicarbazone, that promotes accumulation of nonresolved, genomic concatemers (155-157). However, this strategy were not completely successful, and only partial BACs were generated. Another strategy, reposition of mini-F closer to the inverted terminal repeats, were implied as well. However, this didn't provide expected results either (Xu, unpublished data). With the partial BACs without the A and G segments, we were not able to generate chimeric viruses with these segments exchanged. Nevertheless, the four genes, that represent the major genetic differences in these two segments, were separately introduced into the BR genome as discussed in the previous section. Since the attempts to insert 20 kb to 40 kb fragment to CPXV BR genome *via* Red recombination were not successful due to the high amount of mutations in the large PCR products, for the generation of chimeric viruses the final modifications were made in the cell culture. The Vero cells were transfected with pBRF deletion mutants and RatPox09 genome segments. Chimeric viruses were recovered using fowlpox virus or shope fibroma virus as a helper. Later, miniF vector sequences present in pBRF were removed and the thymidine kinase gene repaired by transfection with a TK-containing plasmid. Before further experimentation, all mutant viruses were confirmed by whole-genome sequencing. Interestingly, nearly 20 % of the mutants had to be corrected or repeatedly generated, demonstrating the need of NGS confirmation. Even though BAC technology was used, the last step of chimeric virus generation was recombination in the cell culture and all identified sequence modifications were located within the less conserved and less stable terminal part of the CPXV genome, where higher mutation rates are expected and often seen (201).

4.3. Cowpox virus replication in a three-dimensional skin model

We tested the suitability of a 3D skin model to assess CPXV replication and virulence prediction by investigating the tissue damage, cell cycle status and regulation in the Phenion® Full-Thickness Skin Model infected with CPXV BR and RatPox09 strains. The Phenion® Full-Thickness Skin Model resembles native human skin in its histological organization. This model consists of human primary fibroblasts and keratinocytes from single donor origin. Organotypic epithelial raft cultures has been already described as a substitute for animal models (203). Moreover, the pathogenesis of several different viruses, including papillomaviruses, adenoviruses, parvoviruses, poxviruses and herpesviruses were tested onto 3D skin substitutes (202, 204). In the case of poxviruses, they were used to test pharmacokinetics of antiviral drugs

for CPVX and VACV infections (205, 206). The previous studies have shown, that he cytopathogenic effects of poxvirus infected organotypic skin raft cultures are comparable to those seen in clinical lesions induced by poxviruses (205, 206). This makes the skin model preferable model to CAM, which is often used in CPXV research. Even though, chicken (*Gallus gallus domesticus*) is not a natural host to CPXV and the CAM composed of chorionic epithelium, the mesenchyme and the allantoic epithelium doesn't represent mammalian tissue.

In this thesis, the cells were infected with 10^5 $TCID_{50}$ of CPXV BR and RatPox09. CPXV infection of the 3D skin model caused cytopathic effects, including ballooning keratinocytes and intracytoplasmic Guarnieri bodies as seen in histological sections of infected mammal skin after systemic or local *in vivo* infection. Productive CPXV infection of the 3D skin model was confirmed by anti-A27 antibody staining (Figure 17). Interestingly, there were no differences in tissue damage recognized between CPXV RatPox09 and Brighton Red infected 3D skin models (Figure 16).

Previous research has documented, that two well-known poxviruses, VACV and Myxoma virus, alter the cell cycle progression (207- 209). To analyze the impact of CPXV BR and RatPox09 infection on the cell cycle status in a 3D skin model, cell cycle markers were indicated with monoclonal and polyclonal antibodies. As a marker of M phase cells, anti-Histone H3 phospho S10 antibody was used (210). Histone H3 phospho S10 was strongly expressed in infected cells; interestingly, not only in the nucleus of infected cells, but also in the cytoplasm (Figure 17). Apparently, phosphorylation of the serine residue at position 10 of histone H3 is not only linked to highly condensed mitotic chromosomes and relaxed chromatin of some genes activated during Interphase (211). H3 S10 phosphorylation also occurs, when cells are exposed to various death stimuli (212). Another tested cell cycle marker, Cyclin B plays a role in control of the M phase while Cyclin E is important for G_1-S phase transition (213). Both cyclins were expressed similarly in CPXV infected and non-infected cells of the 3D skin model (Figure 18). As a marker for progression from G_0 to G_1, anti-Cyclin D1 antibody was used. Cyclin D1 was slightly down-regulated in infected cells (Figure 18). Although little is known about cyclin D1 down regulation during CPXV infection, previous reports have shown that shorter murine Schlafen (Slfn) gene, m-slfn1, encodes a protein that causes arrest of fibroblast growth by inhibition of cyclin D1 *in vitro* (214). It has been demonstrated that a single copy of Schlafen gene is present in all sequenced OPVs, CPXV included (215, 216). Phylogenetic analyses have shown the CPXV (BR and Ratpox09 alike) v-slfn genes to be most closely related to the mouse and rat Slfn genes, including m-slfn1 (215). Therefore, it would be tempting to speculate, that the expression of CPXV Schlafen homolog may cause a slight reduction of cyclin D expression, as seen in CPXV infected skin model. However, future studies will be necessary to either confirm or deny it.

In conclusion, this study has shown that, while CPXV skin replication can be successfully modeled using this *in vitro* system, an evaluation of overall virulence of different CPXV strains is not possible, likely because key steps in the pathogenesis such as development of viremia and innate or non-specific immune response is absent.

4.4. Animal experiments

Previous infection experiments with CPXV BR and Ratpox in Wistar rats were conducted and published by Hoffmann et al, Kalthoff et al and Breithaupt et al (119, 158, 160). The experimental design of this thesis complied with these experiments published previously. An infectious dose of $10^{5.5}$ $TCID_{50}$ per animal was chosen and 5 -week old Wistar rats were infected with mutant viruses with Ratpox09 NMDAr and CrmE, ORFs with homologs of known

function in VACV, inserted and genomic segment F chimera virus. As well the segment F chimera were selected for animal studies. The segment F contains ATI and p4c genes, the sequence of these two genes differs between BR and Ratpox09. Moreover, control groups infected with either RatPox09, wild type BR or BAC derived BR, were included. Furthermore, two additional rats served as noninfected negative controls. Over a period of 21 days, the rats were monitored daily and nasal swabs were taken every other day. Rats infected with the CPXV BR and segment F chimera showed only mild symptoms: nasal discharge, moderate activity and rough fur. These results are consistent with clinical signs described for CPXV BR infections in rats in previous studies (119). Furthermore, most animals infected with Ratpx09, CrmE and NMDAr mutant viruses exhibited more severe symptoms: inflated stomachs, moderate to severe respiratory distress and body weight loss. Similar clinical signs were registered in previous RatPox09 infection (158, 160). Nevertheless, Kalthoff et al previously described the development of pox like lesions in all RatPox09 infected Wistar rats, when during this study, only one, BR_RatPox09 CrmE infected, rat developed pox like lesion (160). This might be explained, rats with severe course of the disease were euthanized early in this study and pox like lesions were shown to develop in later stages of disease. Similarly, in the study of Breithaupt et al, intranasally RatPox09 infected rats were euthanized 8 dpi and only 1 out of 5 animals developed pox like lesion. Unsurprisingly, 6 of the 8 RatPox09 infected Wistar rats had to be euthanized as their health deteriorated dramatically. In previous reports, up to 100 % mortality rates of rats infected with RatPox09 were described (158, 160). Additionally, 2 out of 10 with BR_RatPox09 NMDAr and 1 out of 10 BR_RatPox09 CrmE infected rats succumbed to the disease. When no CPXV BR and BR_RatPox09 sF rats were euthanized before the end of the experiment. (Figure 20 B). Moreover, the RatPox09, NMDAr and CrmE mutants, but not segment F chimera, infected rats attained significantly higher clinical scores than BAC derived BR or wt BR infected rats ($p \leq 0.05$, Anova) (Figure 20 A).

Somewhat counterintuitive, a study by Gubser et al have shown, that mice infected with a VACV vGAAP (98 % similarity with RatPox09 NMDAr) -negative mutant had more severe illness and higher virus titer in lungs (92). However, there were quite a few differences in the experimental design in comparison with our study. First of all, the mutants were generated homologues recombination in cell culture, when in this study RatPox09 NMDAr gene was inserted using *en passant* Red recombination and the final generated viruses were confirmed by full genome sequencing. Secondly, the contribution of GAAP to VACV virulence were tested in VACV background and a murine model. Whether the reason of this different observation is related to the different virus and animal model or differences of method used for generation of the mutants, remains an open question.

Nevertheless, the induction of stronger symptoms with CPXV BR with RatPox09 CrmE inserted was in line with data published for VACV. VACV CrmE is a well described virulence factor. Deletion of CrmE in VACV strain USSR in intranasal mouse infection model resulted in a lower weight loss in mice, whereas overexpression of the protein led to an increased virulence (103). Nevertheless, all analyzed symptoms were of a more general nature: severe clinical signs, such as pox lesions, were not detected in wild type and mutant virus infected animals.

Summing up the results, it can be concluded that, insertion of sequence of putative RatPox09 genes, NMDAr and CrmE, but not the genomic segment F, into strain BR, results in increase of pathogenicity. However, the insertion of these individual ORFs is not sufficient to recreate the pathological effect of RatPox09. It is tempting to speculate, that combination of these two ORFs or/and addition of putative genes D7L and 7tGp leads to the increase of pathogenicity of RatPox09.

5. Outlook

So far, only a couple of generated mutants were used to assess the effect of the putative newly recognized virulence factors on the course of the disease in the *in vivo* model. Since the putative genes CrmE and NMDAr were identified to contribute to increase of RatPox09 virulence, but not sufficient to recreate RatPox09 pathotype, mutants with combination of these ORFs and other putative virulence markers inserted, will be tested in rat model.

Moreover, it would be interesting to investigate the antiapoptotic function of CPXV NMDAr protein. This could be achieved by apoptosis essays adapted from the work of Carrara and colleges (216). Additionally, the putative CPXV BTB/kelch protein D7L could be tested for interactions with cullin-3 and inhibition of NF-κB signaling. This could be evaluated by assessing the interactions between cullin-3 and the virus-encoded BTB/kelch protein by means of co-immunoprecipitation and co-localization using confocal laserscan microscopy. Intracellular localization of NF-κB (nuclear translocation of p65) can be determined by indirect immunofluorescence and live cell imaging after stimulation with recombinant human, murine and rat TNF-α or IL-1α. In the future experiments, the subcellular localization of D7L in infected cells can be determent. For that purpose, Vero cells as well as rat and vole fibroblasts can be transfected with eGFP-expressing RatPox09-D7L and pcDNA-Flag-cullin-3 expression plasmids and half of the cells subsequently infected with parental CPXV RatPox09.

To functionally characterize the CPXV 7tGP, the subcellular localization using a specific polyclonal antibody that we are currently generating should be determined. Using various truncated versions of the proteins and mutants in which the one prominently predicted C-terminal transmembrane domain is deleted, combined with cell surface biotinylation the putative topology of the protein in membranes can be determined. To monitor the hypothesized subversion of T cell responses by CPXV 7tGP, the protocol developed by Alzhanova and colleagues can be adapted (193). We also predict that the function of 7tGP in inducing T cell anergy may be species-specific, such that 7tGP may only be active in a rodent (vole) setting as a major factor of adaptation.

In summary, I have identified CPXV genes that contribute or might contribute to CPXV virulence and generated mutants that can be used for further investigation. Further studies should be directed at addressing the role of these proteins.

Summary

New cowpox virus (CPXV) infections occur naturally in Germany in increasing numbers. It is striking that an infection of the pet rats with these newly occurring CPXV strains often leads to a lethal outcome. Likewise, a CPXV isolate from a pet rat that as well caused human infection in Southern Germany, RatPox09, causes severe disease in Wistar rats, whereas infection of rats with the well-characterized strain Brighton Red (BR) results only in mild symptoms. Nevertheless, these two strains are highly similar on genomic level: the calculated sequence identity between RatPox09 and BR is 92%. However, with the help of proteome similarity plots, six products with major differences between RatPox09 and BR were identified. Though, minor sequence modifications of unknown impact were found dispersed all over the genome too. The thesis at hand, concentrates on genomic differences between the two CPXV strains, mentioned above. First of all, we analyzed the sequence of the genes of major differences and we generated gain of function mutants with single or multiple genes exchanged. Secondly, for identification of additional virulence factors, we used a novel approach to generate BR-RatPox09 chimeric viruses with approximately 20-40 kbp genome segments exchanged. This was achieved by combining markerless *en passant* Red recombination and a classical method, homologous recombination in infected vertebrate cells. Since, these CPXV strains of different pathogenic potential *in vivo*; shows similar growth characteristics *in vitro*, animal model seems to be the only suitable method to test the virulence of the recombinant viruses. Nevertheless, *in vivo* models, are not favorable experimental models due to many reasons, including: aspects of animal protection, their long duration and high requirement of labor. In search of a way to reduce the need for animal experiments for testing new recombinant viruses, we evaluated a three-dimensional (3D) skin model as a possible surrogate for animal experiments. We monitored CPXV lesion formation, viral gene expression and cell cycle patterns after infection of 3D skin cultures with RatPox09 and BR. Infected 3D skin cultures exhibited histological alterations that were similar to those of mammal skin infections, but there were no differences in gene expression patterns and tissue damage between the two CPXV strains in the model system. To be brief, 3D skin cultures reflect the development of pox lesions in the human skin, but seem not to allow differentiation between more or less virulent virus strains, a distinction that is made possible by experimental infection in suitable animal models. Therefore, *in vivo* infection model was applied. CPXV RatPox09 and NMDAr and CrmE mutants, but not segment F chimera, infected rats attained significally higher clinical scores than BAC derived BR or wt BR infected rats ($p \leq 0.05$, Anova). However, 6 out of the 8 RatPox09 infected Wistar rats had to be euthanized as their health deteriorated dramatically. Although only 2 out of 10 with BR_RatPox09 NMDAr and 1 out of 10 BR_RatPox09 CrmE infected rats succumbed to the disease. But none of CPXV BR and BR_RatPox09 sF infected rats did. Summing up the results, it can be concluded that, insertion of sequence of putative RatPox09 genes, NMDAr and CrmE, but not the genomic segment F, into strain BR, results in increase of pathogenicity. However, the insertion of these individual ORFs is not sufficient to recreate the pathological effect of RatPox09.

Zusammenfassung

Die Virulenzfaktoren des Kuhpockenvirus

Die Zahl der Kuhpocken Virus Infektionen in Deutschland steigt beständig. Dabei ist auffallend, dass die Infektionen bei als Haustier gehaltenen Ratten mit den neu auftretenden Kuhpocken Stämmen oft einen letalen Verlauf nehmen. Das Kuhpocken Isolat von einer Haustierratte, RatPox09, hat in Süddeutschland auch zu Infektionen beim Menschen geführt. Gleichzeitig verursacht es bei Experimenten ernsthafte Erkrankungen bei Wistar Ratten, wohingegen die Infektion von Ratten mit dem gut charakterisiertem Brighton Red (BR) Stamm, nur zu schwachen Symptomen führt. Dabei ist anzumerken, dass diese beiden Stämme sich genetisch stark ähneln: Die berechneten Übereinstimmungen der Sequenzen von RatPox09 und BR ist 92%. Wie in vorheriger Publikation beschrieben, wurden sechs Genprodukte mit gravierenden Unterschieden zwischen RatPox09 und BR identifiziert. Zusätzlich wurden geringfügige Sequenz Modifikationen, mit unbekannten Wirkungen, über das Genom verteilt gefunden. Diese These konzentriert sich auf die genetischen Unterschiede der beiden Kuhpocken Stämme. Im ersten Schritt wurde die Sequenzen der möglichen Virulenz Faktoren analysiert, dann Brighton Red Einzelgen Knock-in Mutanten konstruiert, die die mögliche Virulenz Faktoren tragen. Im zweiten Schritt, zur Identifizierung zusätzlicher Virulenz Faktoren, wurde ein neuer Ansatz gefunden um BR-RatPox09 Chimäre Viren herzustellen, indem annähernd 20-40 kbp Genome Segmente ausgetauscht wurden. Das wurde mit Hilfe einer zweistufigen Red-Mutagenese erreicht. Zusätzlich wendeten wir noch eine klassische Methode an, die homologe Rekombination in infizierten Vertebraten Zellen. Dadurch, dass diese Kuhpocken Stämme mit sehr unterschiedlichem pathogenem Potential *in vivo*; welche aber sehr ähnliche Wachstumscharakteristiken *in vitro* zeigen, scheinen Tiermodelle die einzige angemessene Methode zu sein, die Virulenz der rekombinanten Viren zu testen.
Aus unterschiedlichen Gründen sind Tiermodelle nicht zu bevorzugen: einerseits des Tierschutzes wegen, aber auch ihre langen Laufzeiten und der hohe Bedarf an Laborkapazitäten sind ungünstig. Auf der Suche nach einer Methode den Einsatz von Tiermodellen bei den Tests neuer rekombinanter Viren zu reduzieren, haben wir ein dreidimensionales(3D) Hautmodell getestet, als einen möglichen Ersatz für *in vivo* Versuche. Es waren Kuhpocken Läsionen zu beobachten, wie auch virale Genexpressionen und Muster im Zellzyklus, nach der Infektion von 3D Hautkulturen mit RatPox09 und BR. Infizierte 3D Haut Kulturen zeigten histologische Veränderungen, ähnlich der infizierten Haut von Säugetieren, aber es gab keinen Unterschied in den Genexpressionsmustern und Gewebeschäden zwischen den zwei Kuhpocken Stämmen, in diesem Modellsystem.
Kurz gesagt, 3D Hautkulturen spiegeln die Entwicklung der Schädigung durch Pockenviren in der Menschlichen Haut wieder, erlauben aber keine Differenzierung zwischen mehr oder weniger virulenten Stämmen, eine Unterscheidung die durch experimentelle Infektion bei Tiermodellen aber möglich wird. Deswegen wurde die BR Mutanten in einem Infektionsmodell in Wistar Ratten *in vivo* getestet. Mit Kuhpocken RatPox09, NMDAr und CrmE Mutanten, aber nicht die Segment F Chimära, infizierte Ratten erzielten signifikant höhere klinische Werte als BR infizierte Ratten ($p \leq 0.05$, Anova).
Dabei ergab sich das 6 von 8 RatPox09 infizierte Wistar Ratten eingeschläfert werden mussten, da ihr gesundheitlicher Zustand sich dramatisch verschlechtertet. Obwohl nur bei 2 von 10 mit

BR_RatPox09_NMDAr und bei 1 von 10 mit BR_RatPox09_CrmE infizierten Ratten der Ausbruch der Krankheit zur Einschläferung führte.
Zusammengefasst kann die Schlussfolgerung gezogen werden, dass RatPox09 Gene NMDAr und CrmE, aber nicht das genetische Segment F, dazu beisteuern die pathogene Wirkung des CPXV RatPox09 Stamm zu verstärken. Es hat sich aber herausgestellt: Das Insertion dieser individuelle offenere Leserahmen in CPXV BR ist nicht ausreichend, um die pathologische Wirkung von RatPox09 zu erreichen.

References

1. **Moss, B**. Poxviridae: the viruses and their replication, 2007. Fields Virology, 5 ed, **2:**2905-2946.
2. **Van Regenmortel, M. H., C. M. Fauquest, D. H. Bishop, E. B. Carstens, M. K. Estes, S. M. Lemon, J. Maniloff, M. A. Mayo, D. J. McGoech, C. R. Pringle, R. B. Wickner.** 2000. Virus Taxonomy. Academic Press; San Diego.
3. **Fauquet, C. M., M. A. Mayo, J. Maniloff, U. Desselberger, L. A. Ball.** 2005. Virus Taxonomy: VIIIth Report of the International Committee on Taxonomy of Viruses; Academic Press (Elsevier): London, UK.
4. **Bratke, K. A., A. McLysaght, S. Rothenburg**. 2013. A survey of host range genes in poxvirus genomes. Infection, genetics and evolution. Journal of molecular epidemiology and evolutionary genetics in infectious diseases. **14**:406–425.
5. **Hughes, A. L., R. Friedman**. 2005. Poxvirus genome evolution by gene gain and loss. Molecular phylogenetics and evolution. **35**:186–195.
6. **Smith, G. L., and G. McFadden**. 2002. Smallpox: anything to declare? Nature Reviews Immunology. **2**:521-7.
7. **Henderson, D.A.** 2011. The eradication of smallpox—An overview of the past, present, and future. Vaccine. **295**: D7–D9.
8. **Parrino, J., and B. S. Graham.** 2006. Smallpox vaccines: Past, present, and future. The Journal of Allergy and Clinical Immunology **118**:1320-6
9. **Hopkins, D. R.** 1980. Ramses V. Earliest known victim? World Health .22-26**.**
10. **Fenner, F., D. A. Henderson, I. Arita, Z. Jezek, I. D. Ladnyi**. 1988. Smallpox and its eradication. World Health Organization.
11. **Baxby, D**. 1977. Poxvirus hosts and reservoirs. Archives of Virology, vol.55, **3**:169–179.
12. **Jenner, E**. 1909–1914. The Three Original Publications on Vaccination against Smallpox. P.F. Collier & Son: New York, NY, USA. Volume 38, Part 4 of 8.
13. **Moss, B.** 1996. Genetically engineered poxviruses for recombinant gene expression, vaccination, and safety. Proceedings of the National Academy of Sciences of the United States of America. 93(21):11341-8.
14. **Fenner, F.** 2000. Adventures with poxviruses of vertebrates. FEMS Microbiology Reviews **24:**123-133
15. **Fenner, F.** 1996. Poxviruses. In: Field's Virology, ed. Fields BN, Knipe DM, and Howley PM, 3rd ed., 2673–2702.
16. **Fenner, F., R. Wittek, K. R. Dumbell**. 1989. The Orthopoxviruses. Academic Press, Inc, San Diego, CA.
17. **Shah, S.** 2013. New threat from poxviruses. Scientific American **308:**66 - 71
18. **Parker, A., R. Nuara, M. L. Buller, and D. A. Schultz**. 2007. Human monkeypox: an emerging zoonotic disease. Future Microbiology, vol.2, **1**:17–34.
19. **Delhon, G., E. R. Tulman, C. L. Afonso, Z. Lu, A. de la Concha-Bermejillo, H. D. Lehmkuhl, M. E. Piccone, G. F. Kutish, D. L. Rock**. 2004. Genomes of the parapoxviruses ORF virus and bovine papular stomatitis virus. Journal of Virology. 20, **78**: 168–177.
20. **Nazarian, S. H., J. W. Barrett, A. M. Frace, M. Olsen-Rasmussen, M. Khristova, M. Shaban, S. Neering, Y. Li, I. K. Damon, J. J. Esposito, K. Essani, G**. **McFadden**. 2007. Comparative genetic analysis of genomic DNA sequences of two human isolates of Tanapox virus. Virus Research. **129**:11–25.
21. **Tulman, E., C. Afonso, Z. Lu, L. Zsak, G. Kutish, D. Rock.** 2004. The genome of canarypox virus. Journal of Virology. **78**: 353–366

22. **Lefkowitz, E. J., C. Wang, and C. Upton**. 2006. Poxviruses: past, present and future. Virus Research. **117**:105-118.
23. **Gubser, C., S. Hue, P. Kellam, and G. L. Smith.** 2004. Poxvirus genomes: a phylogenetic analysis. Journal of General Virology. **85**:105-117.
24. **Upton, C., S. Slack, A. L. Hunter, A. Ehlers, and R. L. Roper.** 2003. Poxvirus orthologous clusters: toward defining the minimum essential poxvirus genome. Journal of Virology. **77**:7590-7600.
25. **Hendrickson, R. C., C. Wang, E. L. Hatcher, and E. J. Lefkowitz.** 2010. Orthopoxvirus genome evolution: the role of gene loss. Viruses. **2**:1933-1967.
26. **Stanford, M. M., G. McFadden, G. Karupiah, G. Chaudhri.** 2007. Immunopathogenesis of poxvirus infections: forecasting the impending storm. Immunology and Cell Biology. **85**:93–102.
27. **Johnston, J. B. and G. McFadden**. 2004. Technical knockout: understanding poxvirus pathogenesis by selectively deleting viral immunomodulatory genes. Cellular Microbioly. **6**: 695–705.
28. **Alzhanova, D., and K. Früh**. 2010. Modulation of the host immune response by cowpox virus. Microbes and Infection. **12**:900-909.
29. **Barrett, J. W., J. X. Cao, S. Hota-Mitchell, G. McFadden**. 2001. Immunomodulatory proteins of myxoma virus. Seminars in Immunology. **13**:73–84.
30. **Haller, S. L., C. Peng, G. McFadden, S. Rothenburg**. 2014. Poxviruses and the evolution of host range and virulence. Infection, Genetics and Evolution. **21**: 15–40.
31. **Haig, D. M**. 2006. Orf virus infection and host immunity. Current Opinion in Infectious Diseases. **19**:127–131.
32. **Massung, R. F., J. C. Knight, and J. J. Esposito.** 1995. Topography of variola smallpox virus inverted terminal repeats. Virology. **211**:350-355.
33. **Smith, G. L., Y. S. Chan, S. T. Howard**. 1991. Nucleotide sequence of 42 kbp of vaccinia virus strain WR from near the right inverted terminal repeat. Journal of General Virology. 72:1349–1376.
34. **Baroudy, B. M., S. Venkatesan, and B. Moss**. 1982. Incompletely base-paired flip-flop terminal loops link the two DNA strands of the vaccinia virus genome into one uninterrupted polynucleotide chain. Cell. **28**:315-324.
35. **Geshelin P. and K. I. Berns**. 1974. Characterization and localization of the naturally occurring cross-links in vaccinia virus DNA. Journal of Molecular Biology. **88**:785– 796.
36. **Winters, E., B. M. Baroudy, B. Moss.** 1985. Molecular cloning of the terminal hairpin of vaccinia virus DNA as an imperfect palindrome in an Escherichia coli plasmid. Gene. **37**:221–228.
37. **Merchlinsky, M., C. F. Garon, B. Moss**. 1988. Molecular cloning and sequence of the concatemer junction from vaccinia virus replicative DNA. Viral nuclease cleavage sites in cruciform structures. Journal of Molecular Biology. **199**:399–413.
38. **Hiller, G. and K. Weber**. 1985. Golgi-derived membranes that contain an acylated viral polypeptide are used for vaccinia virus envelopment. Journal of Viroly. **55**:651–659
39. **Schmelz M., B. Sodeik, M. Ericsson, E. J. Wolffe, H. Shida, G. Hiller, G. Griffiths**. 1994. Assembly of vaccinia virus: The second wrapping cisterna is derived from the trans Golgi network. Journal of Viroly. **68**:130–147.
40. **Tooze, J., M. Hollinshead, B. Reis, K. Radsak, H. Kern**. 1993. Progeny vaccinia and human cytomegalovirus particles utilize early endosomal cisternae for their envelopes. European Journal of Cell Biology. **60**:163–178.
41. **Condit, R. C., N. Moussatche, and P. Traktman**. 2006. In a nutshell: structure and assembly of the vaccinia virion. Advances in Virus Research. **66**:31-124
42. **Hollinshead, M., A. Vanderplasschen, G. L. Smith, D. J. Vaux.** 1999. Vaccinia virus intracellular mature virions contain only one lipid membrane. Journal of Viroly. **73**:1503–1517

43. **Heuser, J**. 2005. Deep-etch EM reveals that the early poxvirus envelope is a single membrane bilayer stabilized by a geodetic "Honeycomb" Surface coat. The Journal of Cell Biology. **169**:269–283.
44. **Blasco, R. and B. Moss.** 1992. Role of cell-associated enveloped vaccinia virus in cell-to-cell spread. Journal of Viroly. **66**: 4170–4179.
45. **Sanderson, C. M., F. Frischknecht, M. Way, M. Hollinshead, G. L. Smith**. 1998. Roles of vaccinia virus EEV-specific proteins in intracellular actin tail formation and low pH-induced cell-cell fusion. Journal of General Virology. **79**:1415–1425.
46. **Dales, S. and L. Siminovitch.** 1961. The development of vaccinia virus in Earle's L strain cells as examined by electron microscopy. J Biophys Biochem Cytol. **10**: 475–503
47. **Armstrong, J. A., D. H. Metz, M. R. Young.** 1973. The mode of entry of vaccinia virus into L cells. Journal of General Virology. **21**:533–537.
48. **Carter, G. C., M. Law, M. Hollinshead, G. L. Smith**. 2005. Entry of the vaccinia virus intracellular mature virion and its interactions with glycosaminoglycans. Journal of General Virology. **86**:1279–1290.
49. **Huang, C. Y., T. Y. Lu, C. H. Bair, Y. S. Chang, J. K. Jwo, W. Chang**. 2008. A novel cellular protein, VPEF, facilitates vaccinia virus penetration into HeLa cells through fluid phase endocytosis. Journal of Virology. **82**:7988–7999.
50. **Mercer, J. and A. Helenius**. 2008. Vaccinia virus uses macropinocytosis and apoptotic mimicry to enter host cells. Science. **320**:531–535
51. **Mercer, J., S. Knebel, F. I. Schmidt, J. Crouse, C. Burkard, A. Helenius**. 2010. Vaccinia virus strains use distinct forms of macropinocytosis for host-cell entry. Proceedings of the National Academy of Sciences of the United States of America. **107**:9346–9351.
52. **Moser, T. S., R. G. Jones, C. B. Thompson, C. B. Coyne, S. Cherry.** 2010. A kinome RNAi screen identified AMPK as promoting poxvirus entry through the control of actin dynamics. PLoS Pathogens. **6(6):**e1000954
53. **Moss B**. 2006. Poxvirus entry and membrane fusion. Virology. **344**:48–54.
54. **Sandgren K. J., J. Wilkinson, M. Miranda-Saksena, G. M., McInerney, K. Byth-Wilson, P. J. Robinson, A. L. Cunningham**. 2010. A differential role for macropinocytosis in mediating entry of the two forms of vaccinia virus into dendritic cells. Plos Pathogens. **6:**e1000866
55. **Hsiao, J.C.; C. S. Chung, W. Chang.** 1999. Vaccinia virus envelope D8L protein binds to cell surface chondroitin sulfate and mediates the adsorption of intracellular mature virions to cells. Journal of Virology. **73**:8750–8761.
56. **Chung, C. S., J. C. Hsiao, Y. S. Chang, W. Chang**. 1998. A27L protein mediates vaccinia virus interaction with cell surface heparin sulfate. Journal of Virology. **72**:1577–1585.
57. **Hsiao, J. C., C. S. Chung, W. Chang**. 1998. Cell surface proteoglycans are necessary for A27L protein- mediated cell fusion: Identification of the N-terminal region of A27L protein as the glycosaminoglycan-binding domain. Journal of Virology. **72**:8374–8379.
58. **Lin, C.L., C. S. Chung, H. G. Heine, W. Chang.** 2000. Vaccinia virus envelope H3L protein binds to cell surface heparan sulfate and is important for intracellular mature virion morphogenesis and virus infection *in vitro* and *in vivo*. Journal of Virology. **74**:3353–3365.
59. **Vazquez, M. I. and M. Esteban**. 1999. Identification offunctional domains in the 14-kilodalton envelope protein (A27L) of vaccinia virus. Journal of Virology. **73**:9098–9109.
60. **da Fonseca, F. G., E. J. Wolffe, A. Weisberg, B. Moss.** 2000. Effects of deletion or stringent repression of the H3L envelope gene on vaccinia virus replication. Journal of Virology. **74**:7518–7528.
61. **Ward, B. M.** 2005. Visualization and characterization of the intracellular movement of vaccinia virus intracellular mature virions. Journal of Virology. **79**:4755–4763.
62. **McKelvey, T. A., S. C. Andrews, S. E. Miller, C. A. Ray, D. J. Pickup**. 2002. Identification of the orthopoxvirus p4c gene, which encodes a structural protein that directs

intracellular mature virus particles into A-type inclusions. Journal of Virology. **76**:11216–11225.
63. **Chang, S. J., Y. X. Chang, R. Izmailyan, Y. L. Tang, W. Chang.** 2010. Vaccinia virus A25 and A26 proteins are fusion suppressors for mature virions and determine strain-specific virus entry pathways into hela, CHO-K1, and L cells. Journal of Virology. **84**:8422–8432.
64. **Patel, D. D., D. J. Pickup, W. K. Joklik.** 1986. Isolation of cowpox virus A-type inclusions and characterization of their major protein component. Virology. **149**:174–189.
65. **Amegadzie, B. Y., J. R. Sisler, B. Moss**. 1992. Frame-shift mutations within the vaccinia virus A-type inclusion protein gene. Virology. **186**:777–782.
66. **Law, M., G. C. Carter, K. L. Roberts, M. Hollinshead, G. L. Smith**. 2006. Ligand-induced and non-fusogenic dissolution of a viral membrane. Proceedings of the National Academy of Sciences of the United States of America. **103**:5989–5994.
67. **Schmidt, F. I., C. K. Bleck, A. Helenius, J. Mercer**. 2011. Vaccinia extracellular virions enter cells by macropinocytosis and acid-activated membrane rupture. The EMBO Journal. **30**:3647–3661.
68. **Bengali, Z., A. C. Townsley, B. Moss.** 2009. Vaccinia virus strain differences in cell attachment and entry. Virology. **389:**132–140.
69. **Chang, S.J., A. C. Shih, Y. L. Tang, W. Chang**. 2012. Vaccinia Mature Virus Fusion Regulator A26 Protein Binds to A16 and G9 Proteins of the Viral Entry Fusion Complex and Dissociates from Mature Virions at Low pH. Journal of Virology. **86:**3809–3818.
70. **Moss, B.** 2013. Poxvirus DNA Replication. Cold Spring Harbor Perspectives in Virology. **5(9)**: a010199
71. **Buller, R. M., G. J. Palumbo.** 1991. Poxvirus Pathogenesis. Microbological Reviews. **55(1):**80-122.
72. **Tolonen, N., L. Doglio, S. Schleich, J. Krijnse Locke**r. 2001. Vaccinia virus DNA replication occurs in endoplasmic reticulum-enclosed cytoplasmic mini-nuclei. Molecular Biology of the Cell. **12**:2031– 2046.
73. **Du, S. and P. Traktman**. 1996. Vaccinia virus DNA replication: Two hundred base pairs of telomeric sequence confer optimal replication efficiency on minichromosome templates. PNAS. **93**: 9693-9698.
74. **Smith, G. L., and M. Law**. 2004. The exit of vaccinia virus from infected cells. Virus Research. **106**:189-97.
75. **Seet, B. T., J. B. Johnston, C. R. Brunetti, J. W. Barrett, H. Everett, C. Cameron, J. Sypula, S. H. Nazarian, A. Lucas, and G. McFadden.** 2003. Poxviruses and immune evasion. Annual review of immunology **21**:377-423.
76. **Moss, B. and J. L. Shisler.** 2001. Immunology 101 at poxvirus U: immune evasion genes. Seminars in Immunology. **13**:59–66.
77. **McFadden, G**. 2005. Poxvirus tropism. Nature Reviews Microbiology. **3:**201-213.
78. **Johnston, J. B., and G. McFadden**. 2003. Poxvirus immunomodulatory strategies: current perspectives. Journal of Virology. **77**:6093-6100.
79. **Nash, P., J. Barrett, J. X. Cao, S. Hota-Mitchell, A. S. Lalani, H. Everett, X. M. Xu, J. Robichaud, S. Hnatiuk, C. Ainslie, B. T. Seet, G. McFadden.** 1999. Immunomodulation by viruses: the myxoma virus story. Immunological Reviews. **168**:103–120.
80. **Tait, S. W. and D. R. Green.** 2010. Mitochondria and cell death: outer membrane permeabilization and beyond. Nature Reviews Molecular Cell Biology. **11**:621–632.
81. **Kvansakul, M., H. Yang, W. D. Fairlie, P. E. Czabotar, S. F. Fischer, M. A. Perugini, D. C. Huang, P.M: Colman**. 2008. Vaccinia virus anti-apoptotic F1L is a novel Bcl-2-like domain-swapped dimer that binds a highly selective subset of BH3-containing death ligands. Cell Death and Differentiation. 15:1564–1571.

82. **Wasilenko, S., T. L. Stewart, A. F. Meyers, M. Barry**. 2003. Vaccinia virus encodes a previously uncharacterized mitochondrialassociated inhibitor of apoptosis Proceedings of the National Academy of Sciences of the United States of America. **100:**14345–14350.
83. **Wasilenko, S. T., L. Banadyga, D, Bond, M. Barry.** 2005. The vaccinia virus F1L protein interacts with the proapoptotic protein Bak and inhibits Bak activation. Journal of Virology **79**:14031–14043.
84. **Postigo, A., J. R. Cross, J. Downward, M. Way.** 2006. Interaction of F1L with the BH3 domain of Bak is responsible for inhibiting vaccinia-induced apoptosis Cell Death and Differentiation. **13**:1651–1662.
85. **Gerlic, M., B. Faustin, A. Postigo, E. C.-W. Yu, M. Proell, N. Gombosuren, M. Krajewska, R. Flynn, M. Croft, M. Way, A. Satterthwait, R. C. Liddington, S. Salek-Ardakani, S. Matsuzawa, J. C. Reed.** 2013. Vaccinia virus F1L protein promotes virulence by inhibiting inflammasome activation. Proceedings of the National Academy of Sciences of the United States of America. 110:7808–7813.
86. **Aoyagi, M., D. Zhai, C. Jin, A. E. Aleshin, B. Stec, J. C. Reed, R. C. Liddington.** 2007. Vaccinia virus N1L protein resembles a B cell lymphoma-2 (Bcl-2) family protein. Protein Science. **16**:118–124.
87. **Cooray, S., M. W. Bahar, N. G. Abrescia, C. E. McVey, N. W. Bartlett, R. A. Chen, D. I. Stuart, J. M. Grimes, G. L. Smith.** 2007. Functional and structural studies of the vaccinia virus virulence factor N1 reveal a Bcl-2-like anti-apoptotic protein. Journal of General Virology. **88**: 1656–1666.
88. **Ray, C. A., R. A. Black, S. R. Kronheim, T. A. Greenstreet, P. R. Sleath, G.S. Salvesen, D. J. Pickup**. 1992. Viral inhibition of inflammation: cowpox virus encodes an inhibitor of the interleukin-1b converting enzyme. Cell. **69**, 597–604.
89. **Zhou, Q., S. Snipas, K. Orth, M. Muzio, V. M. Dixit, G. S. Salvesen.** 1997. Target protease specificity of the viral serpin CrmA. Analysis of five caspases. The Journal of Biological Chemistry. **272**:7797–7800.
90. **Garcı´a-Calvo, M., E. P. Peterson, B. Leiting, R. Ruel, D. W. Nicholson N. A: Thornberry**. 1998. Inhibition of human caspases by peptide-based and macromolecular inhibitorsThe Journal of Biological Chemistry. **273**:32608–32613.
91. **Gubser, C. and G.L:Smith**. 2002. The sequence of camelpox virus shows it is most closely related to variola virus, the cause of smallpox. Journal of General Virology. **83**:855–872.
92. **Gubser, C., D. Bergamaschi, M. Hollinshead, X. Lu, F. J. van Kuppeveld, and G. L. Smith**. 2007. A new inhibitor of apoptosis from vaccinia virus and eukaryotes. PLoS Pathogens. **3(2)**:e17
93. **Dasgupta, A., E. Hammarlund, M. K. Slifka, and K. Früh.** 2007. Cowpox virus evades CTL recognition and inhibits the intracellular transport of MHC class I molecules. Journal of Immunology. **3**:1654–1661.
94. **Byun, M., M. C. Verweij, D. J. Pickup, E. J. H. J. Wiertz, T. H. Hansen, andW. M. Yokoyama.** 2009. Two mechanistically distinct immune evasion proteins of cowpox virus combine to avoid antiviral CD8 T cells. Cell Host and Microbe. **5**:422–432.
95. **Janeway, C. A. Jr.** 2001. How the immune system protects the host from infection. Microbes and Infection. **3**:1167–1171.
96. **Guidotti, L. G., F. V. Chisari**. 2001. Noncytolytic control of viral infections by the innate and adaptive immune response. Annual Review of Immunology. **19**:65–91
97. **Rossi, D., A. Zlotnik**. 2000. The biology of chemokines and their receptors. Annual Review of Immunology. **18**:217–242.
98. **Alcami, A., U. H. Koszinowski**. 2000. Viral mechanisms of immune evasion. Trends in Immunology. **8**:410–418.

99. **Unterholzner, L., A. G: Bowie.** 2008. The interplay between viruses and innate immune signaling: recent insights and therapeutic opportunities. Biochemical Pharmacology. **75**:589–602.
100. **Hu, F. Q., C. A. Smith, and D. J. Pickup.**1994. Cowpox virus contains two copies of an early gene encoding a soluble secreted form of the type II TNF receptor. Virology. **204**:343–356.
101. **Smith, C. A., F. Q. Hu, T. D. Smith, C. L. Richards, P. Smolak, R. G. Goodwin, and D. J. Pickup**. 1996. Cowpox virus genome encodes a second soluble homologue of cellular TNF receptors, distinct from CrmB that binds TNF but not LT alpha. Virology. **223**:132–147.
102. **Loparev, V. N., J. M. Parsons, J. C. Knight, J. F. Panus, C. A. Ray, R. M. Buller, D. J. Pickup, and J. J. Esposito**.1998. A third distinct tumor necrosis factor receptor of orthopoxviruses Proceedings of the National Academy of Sciences of the United States of America. **95**:3786–3791.
103. **Reading, P. C., A. Khanna and G. L. Smith.** 2002. Vaccinia virus CrmE encodes a soluble and cell surface tumor necrosis factor receptor that contributes to virus virulence. Virology. **292**:285-298
104. **Alcami, A.** 2003. Viral mimicry of cytokines, chemokines and their receptors. Nature Reviews Immunology**. 3**:36–50.
105. **Xiang, Y., and B. Moss.** 2001. Correspondence of the functional epitopes of poxvirus and human interleukin-18-binding proteins. Journal of Virology. 75:9947-9954.
106. **Calderara, S., Y. Xiang, and B. Moss**. 2001. Orthopoxvirus IL-18 binding proteins: affinities and antagonist activities. Virology. **279**:22-26.
107. **Smith, V. P., N. A. Bryant, and A. Alcami.** 2000. Ectromelia, vaccinia and cowpox viruses encode secreted interleukin-18-binding proteins. Journal of General Virology. **81**:1223-1230.
108. **Smith, S. A. and G. J. Kotwal.** 2002. Immune response to poxvirus infections in various animals. Critical Reviews in Microbiology. **28:** 149–185.
109. **Riedel S.** 2005 Edward Jenner and the history of smallpox and vaccination. Baylor University Medical Center Proceedings. **18(1):** 21–25
110. **Essbauer, S., M. Pfeffer, and H. Meyer.** 2010. Zoonotic poxviruses. Veterinary Microbiology **140**:229-236.
111. **Esposito, J. J. and J.C. Knight.** 1985. Orthopoxvirus DNA: a comparison of restriction profiles and maps. Virology. **143,** 230e251.
112. **Baxby, D. and M. Bennett M.** 1997. Cowpox: a re-evaluation of the risks of human cowpox based on new epidemiological information Archives of Virology. Supplementa. **13**:1–12.
113. **Yeruham, I., A. Nyska, A. Abraham, R. Algazi.** 1996. Occurrence of cowpox-like lesions in cattle in Israel. Revue d'élevage et de médecine vétérinaire des pays tropicaux. **49**: 299–302
114. **Bennett, M., A. J. Crouch, M. Begon, B. Duffy, S. Feore, R. M. Gaskell, D.F: Kelly, C. M. McCracken, L. Vicary, D. Baxby.** 1997. Cowpox in British voles and mice. Journal of Comparative Pathology **116**: 35–44.
115. **Kinnunen, P. M., H. Henttonen, B. Hoffmann, E. R. Kallio, C. Korthase J. Laakkonen, J. Niemimaa, A. Palva, M: Schlegel, H. S. Ali, P. Suominen, R. G. Ulrich, A. Vaheri, O. Vapalahti.** 2011. Orthopox virus infections in Eurasian wild rodents. Vector Borne Zoonotic Disease. **11**: 1133–1140
116. **Chantrey, J., H. Meyer, D. Baxby, M. Begon, K. J. Bown, S. M. Hazel, T. Jones, W. I. Montgomery, and M. Bennett.** 1999. Cowpox: reservoir hosts and geographic range. Epidemiology and infection **122**:455-460.

117. **Crouch, A. C., D. Baxby, C. M. McCracken, R. M. Gaskell, and M. Bennett.** 1995. Serological evidence for the reservoir hosts of cowpox virus in British wildlife. Epidemiology and Infection. **115**:185-191.
118. **Hazel, S. M., M. Bennett, J. Chantrey, K. Bown, R. Cavanagh, T. R. Jones, D. Baxby, M. Begon.** 2000. A longitudinal study of an endemic disease in its wildlife reservoir: cowpox and wild rodents. Epidemiology and infection. **124**:551-562
119. **Hoffmann, D., A. Franke, M. Jenckel, A. Tamošiūnaitė, J. Schluckebier H. Granzow, B. Hoffmann, S. Fischer, R. G. Ulrich, D. Höper, K. Goller, N. Osterrieder, M. Beer.** 2015. Out of the reservoir: Phenotypic and genotypic characterization of a novel cowpox virus isolated from a common vole. Journal of Virology. 89(21):10959-69
120. **Campe, H., P. Zimmermann, K. Glos, M. Bayer, H. Bergemann, C. Dreweck, P. Graf, B. K. Weber, H. Meyer, M. Büttner, U. Busch, A. Sing.** 2009. Cowpox virus transmission from pet rats to humans, Germany. Emerging infectious diseases. **15**:777-780
121. **Carletti, F., L. Bordi, C. Castilletti, A. Di Caro, L. Falasca, C. Gioia, G. Ippolito, S. Zaniratti, A. Beltrame, P. Viale, M. Rosaria Capobianchi.** 2009. Cat-to human orthopoxvirus transmission, northeastern Italy. Emerging infectious diseases. **15:**499–500
122. **Hobi, S., R. S. Mueller, M. Hill, A. Nitsche, T. Löscher, W. Guggemos, S. Ständer, D. Rjosk-Dendorfer, A. Wollenberg.** 2015. Neurogenic inflammation and colliquative lymphadenitis with persistent orthopox virus DNA detection in a human case of cowpox virus infection transmitted by a domestic cat. British Journal of Dermatology. **10**:1111 – 13700
123. **Vogel, S., M. Sardy, K. Glos, H. C. Korting, T. Ruzicka T A. Wollenberg.** 2012. The Munich outbreak of cutaneous cowpox infection: transmission by infected pet rats. Acta Dermato Venereologica. **92**:126–31.
124. **Ninove, L., Y. Domart, C. Vervel, C. Voinot, N. Salez, D. Raoult, H. Meyer, I. Capek, C. Zandotti, and R. N. Charrel**. 2009. Cowpox virus transmission from pet rats to humans, France. Emerging infectious diseases. **15**:781-784.
125. **Tryland, M., M. I. Okeke, C. H. Segerstad, T. Morner, T. Traavik M. P. Ryser-Degiorgis.** 2011. Orthopoxvirus DNA in Eurasian lynx, Sweden. Emerging infectious diseases. **17**: 626–632
126. **Cardeti, G., A. Brozzi, C. Eleni, N. Polici, G. D'Alterio, F. Carletti, M. T. Scicluna, C. Castilletti, M. R. Capobianchi, A. Di Caro, G. L. Autorino, D. Amaddeo.** 2011. Cowpox virus in llama, Italy. Emerging infectious diseases. **17**: 1513–1515.
127. **Favier, A. L., O. Flusin, S. Lepreux, H. Fleury, C. Labreze A. Georges, J. M. Crance, F. Boralevid** 2011. Necrotic ulcerated lesion in a young boy caused by cowpox virus infection. Case Reports in Dermatology. **3**:186–194.
128. **Świtaj, K., P. Kajfasz, A. Kurth, A. Nitsche.** 2015. Cowpox after a cat scratch - case report from Poland. Annals of Agricultural and Environmental Medicine. **3**:456-8
129. **Marrenikova, S. S., N. N: Maltseva, V. I. Korneeva, N. M. Garanina**. 1977. Outbreak of pox disease among carnivora (felidae) and edentate. The Journal of Infectious Diseases. **135**: 358–366
130. **Stemmler, M., H. Neubauer, H. Meyer.** 2001. Comparison of closely related orthopoxvirus isolates by random amplified polymorphic DNA and restriction length polymorphism analysis. Journal of Veterinary Medicine. **B48**:647–654
131. **Boulanger, D., A. Crouch, B. Brochier, M. Bennett, J. Clement, R. M. Gaskell, D. Baxby, P. P. Pastoret.** 1996. Serological survey for orthopoxvirus infection of wild mammals in areas where a recombinant rabies virus is used to vaccinate foxes. Veterinary Record. **138:** 247–249
132. **Smith, K. C., M. Bennett, D. C. Garrett.** 1999. Skin lesions caused by orthopoxvirus infection in a dog. Journal of Small Animal Practice. **40**: 495–497

133. **Ellenberger, C., K. F. Schuppel, M. Mohring, A. Reischauer, M. Alex, C. P. Czerny, A. Fercho, H. A. Schoon**. 2005. Cowpox virus infection associated with a streptococcal septicaemia in a foal. Journal of Comparative Pathology. **132**:101–105
134. **Meyer, H., C. Schay, H. Mahnel, M. Pfeffer.** 1999. Characterization of orthopoxviruses isolated from man and animals in Germany. Archives of Virology. **144**:491–501
135. **Pilaski, J., A. Rosen, G. Darai.** 1986. Comparative analysis of the genomes of orthopoxviruses isolated from elephant, rhinoceros, and okapi by restriction enzymes. Archives of Virology. **88**:135–142
136. **Wisser, J., J. Pilaski, G. Strauss, H. Meyer, G. Burck, U. Truyen, M. Rudolph, K. Frolich.** 2001. Cowpox virus infection causing stillbirth in an Asian elephant (Elephas maximus). Veterinary Record. **149**: 244–246
137. **Wienecke, R., H. Wolff, M. Schaller, H. Meyer, G. Plewig.** 2000. Cowpox virus infection in an 11-year-old girl. Journal of the American Academy of Dermatology. **42**:892–894.
138. **Vorou, R. M., V. G. Papavassiliou, I. N. Pierroutsakos**. 2008. Cowpox virus infection: an emerging health threat. Current Opinion in Infectious Diseases. **21**:153–156.
139. **Nitsche, A. and G. Pauli.** 2007 Sporadic human cases of cowpox in Germany. Eurosurveillance. **12**:E070419.
140. **Baxby, D., M. Bennett, B. Getty B.** 1994. Human cowpox 1969–93: a review based on 54 cases. British Journal of Dermatology.**131**:598–607.
141. **Eis-Hubinger, A. M., A. Gerritzen, K. E. Schneweis, B. Pfeiff, H. Pullmann, A. Mayr, C. P. Czerny**. 1990. Fatal cowpox-like virus infection transmitted by cat. The Lancet 336:880
142. **Marennikova, S. S., E. M. Shelukhina, V. A: Fimina.** 1978. Pox infection in white rats. Laboratory Animals. **12(1):**33–36.
143. **Pfeffer, M., S. Pfleghaar, B. D. Von, O. R. Kaaden, H. Meyer.** 2002. Retrospective investigation of feline cowpox in Germany. Veterinary Record. **150**:50-51
144. **Schöniger, S., D. L. Chan, M. Hollinshead, K. Humm, G. L. Smith, P. M. Beard.** 2007. Cowpox virus pneumonia in a domestic cat in Great Britain. Veterinary Record. **160**: 522-523
145. **Carroll, D. S., G. L: Emerson, Y. Li, S. Sammons, V. Olson, M Frace, Y. Nakazawa, C. P. Czerny, M. Tryland, J. Kolodziejek, N. Nowotny, M. Olsen-Rasmussen, M. Khristova, D. Govil, K. Karem, I. K. Damon, H. Meyer.**. 2011. Chasing Jenner's vaccine: revisiting cowpox virus classification. PLoS One. **6**:e23086
146. **Fenner, F and F. M. Burnet**. 1957. A short description of the poxvirus group (vaccinia and related viruses). Virology. **4**: 305–314
147. **Dabrowski, P. W., A. Radonic, A. Kurth, A. Nitsche.** 2013. Genome-wide comparison of cowpox viruses reveals a new clade related to Variola virus. PLoS One. **8**: e79953.
148. **Hansen, H., M. I. Okeke, O. Nilssen, T. Traavik.** 2009. Comparison and phylogenetic analysis of cowpox viruses isolated from cats and humans in Fennoscandia. Archives of Virology. **154**:1293–1302
149. **Duraffour, S., B. Mertens, H. Meyer, J. J. van den Oord, T. Mitera, P. Matthys, R. Snoeck, G. Andrei G**. 2013. Emergence of cowpox: study of the virulence of clinical strains and evaluation of antivirals. PLoS One. **8**:e55808.
150. **Becker, C., A. Kurth, F. Hessler, H. Kramp, M. Gokel, R. Hoffmann, A. Kuczka, A. Nitsche**. 2009. Cowpox virus infection in pet rat owners—not always immediately recognized. Deutsches Arzteblatt International. **106**: 329-334
151. **Brune, W., M. Messerle and U. H. Koszinowski.** 2000. Forward with BACs: new tools for herpesvirus genomics. Trends in Genetics. **16:**254-9.

152. **Zhang, Y., F. Buchholz, J. P. Muyrers, and A. F. Stewar**t. 1998. A new logic for DNA engineering using recombination in Escherichia coli. Nature Genetics. **20**:123-128
153. **Domi, A. and B. Moss**. 2002. Cloning the vaccinia virus genome as a bacterial artificial chromosome in Escherichia coliand recovery of infectious virus in mammalian cells. Proceedings of the National Academy of Sciences of the United States of America. **99**:12415-12420.
154. **Messerle, M., I. Crnkovic, W. Hammerschmidt, H. Ziegler, and U. H. Koszinowski**. 1997. Cloning and mutagenesis of a herpesvirus genome as an infectious bacterial artificial chromosome. Proceedings of the National Academy of Sciences of the United States of America. **94**:14759-14763.
155. **Cottingham, M. G., R. F. Andersen, A. J. Spencer, S. Saurya, J. Furze, A. V. Hill, and S. C. Gilbert**. 2008. Recombination-mediated genetic engineering of a bacterial artificial chromosome clone of modified vaccinia virus Ankara (MVA). PLoS. ONE. 3:e1638.
156. **Meisinger-Henschel, C., M. Spath, S. Lukassen, M. Wolferstatter, H. Kachelriess, K. Baur, U. Dirmeier, M. Wagner, P. Chaplin, M. Suter and J. Hausmann.** 2010. Introduction of the six major genomic deletions of modified vaccinia virus Ankara (MVA) into the parental vaccinia virus is not sufficient to reproduce an MVA-like phenotype in cell culture and in mice. Journal of Virology. **84**:9907-9919.
157. **Roth, S. J., D. Hoper, M. Beer, S. Feineis, B. K. Tischer, and N. Osterrieder.** 2011. Recovery of infectious virus from full-length cowpox virus (CPXV) DNA cloned as a bacterial artificial chromosome (BAC). Veterinary Research. **42**:3
158. **Breithaupt, A., D. Kalthoff, F., Deutskens, P. Konig, B Hoffmann, M. Beer, H. Meyer, J. P. Teifke**. 2012. Clinical course and pathology in rats (Rattus norvegicus) after experimental cowpox virus infection by percutaneous and intranasal application. Veterinary pathology. **49**:941-949.
159. **Martinez, M. J., M. P. Bray and J. W. Huggins.** 2000. A mouse model of aerosoltransmitted orthopoxviral disease: morphology of experimental aerosol-transmitted orthopoxviral disease in a cowpox virus-BALB/c mouse system. Archives of Pathology and Laboratory Medicine. **124**:362-377
160. **Kalthoff, D., P. König, H. Meyer, M. Beer, B. Hoffmann.** 2011. Experimental cowpox virus infection in rats. Veterinary microbiology. **153:**382-386.
161. **Schat, K. A.** 1998. A Laboratory Manual for the Isolation and Identification of Avian Pathogens. American Association of Avianian Pathologist. 223–234
162. **Tischer, B. K., G. A. Smith, and N. Osterrieder**. 2010. En passant mutagenesis: a two-step markerless red recombination system. Methods in molecular biology **634**:421-30.
163. **Tischer, B. K., J. von Einem, B. Kaufer, and N. Osterrieder.** 2006. Two-step redmediated recombination for versatile high-efficiency markerless DNA manipulation in Escherichia coli. Biotechniques. **40**:191-7.
164. **Wussow, F., H. Fickenscher, and B. K. Tischer**. 2009. Red-mediated transposition and final release of the mini-F vector of a cloned infectious herpesvirus genome. PLoS. ONE. **4**:e8178.
165. **Scaramozzino, N., A. Ferrier-Rembert. A. L. Favier, C. Rothlisberger, S. Richard, J. M. Crance, H. Meyer, D. Garin.** 2007. Real-time PCR to identify variola virus or other human pathogenic orthopox viruses. Clinical Chemistry. **53**:606–613
166. http://www.ncbi.nlm.nih.gov/
167. **Shchelkunov, S. N., P. F. Safronov, A. V. Totmenin, N. A. Petrov, O. I. Ryazankina, V. V. Gutorov, G. J. Kotwal.** 1988. The genomic sequence analysis of the left and right species-specific terminal region of a cowpox virus strain reveals unique sequences and a cluster of intact ORFs for immunomodulatory and host range proteins. Virology. **243(2)**:432-60
168. **Morikawa, S., T. Sakiyama, H. Hasegawa, M. Saijo, A. Maeda, I. Kurane, G. Maeno, J. Kimura, C. Hirama, T. Yoshida, Y. Asahi-Ozaki, T. Sata, T. Kurata, A. Kojima.**

2005. An attenuated LC16m8 smallpox vaccine: analysis of full-genome sequence and induction of immune protection. Journal of Virology. **79(18):**11873-91.
169. **Afonso, C. L., E. R. Tulman, Z. Lu, L. Zsak, N. T. Sandybaev, U. Z. Kerembekova, V. L. Zaitsev, G. F. Kutish, D. L. Rock.** 2002. The genome of camelpox virus. Virology. **295(1):**1-9.
170. **Mavian, C., A. López-Bueno, N. A. Bryant, K. Seeger, M. A. Quail, D. Harris, B. Barrell, A. Alcamí.** 2014. The genome sequence of ectromelia virus Naval and Cornell isolates from outbreaks in North America. Virology. **462-463:**218-26
171. **Mendez-Rios, J. D., C. A. Martens, D. P. Bruno, S. F. Porcella, Z. M. Zheng, B. Moss.** 2012. Genome sequence of erythromelalgia-related poxvirus identifies it as an ectromelia virus strain. PLoS One. **7(4):**e34604.
172. **Tulman, E. R., G. Delhon, C. L. Afonso, Z. Lu, L. Zsak, N. T. Sandybaev, U. Z. Kerembekova, V. L. Zaitsev, G. F. Kutish, D. L. Rock.** Genome of horsepox virus. Journal of Virology. **80(18):**9244-58.
173. **Goujon, M., McWilliam, H., Li, W., Valentin, F., Squizzato, S., Paern, J., Lopez, R.** 2010. A new bioinformatics analysis tools framework at EMBL-EBI. Nucleic. Acids Research**. 38**:695-9.
174. **Nakazawa,Y., M. R. Mauldin, G.L. Emerson, M. G., Reynolds, R.R. Lash, J. Gao, H. Zhao, Y. Li, J. J. Muyembe, P.M. Kingebeni, O. Wemakoy, J. Malekani, K. L. Karem, I. K. Damon. and D. S. Carroll**. 2015. A phylogeographic investigation of African monkeypox. Viruses. **7(4):**2168-84.
175. **Tamošiūnaitė, A.**, **D. Hoffmann, A. Franke, J. Schluckebier, K. Tauscher, B. K. Tischer, M. Beer, R. Klopfleisch, N. Osterrieder**. 2016. Histopathological and Immunohistochemical Studies of Cowpox Virus Replication in a Three-Dimensional Skin Model. Journal of Comperative Pathology. **155(1):**55-61.
176. **Chae, H. J., H. R. Kim, C. Xu, B. Bailly-Maitre, M. Krajewska M**. 2004. BI-1 regulates an apoptosis pathway linked to endoplasmic reticulum stress. Molecular Cell **15**:355–366.
177. **Xu. Q., J. C. Reed.** 1998. Bax inhibitor-1, a mammalian apoptosis suppressor identified by functional screening in yeast. Molecular Cell. **1**: 337–346.
178. **Lee, S., M. Jo, J. Lee, S. S. Koh, and S. Kim** .2007. Identification of novel universal housekeeping genes by statistical analysis of microarray data. Journal of biochemistry and molecular biology. **40**:226–231
179. **Lefkowitz, E. J., C. Upton, S. S. Changayil, C. Buck, P. Traktman, R. M. Buller.** 2005. Poxvirus Bioinformatics Resource Center: a comprehensive Poxviridae informational and analytical resource. Nucleic Acids Research. **33**:D311-D316.
180. **Saraiva, M., A. Alcami**. 2001. CrmE, a novel soluble tumor necrosis factor receptor encoded by poxviruses. Journal of Virology. **75**:226-233.
181. **Graham, S. C., M. W. Bahar, N. G. Abrescia, G. L. Smith, D. I. Stuart, J. M, J. M. Grimes.** 2007. Structure of CrmE, a virus-encoded tumour necrosis factor receptor. Journal of Molecular Biology. **372**:660-671.
182. **Ito, N., S. E. Phillips, K. D. Yadav, P. F. Knowles.** 1994. Crystal structure of a free radical enzyme, galactose oxidase. Journal of Molecular Biology. **238**:794–814.
183. **Prag, S., J. C. Adams.** 2003. Molecular phylogeny of the kelchrepeat superfamily reveals an expansion of BTB/kelch proteins in animals. BMC Bioinformatics. **4:**42.
184. **Ahmad, K. F., C. K: Engel, G.G. Prive**. 1998. Crystal structure of the BTB domain from PLZF. Proceedings of the National Academy of Sciences of the United States of America. **95**:12123–12128.
185. **Bardwell, V. J., R. Treisman, R.** 1994. The POZ domain: a conserved protein–protein interaction motif. Genes and Development. **8:**1664–1677.

186. **Furukawa, M., He, Y.J., Borchers, C., Xiong, Y.** 2003. Targeting of protein ubiquitination by BTB-Cullin 3-Roc1 ubiquitin ligases. Nature Cell Biology. **5 (11)**:1001–1007
187. **Geyer, R., Wee, S., Anderson, S., Yates, J., Wolf, D.A.** 2003. BTB/POZ domain proteins are putative substrate adaptors for cullin 3 ubiquitin ligases. Molecular Cell **12 (3)**: 783–790.
188. **Pintard, L., Willis, J.H., Willems, A., Johnson, J.L., Srayko, M., Kurz, T., Glaser, S., Mains, P.E., Tyers, M., Bowerman, B., Peter, M.** 2003. The BTB protein MEL-26 is a substrate-specific adaptor of the CUL-3 ubiquitinligase. Nature. **425 (6955)**:311–316.
189. **Xu, L., Wei, Y., Reboul, J., Vaglio, P., Shin, T.H., Vidal, M., Elledge, S.J., Harper, J.W.** 2003. BTB proteins are substrate-specific adaptors in an SCF-like modular ubiquitin ligase containing CUL-3. Nature. **425 (6955**):316–321.
190. **Wilton, B. A., S. Campbell, N. Van Buuren, R. Garneau, M. Furukawa, Y. Xiong, M. Barry** .2008. Ectromelia virus BTB/kelch proteins, EVM150 and EVM167, interact with cullin-3-based ubiquitin ligases. Virology. **374**:82 99.
191. **Wang, Q., K. Burles, B. Couturier, C. M. Randall, J. Shisler, M. Barry.** 2014. Ectromelia virus Encodes a BTB/kelch protein, EVM150 that inhibits NF-kappaB signaling. Journal of virology. **88:**4853-4865.
192. **Kochneva, G. V., I. V. Kolosova, T. A. Lupan, G. F. Sivolobova, P. V. Iudin, A. A. Grazhdantseva, E.I. Riabchikova, N. I. Kandrina, S. N. Shchelkunov .** (2009) Orthopoxvirus genes for kelch-like proteins: III. Construction of mousepox (ectromelia) virus variants with targeted gene deletions. Molecular Biology. **43 (4):**567–572.
193. **Kochneva, G., I. Kolosova, T. Maksyutova, E. Ryabchikova, and S. Shchelkunov.** 2005. Effects of deletions of kelch-like genes on cowpox virus biological properties. Archives of Virology. 150:1857-1870.
194. **Alzhanova, D., E. Hammarlund, J. Reed, E. Meermeier, S. Rawlings, C. A. Ray, D. M. Edwards, B. Bimber, A. Legasse, S. Planer, J. Sprague, M. K. Axthelm, D. J. Pickup, D. M. Lewinsohn, M. C. Gold, S. W. Wong, J. B. Sacha, M. K. Slifka, K. Früh.** 2014. T cell inactivation by poxviral B22 family proteins increases viral virulence. PLoS Pathogens. **10(5):** e1004123
195. **Reynolds, S. E., B. Moss.** 2015. Characterization of a large, proteolytically processed cowpox virus membrane glycoprotein conserved in most chordopoxviruses. Virology. **483:**209-17
196. **Horst, D., M. C. Verweij, A. J. Davison, M. E. Ressing, E. J: Wiertz.** 2011. Viral evasion of T cell immunity: ancient mechanisms offering new applications. Current opinion in immunology. **23:** 96–103.
197. **Howard, A. R., A. S. Weisberg, B. Moss.** 2010. Congregation of orthopoxvirus virions in cytoplasmic A-type inclusions is mediated by interactions of a bridging protein (A26p) with a matrix protein (ATIp) and a virion membrane-associated protein (A27p). Journal of Virology. **84:**7592–7602.
198. **Chiu, W. L., C. L. Lin, M. H. Yang, D. L. Tzou, W. Chang.** 2007. Vaccinia virus 4c (A26L) protein on intracellular mature virus binds to the extracellular cellular matrix laminin. Journal of Virology. **81**:2149–2157.
199. **Howard, A. R., T. G. Senkevich, B. Moss.** 2008. Vaccinia virus A26 and A27 proteins form a stable complex tethered to mature virions by association with the A17 transmembrane protein. Journal of Virology. **82**:12384–12391
200. **Kastenmayer, R. J., L. Maruri-Avidal, J. L. Americo, P. L. Earl, A. S. Weisberg, B. Moss.** 2014. Elimination of A-type inclusion formation enhances cowpox virus replication in mice: implications for orthopoxvirus evolution. Virology. **452-453**:59-66.
201. . **Committee on the Assessment of Future Scientific Needs for Live Variola Virus IoM.** 2009. Live Variola Virus: Considerations for Continuing Research. National Academies Press.

202. **Meyers, C., M. Mane, N. Kokorina, S. Alam, P. L. Hermonat.** 2000. Ubiquitous human adeno-associated virus type 2 autonomously replicates in differentiating keratinocytes of a normal skin model. Virology. **272(2):**338-46.
203. **Roguet, R., C. Cohen, E. Tessonneaud, C. Gagne, M. H. Teissier et al.** 2000. Use of a standardized reconstructed epidermis kit to assess in vitro the tolerance and the efficacy of cosmetics. International Journal of Cosmetic Science. **22**: 409–419.
204. **Andrei, G., S: Duraffour, J. Van den Oord, R. Snoeck.** 2010. Epithelial raft cultures for investigations of virus growth, pathogenesis and efficacy of antiviral agents. Antiviral Research. **85**:431–449.
205. **Duraffour, S., R. Snoeck, R. de Vos, J. van Den Oord, J. M. Crance, D. Garin, D. E. Hruby, R. Jordan, E. De Clercq, G. Andrei G.** 2007. Activity of the anti-orthopoxvirus compound ST-246 against vaccinia, cowpox and camelpox viruses in cell monolayers and organotypic raft cultures. Antiviral Therapy. **12**:1205-1216.
206. **Snoeck, R., A. Holy, C. Wolf-Peeters, J. Van Den Oord, E. De Clersq and G. Andrei.** 2002. Antivaccinia activities of acyclic nucleoside phosphonate derivatives in epithelial cells and organotypic cultures. Antimicrobial Agents and Chemotherapy. **46:**3356-3361.
207. **Wali, A., D. S. Strayer**. 1999. Infection with vaccinia virus alters regulation of cell cycle progression. DNA Cell Biology. **18**:837-843.
208. **Johnston, J. B., G. Wang, J. W. Barrett, S. H. Nazarian, K. Colwill, M. Moran, G. McFadden.** 2005. Myxoma virus M-T5 protects infected cells from the stress of cell cycle arrest through its interaction with host cell cullin-1. Journal of Virology. **79:**10750–10763.
209. **Yoo, N. K., C. W. Pyo, Y. Kim, B. Y. Ahn, S. Y. Choi.** 2008. Vaccinia virus-mediated cell cycle alteration involves inactivation of tumour suppressors associated with Brf1 and TBP. Cellular Microbiology. **10**:583–592.
210. **Hans, F., S. Dimitrov**. 2001. Histone H3 phosphorylation and cell division. Oncogene. **20**:3021–3027.
211. **Prigent, C., S. Dimitrov**. 2003. Phosphorylation of serine 10 in histone H3, what for? Journal of Cell Science. **116**:3677–3685.
212. **Bode, A. M., Z. Dong.** 2005. Inducible covalent posttranslational modification of histone H3. Science's STKE : signal transduction knowledge environment. **281**:re4.
213. **Evans, T., E. T. Rosenthal, J. Youngblom, D. Distel, T. Hunt T.** 1983. Cyclin: a protein specified by maternal mRNA in sea urchin eggs that is destroyed at each cleavage division. Cell. **33**:389–396.
214. **Brady, G., L: Boggan, A. Bowie, L. A. O'Neill.** 2005. Schlafen-1 causes a cell cycle arrest by inhibiting induction of cyclin D1. Journal of Biological Chemistry. **280**:30723–30734.
215. **Bustos, O., N. Naik, G. Ayers, C. Casola, M. A. Perez-Lamigueiro, P. T. Chippindale, E. J. Pritham, E. de la Casa-Esperón**. 2009. Evolution of the Schlafen genes, a gene family associated with embryonic lethality, meiotic drive, immune processes and orthopoxvirus virulence. Gene. **1**:1-11
216. **Gubser, C., R. Goodbody, A. Ecker, G. Brady, L. A. O'Neill, N. Jacobs, G. L. Smith**. 2007. Camelpox virus encodes a Schlafen-like protein that affects orthopoxvirus virulence. Journal of General Virology. **88**:1667–1670.
217. **Carrara, G., N. Saraiva, M. Parsons, B. Byrne, D. L. Prole, C. W. Taylor, G. L: Smith.** 2015. Golgi anti-apoptotic proteins are highly conserved ion channels that affect apoptosis and cell migration. Journal of Biological Chemistry**. 290(18):**11785-801.

List of publications

Tamošiūnaitė, A., D. Hoffmann, A. Franke, J. Schluckebier, K. Tauscher, B. K. Tischer, M. Beer, R. Klopfleisch, N. Osterrieder. 2016. Histopathological and Immunohistochemical Studies of Cowpox Virus Replication in a Three-Dimensional Skin Model. Journal of Comperative Pathology. 155(1):55-61.

Hoffmann, D., A. Franke, M. Jenckel, **A. Tamošiūnaitė**, J. Schluckebier H. Granzow, B. Hoffmann, S. Fischer, R. G. Ulrich, D. Höper, K. Goller, N. Osterrieder, M. Beer. 2015. Out of the reservoir: Phenotypic and genotypic characterization of a novel cowpox virus isolated from a common vole. Journal of Virology. 89(21):10959-69

Xu, Z., D. Zikos, **A. Tamošiūnaitė**, R. Klopfleisch, N. Osterrieder, B. K. Tischer. 2014. Identification of 10 cowpox virus proteins that are necessary for induction of hemorrhagic lesions (red pocks) on chorioallantoic membranes. Journal of Virology. 88(15):8615-28

Talks and poster presentations (conference proceedings)

Tamošiūnaitė, A., D. Hoffmann, R. Klopfleisch, M. Jenckel, M. Beer, B. K. Tischer, K. Osterrieder. 2015. Poster. Identification of new Orthopoxvirus virulence markers in the rodent host. 25st German Society of Virology (GfV) Congress, Bochum, Germany.

Hoffmann, D., A. Franke, **A. Tamošiūnaitė**, N. Osterrieder, M. Beer. 2016. Out of the reservoir: CPXV-infections of bank voles (*Myodes glareolus*). National Symposium of on Zoonoses Research, Berlin.

Franke, A., D. Hoffmann, **A. Tamošiūnaitė**, M. Jenckel, B. Hoffmann, N. Osterrieder, M. Beer. 2014. Cowpox virus virulence factors - genetic definition and in vivo testing. National Symposium of on Zoonoses Research, Berlin.

Franke, A., D. Hoffmann, **A. Tamošiūnaitė,** M. Jenckel, N. Osterrieder, M. Beer. 2016. Cowpox virus-host interactions: Determination of defined virulence factors. International Poxvirus, Asfarvirus and Iridovirus Conference, Strasbourg.

Franke, A., D. Hoffmann, A. Tamošiūnaitė, M. Jenckel, B. Hoffmann, N. Osterrieder, M. Beer. 2016. Cowpox virus-host interactions: Determination of defined virulence factors. 10th Annual Meeting EPIZONE, Madrid.

Acknowledgements

I am very grateful to my supervisor, Prof. Dr. Prof. Klaus Osterrieder, for giving me the opportunity to do my doctoral thesis in his lab, for his expert advices, constructive criticism, seemingly never-ending patience and funding assistance.

I warmly thank to Dr. Karsten Tischer for bringing the ideas to this interesting project.

A lot of thanks go to our collaborators, Martin Beer, Donata Hoffmann and Annika Franke in Friedrich-Loeffler Institut, for helping with the animal experiments

Also, I am very thankful to Prof. Robert Klopfleisch for the help with the histopathological examinations of the infected skin model.

I would also like to thank all past and present members of the Institut für Virologie, FU Berlin, who have supported and helped me during the last years. In particular, I would like to thank Annachiara, Pratik Bart, Renato, Darren, Dušan, Nina, Inês, Timo, Tobi, Ben, Imme, Dimitris, Maren, Jakob, Kathrin, Kia, Walid, Xu, Liuba, Atika and everyone who was not named here.

Also, I am deeply grateful to our technicians Ann and Netti for always having an answer to any technical question.

A special thank you goes to Til for the support, patience and encouragement during the past 4 years of my studies.

Most importantly, I would like to thank my family and friends for never stopping to believe in me.

The last but not the least, many thanks would be given to the support and funding from the Freie Universität Berlin and German Research Foundation (DFG) without which the studies would not have been possible.

Selbständigkeitserklärung

Hiermit bestätige ich, dass ich die vorliegende Arbeit selbständig angefertigt habe. Ich versichere, dass ich ausschließlich die angegebenen Quellen und Hilfen Anspruch genommen habe.

Berlin, den 20. Juli 2017

Aistė Tamošiūnaitė